NONLINEAR ROTORDYNAMICS ANALYSIS

prepared for
George C. Marshall
Space Flight Center
Alabama 35812

under

CONTRACT NAS8 - 37465

Principal Investigator

Sherif T. Noah

Mechanical Engineering Department
Texas A&M University
College Station, Texas 77843

February 1991

TABLE OF CONTENTS

ABSTRACT

Effective analysis tools have been developed for predicting the nonlinear rotordynamic behavior of the SSME turbopumps under steady and transient operating conditions. Using these methods, preliminary parametric studies have been conducted on both generic and actual HPOTP (high pressure oxygen turbopumps) models. In particular, a novel modified harmonic balance/alternating Fourier transform (HB/AFT) method was developed and used to conduct a preliminary study of the effects of fluid, bearing and seal forces on the unbalanced response of a Multi-disk rotor in presence of bearing clearances. A computer program was developed and made available to NASA, Marshall. The method makes it possible to determine periodic, sub-, super- synchronous and chaotic responses of a rotor system. The method also yields information about the stability of the obtained response, thus allowing bifurcation analyses. This provides a more effective capability for predicting the response under transient conditions by searching in proximity of resonance peaks. Preliminary results were also obtained for the nonlinear transient response of an actual HPOTP model using an efficient, newly developed numerical method based on convolution integration. A computer program was developed and made available to NASA Marshal Flight Center. Currently, the HB/AFT is being extended for determining the aperiodic response of nonlinear systems. Initial results shows the method to be promising.

I. INTRODUCTION

Background:

Modern mechanical systems are being recently designed for higher performance, reliability and smooth operation within compact configuration. These requirements often cause significant nonlinear effects which could not be predicted with linear models. Therefore, a more complete picture of their nonlinear dynamic characteristics is required to enhance their efficient design, refinement, monitoring or maintenance.

Modern complex rotating machinery, such as the turbopumps of the space shuttle main engines (SSME), contain various sources of strong nonlinearities. These include clearances and nonlinearity of rolling elements, rubbing in splines and in built-up rotor segments, rubbing at seals and rotor blades, viscous damping and various fluid effects. Observed nonlinear behavior of actual rotor systems include jump discontinuities [1], large subsynchronous motion, [2] - [4], quasi-periodic and possible chaotic motion [5]. As stated by Nataraj and Nelson [6], the future developments in modern machines heavily depends on the ability to identify, understand mathematically and analyze systems involving nonlinear components. This is particularly the case for the proper development, monitoring and analysis of the SSME turbopumps.

Quite often, it is essential to determine the steady state periodic response of rotor systems in the form of self excited limit cycles or forced motion due to rotating imbalance. Accurate prediction of the nonlinear periodic responses and their stability plays a central role in developing a complete picture of the dynamic behavior of nonlinear rotor systems as function of their parameters.

Several methods have recently been advanced for determining the periodic response of low order nonlinear rotor systems, [7] - [10]. For application to large, multi-disk rotor systems, Nataraj and Nelson [6] developed a periodic solution method based on a collocation approach for the response of the rotor. They utilized a subsystem approach to reduce the size of the resulting system of algebraic equations. Ehrich [11] recently analyzed high order subharmonic response and chaos [12] using numerical integration for Jeffcott rotor with a bearing clearance.

Few analysts have addressed the stability of periodic or subharmonic responses of nonlinear rotor systems despite its considerable significance in predicting the response of modern, high performance systems. Most of the stability or bifurcation analyses were concentrated on one dimensional (rectilinear) problems where solution forms are assumed a priori (Shaw and Holmes [13], and Natsiavaas [14]). These approaches are very difficult or not feasible to extend to the two dimensional nonlinear rotor problems.

Complete characterization of the dynamic behavior must include determining the steady state responses and their bifurcation as function of the system parameters. In addition, the transient response of the nonlinear system has to be determined as part of any complete dynamic analysis of the system.

Objectives and Outline of Study

The main objective of this study was to develop reliable and efficient analytical-computational methods of the nonlinear dynamic analysis of large, rotor-housing systems such as the turbopumps of the space shuttle main engines (SSME), and some aspects were then examined to be of the nonlinear behavior of a general multi-disk rotor-housing system.

In the present study, HB (Harmonic Balance)/AFT (Alternating Frequency-Time) method has been developed. Using the method, a study is made of the dynamics and stability of simplified models of the HPOTP (High Pressure Oxygen Turbo Pump) of the SSME (Space Shuttle Main Engine) including clearances between the bearings' outer races and their supports. The method employs an explicit Jacobian form in an iterative procedure which ensures convergence at all parameter values. A dynamic reduction technique [15] is used with the HBM to reduce the system nonlinear differential equations to linear algebraic equations involving only the nonlinear coordinates.

A recently developed convolution approach by the present author for the non-linear transient analysis was carefully tested against direct integration techniques and proved more robust and efficient. Using the HB/AFT method, the response resonances of a multiple-disk rotor as function of the rotor spinning speed (critical speeds) can be located. The convolution approach can then be used effectively to determine the transient response in passing through these critical speeds.

II. ANALYSIS METHODS AND RESULTS

STEADY STATE RESPONSE AND STABILITY

(i) One and Two Dimensional Systems:

The dynamic behavior of strongly nonlinear mechanical systems with piecewise-linear or piecewise-smooth nonlinearities is studied using a newly developed HB (Harmonic Balance) with an AFT (Alternating Frequency Time) robust and efficient algorithm. By employing the harmonic balance approach, the nonlinear differential equations are transformed to nonlinear algebraic equations. Two iterative techniques are available for solving the nonlinear algebraic equations. These are the Newton-Raphson method and a certain version of the Quasi-Newton Algorithm. The Newton-Raphson algorithm requires a laborious and complex calculation of a Jacobian matrix and has a narrow range of initial guesses for achieving convergence. However, the algorithm has superior convergence speed as compared to the corresponding Quasi-Newton method.

The development of the method and its application to an oscillator interacting through a gap with a flexible stop (see Figure 1) can be found in a paper [16], accepted for publication in the Journal of Applied Mechanics of the American Society of Mechanical Engineers (ASME). The method was also applied to a modified Jeffcott rotor model (see Figure 2) supported on bearings, with clearances (see appendix [A] which was also published as a paper in "Nonlinear Dynamics", [17]).

A bifurcation analysis method, based on Flouqet's theory, was also developed for determining the stability of the obtained periodic solutions. For the stability analysis, Poincare mapping is utilized to obtain the fixed points corresponding to the periodic

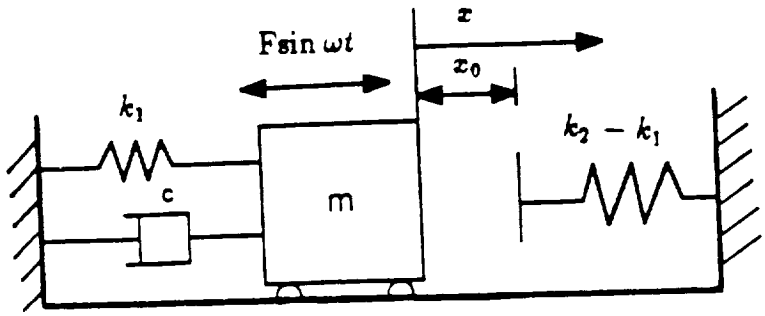

Figure 1-a Oscillator with a gap

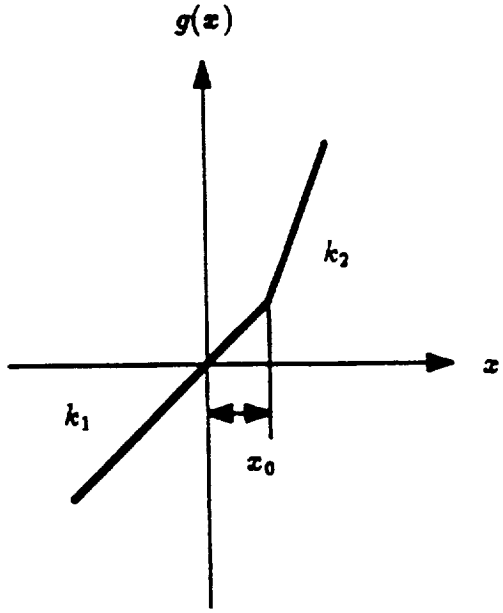

Figure 1-b Piecewise-linear restoring force of oscillator

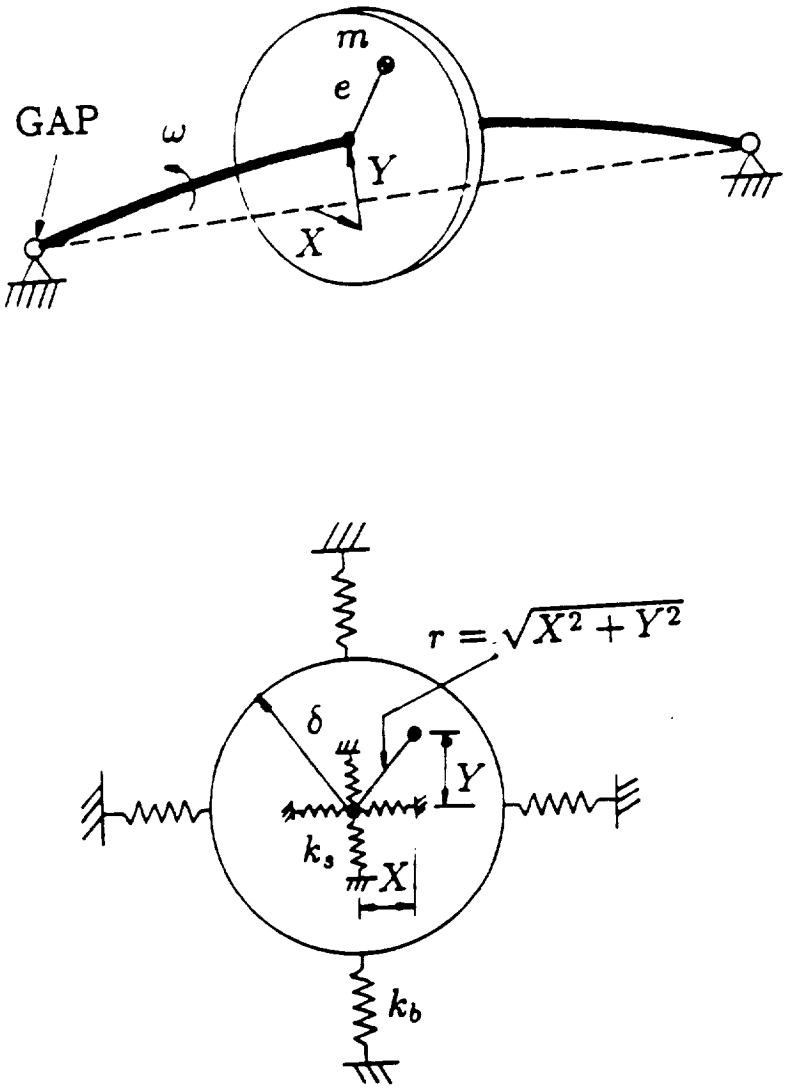

Figure 2. Jeffcott rotor model with a bearing clearance,

solutions (or limit cycles). Small perturbation around the periodic solutions (fixed points) is performed in order to analyze their stability. A first order Jacobian around a fixed point is calculated using numerical integration to obtain the associated monodromy matrix. The eigenvalues of the monodromy matrix are analyzed to determine the bifurcation type (cyclic fold, secondary Hopf or period multiplying).

The bifurcation analysis allows determining ranges of parameters at which the response of a given rotor system would become subsynchronous or chaotic.

(ii) Multi-Disk Rotor Systems

The HB/AFT method was also applied to a two-disk rotor system (see Figure 3) containing a bearing clearance [18,19]. The method generalizes the author's early work [20,21]. Results were obtained for the synchronous, sub-synchronous and chaotic response of the system. The bifurcation analysis developed for this case was also used for predicting the onset of qualitative changes in the dynamic behavior of the system. The extended HB/AFT and bifurcation analysis extended for application to the two-disk rotor system considered, as well as the sample results obtained, are included in Appendix B. The work in this appendix was also accepted for publication in "Nonlinear Dynamics" Journal [18]. A computer program for this case was developed and made available to NASA, Marshall which, if needed, can be readily modified for modeling the turbopumps of the SSME.

NONLINEAR TRANSIENT ANALYSIS

A convolution approach first reported by Noah [22] and Noah, et. al. [23] was further refined and applied to the transient analysis of the generic model shown in Figure 4. A general purpose computer program is written based on this approach, along with a user

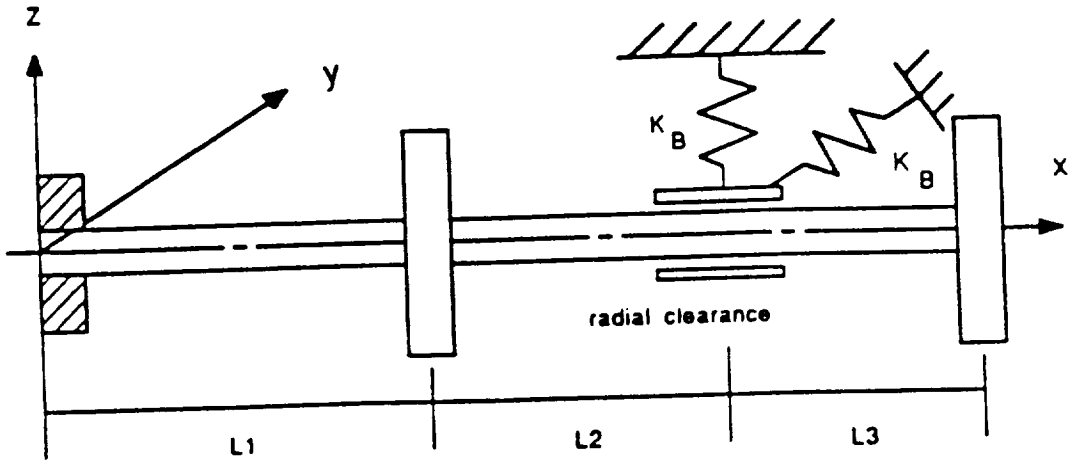

Figure 3. Multi-disk rotor model with a bearing clearance.

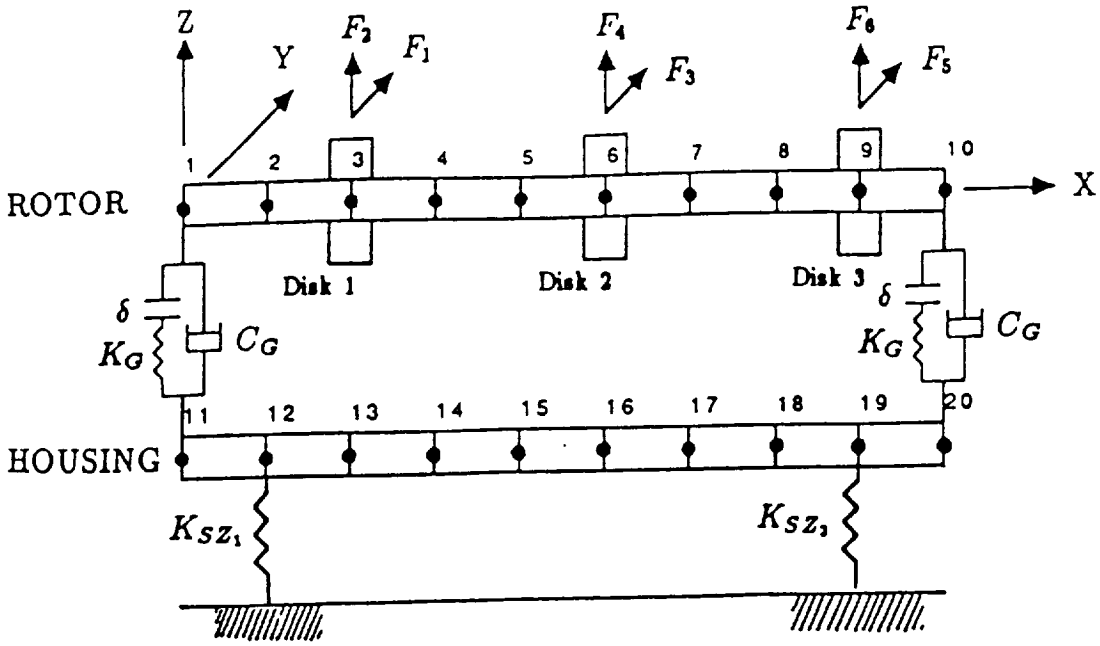

ROTOR: Shaft diameter: OD = 3.0 *inches*, ID = 0.0 *inch*
Material: Steel, $E = 3.0 \times 10^6$ *psi*
Joint length = 3.0 *inches*
Rotor length = 27.0 *inches*

HOUSING: Housing/rotor weight ratio = 6/1

$(EI)_R = 1.1928 \times 10^6$ *lb in*^{3}
$(EI)_H = 2.4 \times 10^6$ *lb in*^{3}

$F_1(t) = m_1 e\dot{\phi}^2 cos\phi t$ $\quad K_{SZ_1} = 4.0 \times 10^4$ *lb/in*
$F_2(t) = m_1 e\dot{\phi}^2 sin\phi t$ $\quad K_{SY_1} = 5.0 \times 10^4$ *lb/in*
$F_3(t) = m_2 e\dot{\phi}^2 cos\phi t$ $\quad K_{SZ_2} = 5.0 \times 10^4$ *lb/in*
$F_4(t) = m_2 e\dot{\phi}^2 sin\phi t$ $\quad K_{SY_2} = 1.5 \times 10^5$ *lb/in*
$F_5(t) = m_3 e\dot{\phi}^2 cos\phi t$ $\quad K_G = 5.0 \times 10^5$ *lb/in*
$F_6(t) = m_3 e\dot{\phi}^2 sin\phi t$ $\quad C_G = 0.0$

Figure 4. The generic model of the SSME turbopump

manual and was provided to NASA, Marshall.

The convolution approach can be applied to a locally nonlinear general rotor housing system with rotor imbalance during start-up or shut-down. In the present work, eigen-coordinates are used to represent both housing and rotor. The local nonlinearities were taken as bearing deadband clearances at the rolling element bearings which support the rotor in its housing. The integral formulation of the rotor motion is represented by its transition matrix and that of the housing by a convolution integral (based on the housing's impulse response).

The convoluted impulse response can only be applied to a system of uncoupled equations while the transition matrix formulation, in addition, can be applied to coupled equations. The transition matrix can therefore be applied to coupled dynamical systems represented by their physical coordinates or, in case of rotors, coupled by the gyroscopic terms in otherwise decoupled modal representation.

Sample of the various tests conducted on the convolution method, to test its accuracy and efficiency, is presented in Figures 5 and 6 for the generic model of Figure 4 under transient loading. It can be seen that the method is more robust and efficient than direct numerical integration.

More complete presentation of the method and the transient response is included in Appendix C. A paper [24] was also published based on this appendix in the ASME Journal of Applied Mechanics.

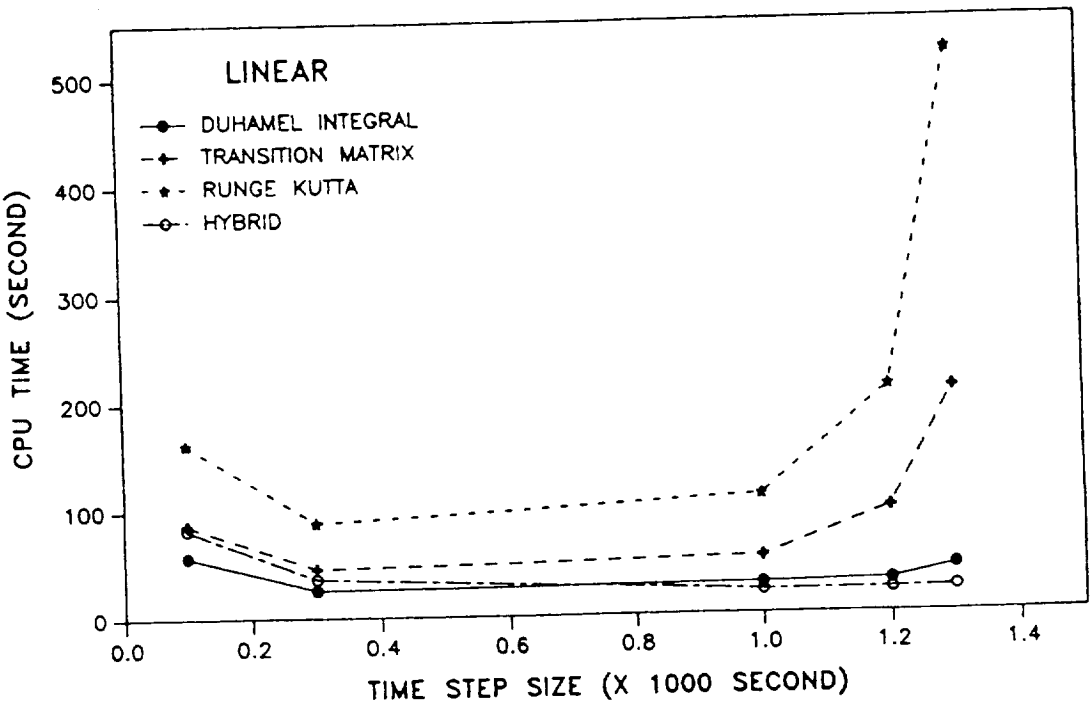

Figure 5. Accuracy of hybrid method and Runge Kutta method

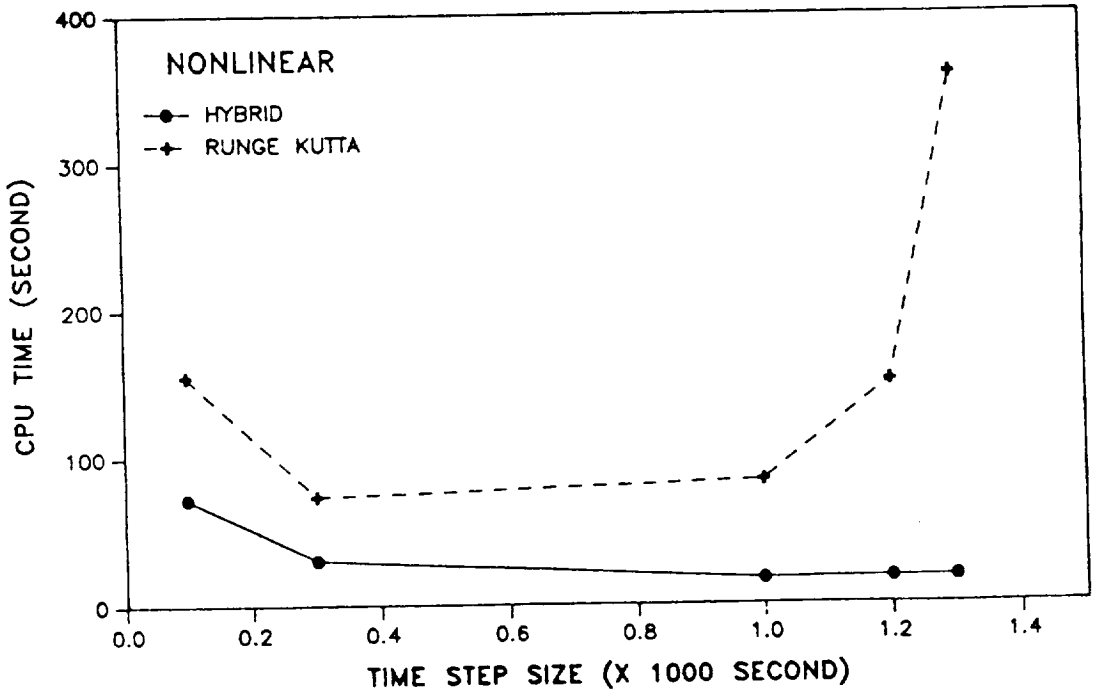

Figure 6. CPU time of hybrid method and Runge Kutta method

III. CONCLUSIONS AND RECOMMENDATIONS

SUMMARY AND CONCLUSIONS

(i) Steady State Analysis:

A robust iterative numerical procedure based on the HBM/AFT method has been developed for obtaining the periodic response of a large rotor/housing system containing bearing clearances. Modern bifurcation theory is utilized to characterize the dynamic behavior of the system. A bifurcation analysis method is developed which provides boundaries of parameter regions at which rotor whirling pattern changes its shape rapidly, resulting in the occurrence of subharmonic, aperiodic or possible chaotic motion.

Results on the effects of parameters on a SDOF (Single Degree of Freedom) system with piecewise-linear response show that, for some combinations of these parameters, the system response exhibits both period doubling and saddle-node bifurcations. Chaotic motion was also observed for finite stiffness ratios. The stability analysis, along with the harmonic balance-based method provide a very powerful tool for better understanding of the behavior of systems with clearances.

The main results obtained using the HBM/AFT approach with a nonlinear Jeffcott rotor[1] with a bearing clearance can be summarized as follows [17]:

1. Increasing the dimensionless support stiffness ratio, $\propto$, causes flip bifurcation to occur which produces period doubled whirling motion (subsynchronous motion).

[1]A Computer program based on this work was submitted to NASA, Marshall.

2. For the same α and a nondimensional frequency ratio, $\acute{\omega}$, an increase in the damping ratio, ς, leads to elimination of the subharmonic motion.

3. With higher values of α, chaotic whirling motion is feasible.

4. Limited results obtained concerning the effect of Coulomb friction indicate that the coefficient of friction, μ, has little effect on the subharmonic response. However, higher μ could eliminate the subharmonics near flip (period doubling) bifurcation boundaries.

5. Increasing the nondimensional cross coupling stiffness ratio γ leads to a Hopf bifurcation which could result in aperiodic whirling.

A further developed HBM, using a DFT (Discrete Fourier Transform)/IDFT (Inverse Discrete Fourier Transform), is employed to obtain the steady-state periodic response for MDOF (multi-degree of freedom) rotor systems with bearing clearances (piecewise-linear type nonlinearity).[2] A dynamic reduction (impedance) technique [15] is utilized to reduce the system to only those of the nonlinear coordinates. The stability analysis is performed via perturbation of the obtained periodic solutions. The reduced and approximated system parameters (mass, damping, and stiffness) are calculated from the determined harmonic coefficients.

A simple MDOF rotor system with a bearing clearance is used for illustration of the method. The results obtained show that: i) the HB/AFT method, as developed here, is robust and efficient; ii) the method leads to accurate bifurcation boundaries for nonlinear MDOF rotor systems and, furthermore; iii) the method can in general be applied to MDOF rotor systems with piecewise-smooth or polynomial type nonlinearities at the bearing

[2]A computer program based on this work was submitted to NASA, Marshall.

supports.

In summary, the major advantages of the HB/AFT approach are:

a) it can provide steady-state periodic solution as well as steady-state quasi-period solutions using modified DFT/IDFT algorithms.

b) its formulation is neither problem nor response pattern dependent, except for selecting the least appropriate numbers of harmonics for the Fourier expansions.

c) it can drastically reduce the computational time while providing high computational accuracy. Especially for nonlinear MDOF systems with lower damping, this approach is much more powerful in delineating the steady-state solutions efficiently.

d) it enables perturbation of the determined periodic solution so that the resulting linear ordinary differential equation with periodic coefficient would yield information about the stability employing Floquet theory. Approximate, but accurate, stability information can then be obtained.

e) using modern dynamical theory, detailed bifurcation boundaries and their type (such as flip, Hopf and fold) can be easily calculated from the perturbed periodic solution as function of the system parameters.

f) by observing the unstable solutions, bifurcation boundaries can be easily obtained as function of system parameters.

(ii) Transient Analysis:

The hybrid convolution approach, further developed in this study, is shown to provide an efficient and accurate closed form integral formulation for determining the transient

response of linear systems coupled through local nonlinearities associated with friction and clearances. A typical application in which the present method proved quite effective is the determination of the transient response of a generic model of the high pressure oxygen turbopump (HPOTP) of a space shuttle main engine (SSME) in presence of bearing clearances (see Appendix C).[3]

The use of the transition matrix is successful in allowing the representation of rotor-system involving skew-symmetric matrices of gyroscopic loads or other nonconservative systems with general velocity dependent matrices. A convolution integral would represent quite effectively other systems with normal modes, such as the housing of the HPOTP or other non-rotating, proportionally damped structures. An application is also made to a generic model of the high pressure oxygen turbopump (HPOTP) of a space shuttle main engine (SSME) in the presence of bearing clearances, constituting the local nonlinearities.

Two iterative techniques, the Jacobi method and the Gauss-Seidel method, were studied. Both were able to correct the predicted coupling forces and converge to the correct force magnitudes with a desired accuracy. The Gauss-Seidel method is more efficient in CPU time especially for a system with large time step and large external forces. For a system with very small external forces, the advantage will not be significant. However, the solution has to be formulated differently so as to accommodate a given type of nonlinear component. If the convolution method is applied to a system with a specific nonlinear component only, Gauss-Seidel scheme could be a better choice. On the other hand, the Jacobi scheme is more flexible in its application. Once the equations of a rotor and its housing are derived, they are ready for use with almost all other types of coupling

[3]A computer program based on this work was submitted to NASA, Marshall.

components.

A generic model of the HPOTP of the SSME was used to test the transient method and conduct parametric studies, typical of nonlinear rotor/housing systems with bearing clearances.

As typical of the effectiveness of the convolution method, firstly, the accuracy and CPU time are studied using both the hybrid convolution approach and Runge Kutta 4th order method. The results show for the given triangular load used in [24] and included in Appendix C that:

1. For a fixed tolerance (1×10^{-8}), the hybrid convolution method is faster and more accurate. The CPU time for the Runge Kutta is 1.42 times of the hybrid method. For more meaningful comparison, the accuracies of the Runge Kutta and convolution methods are made closer by reducing the allowable tolerance for the Runge Kutta to 1×10^{-14}. The CPU time for the Runge Kutta increases quickly from 1.42 times of the hybrid method's CPU to 4.23 times.
2. The hybrid convolution method is also more robust than the Runge Kutta method. The Runge Kutta algorithm failed to converge for time increments greater than 2×10^{-5} seconds. However, the hybrid method will diverge when the time step size is larger than 3.3×10^{-5} seconds.

Secondly, the convolution method is shown to have the potential as a useful tool for determining transient response. For the generic model of the HPOTP, three nonstationary cases have been studied [25]. One is a linear model with no gap. In this case, a closed form solution can be used directly. The other two are nonlinear cases with small and large gaps

(gap size 5×10^{-4} and 1×10^{-3} inches respectively). The gaps are considered as the small and large bearing clearances. The study shows:

1. The reaction force in the deceleration period is much higher than that in the acceleration period. One of the reasons is that the response in the deceleration period has more time to build up since the absolute value of the deceleration is smaller than that of the acceleration.
2. The small gap reduces the approximate first linear critical speed by 9%. However, the large gap reduces the speed by 18%.
3. The small gap reduces the amplitude of the peak bearing forces at the first critical speed of the linear case by 45.2% in bearing 1 and 30.6% in bearing 2. The large gap reduces the amplitude of the peak bearing forces at the first critical speed of the linear case by 49.8% in bearing and 34.9% in bearing 2. The larger gap causes more reduction in peak forces.
4. In contrast to the first critical speed, the second critical speed and its corresponding peak forces in the two bearings in the deceleration period of these three cases are not significantly influenced by the existence or the size of the gap. The average reductions are 0.9% for critical speeds and 2.4% for the corresponding forces.
5. The peak force at the second critical speed is higher than that at the first critical speed. The ratio is 1.78 and 3.94 times in bearings 1 and 2, respectively, for the linear case. For the nonlinear case, the ratios are much higher. For the small gap, the ratios are 3.4 and 5.8 in bearing 1 and 2,

respectively. For the large gap, the ratios are 3.7 and 6.2 in bearing 1 and 2, respectively.

The convolution formulation allows accommodating with ease changes in the nonlinear or linear coupling parameters among the various linear subsystems involved. Besides bearing clearances, other cases of local nonlinearities involving dry friction and impacts were also studied in [25].

RECOMMENDATIONS

The newly devised HB/AFT method proved to be effective in obtaining the steady state solutions for multi-disk rotor systems. Although the impedance (dynamic condensation) method [22,15] is utilized to reduce the systems' equations, the reduction was only possible in physical coordinate systems. In order to adopt the method to generalized coordinate systems, modal representation utilizing a drastically truncated set of modes will be necessary. Further development of the HB/AFT method should be made in order to allow for better reduction techniques in modal coordinates. In addition, the so called internal resonances (in which nonrational relation between the various modes exists) need to be investigated as related to the turbopumps of the SSME.

Further study is needed to complete the development of a preliminary method obtained in this study concerning quasi-periodic response, and to generalize the HB/AFT method to conduct parametric studies on the SSME turbopumps under various operating conditions.

Modern studies have revealed the significance of predicting what is labeled "crisis". This is a generalization of the jump behavior in nonlinear systems. A preliminary study was made and limited results were obtained during the course of the present study. It is recommended that further study be pursued in which the "crisis behavior" in piecewise-smooth systems (specially in applications to rotordynamics) is peculiar. In this connection, the HB/AFT method could prove to be very effective.

For the transient analysis, further work should be made on the analysis and behavior of rotor systems with bearing clearances and rubs. This could include the following:

a. Use approximate methods to replace local nonlinearities with linear

components and then use closed form convolution representation for the solutions.

b. Use other possible iterative techniques, possibly incorporating the Gauss-Seidel technique.

c. Develop other means of increasing the efficiency of the method, including the use of predictor-corrector and other algorithms.

d. Adapt the HB/AFT method to determine domains of attractions of the nonlinear rotor system.

e. Extend the method for application to other local nonlinearities, e.g. Coulomb friction rubs at seals, turbine blades, rotor shrink fits and to impacts due to intermittent contacts.

f. Conduct parametric studies of the turbopumps of the SSME using the current and modified versions of the computer programs provided to NASA, Marshall, developed in this study to examine the significance of the various nonlinear phenomena.

g. Explore the HB/AFT method role in experimental verification, identification, and monitoring of the SSME systems.

Finally, direct comparison should be made of the techniques reported here to those currently used throughout industry. It is anticipated that the techniques described here will yield more information about the dynamic behavior of nonlinear rotor systems in an efficient and systematic manner.

ACKNOWLEDGEMENT

This work was carried out as part of a research project supported by NASA, Marshall Flight Center, under Contract No. NAS8-37465. The authors are grateful to Thomas Fox, the technical monitor, for his enthusiastic support and interest.

REFERENCES

1. Ehrich, F. F., 1966, "Subharmonic Vibrations of Rotors in Bearing Clearances," ASME paper No. 66-MD-1.

2. Bently, D., 1979, "Forced Subrotative Speed Dynamic Action of Rotating Machinery," ASME paper No. 74-PET-16.

3. Muszynska, A., 1984, "Partial Lateral Rotor to Stator Rubs," Proceedings of the Inst. Mech. Engrs. 3rd Intl. Conf. on Vibrations in Rotating Machinery, Univ. of York, 11-13 Sept., pp. 327-335.

4. Beatty, R. F., 1985, "Differentiating Rotor Response Due to Radial Rubbing," (ASME) Journal of Vibration, Acoustics, Stress and Reliability in Design, Vol. 107, pp. 151-160.

5. Neilson, R. D., and Barr, A. D. S., 1988, "Response of Two Elastically Supported Rigid Rotors Sharing a Common Discontinuously Non-linear Support," Proceedings of the Institution of Mechanical Engineers, Heriot-Watt University, 13-15 Sept., pp. 589-598.

6. Nataraj, C. and Nelson, H. D., 1987, "Periodic Solutions in Rotor Dynamic Systems with Nonlinear Supports: A General Approach," American Society Mechanical Engineers Design Conference, October.

7. Yamamoto, T. T., 1954, "On Critical Speeds of a Shaft," Memoirs of the Faculty of Engineering, Nagoya (Japan) University, Vol. 6, No. 2

8. Childs, D. W., 1982, "Fractional-Frequency Rotor Motion due to Nonsymmetric Clearance Effects," ASME Journal of Energy and Power, Vol. 104, pp. 533-541.

9. Saito, S., 1985, "Calculation of Nonlinear Unbalance Response of Horizontal Jeffcott Rotors Supported by Ball Bearings with Radial Clearances," ASME paper No. 85-DET-33.

10. Choi, Y. S. and Noah, S. T., 1987, "Nonlinear Steady-State Response of a Rotor-Support System," ASME Journal of Vibration, Acoustics, Stress and Reliability in Design, Vol. 109, pp. 255-261.

11. Ehrich, F. F., 1988, "High Order Subharmonic Response of High Speed Rotors in Bearing Clearance," ASME Journal of Vibration, Acoustics, Stress and Reliability in Design, Vol. 110, pp. 9-16.

12. Ehrich, F. F., 1990, "Some Observations of Chaotic Vibration Phenomena in High Speed Rotor-Dynamics," accepted for publication in the ASME J. of Vibration and Acoustics.

13. Shaw, S. W. and Holmes, J. P., 1983, "A Periodically Forced Piecewise-Linear Oscillator," Journal of Sound and Vibration, Vol. 108, pp. 129-155.

14. Natsiavas, S., 1989, "Periodic Response and Stability of Oscillators with Symmetric Trilinear Restoring Force. Journal of Sound and Vibration, Vol. 134, pp. 315-331.

15. Fan, U. J. and Noah, S. T., 1990, "Vibration Analysis of Rotor Systems Using Reduced Subsystem Models," AIAA Journal of Propulsion and Power, Vol. 102, pp. 360-368.

16. Kim, Y. B. and Noah, S. T., 1990, "Stability and Bifurcation Analysis of Oscillators with Piecewise-linear Characteristics: A General Approach," accepted for publication in the ASME J. of Applied Mechanics.

17. Kim, Y. B. and Noah, S. T., 1990, "Bifurcation Analysis for a Modified Jeffcott Rotor with a Bearing Clearance," Nonlinear Dynamics Journal, Vol. 1, pp. 221-241. Also presented at the 11th U.S. National Congress of Applied Mechanics, May 21-25, 1990, Universityi of Arizona, Tucson, AZ.

18. Kim, Y. B. and Noah, S. T., 1991, "Response and Bifurcation Analysis of MDOF Rotor System with a Strong Nonlinearity," to appear in Nonlinear Dynamics.

19. Kim, Y. B. and Noah, S. T., 1990, "Bifurcation Analysis for a Multi-Disk Rotor System with Bearing Clearances," presented at the Third Conference on Nonlinear Vibrations, Stability and Dynamics of Structures and Mechanisms, VPI and State University, Blacksburg, VA, June 25-27.

20. Kim, Y. B., Noah, S. T. and Choi, Y. S., 1990, "Periodic Response of Multi Disk Rotors with Bearing Clearances," Journal of Sound and Vibration, Vol. 143, No. 3.

21. Kim, Y. B. and Noah, S. T., 1989, "Steady-State Analysis of a Nonlinear Rotor-Housing System," to appear in ASME Journal of Turbomachinery, also presented at the Gas Turbine and Aeroengine Congress, June 11-14, 1990, Brussel, Belgium. Paper No. 90-GT-328.

22. Noah, S. T., 1986, "Hybrid Methods for Rotordynamic Analysis," Final NASA Report, G. C. Marshall Space Flight Center, Alabama, under contract No. NAS8-36182, December, 1986.

23. Noah, S. T., Chiang, I. F., and Kim, Y. B., 1988, "Dynamic Analysis of Nonlinear Rotor/Housing Systems," MSFC Advanced High Pressure O_2/H_2 Technology Conference Proceedings, G. Marshall Space Flight Center, Huntsville, Alabama.

24. Chiang, I. F. and Noah, S. T., 1990, "A Convolution Approach for the Transient Analysis of Locally Nonlinear Rotor Systems," ASME J. Applied Mechanics. Also presented at the ASME Winter Annual meeting, November, 1990, Dallas, Texas.

25. Chiang, I. F., "Efficient Transient Analysis of Mechanical Systems with Local Nonlinearities," Ph.D. Dissertation, Mechanical Engineering Dept., Texas A&M University, August, 1990.

APPENDIX A

"Bifurcation Analysis for a Modified Jeffcott Rotor with Bearing Clearances," Kim, Y.B. and Noah, S.T., Nonlinear Dynamics, Vol. 1, pp. 221-241, 1990.

Bifurcation Analysis for a Modified Jeffcott Rotor with Bearing Clearances

Y. B. KIM and S. T. NOAH
Mechanical Engineering Department, Texas A&M University, College Station, TX 77843-3123, U.S.A.

Abstract. A HB (Harmonic Balance)/AFT (Alternating Frequency/Time) technique is developed to obtain synchronous and subsynchronous whirling motions of a horizontal Jeffcott rotor with bearing clearances. The method utilizes an explicit Jacobian form for the iterative process which guarantees convergence at all parameter values. The method is shown to constitute a robust and accurate numerical scheme for the analysis of two dimensional nonlinear rotor problems. The stability analysis of the steady-state motions is obtained using perturbed equations about the periodic motions. The Floquet multipliers of the associated Monodromy matrix are determined using a new discrete HB/AFT method. Flip bifurcation boundaries were obtained which facilitated detection of possible rotor chaotic (irregular) motion as parameters of the system are changed. Quasi-periodic motion is also shown to occur as a result of a secondary Hopf bifurcation due to increase of the destabilizing cross-coupling stiffness coefficients in the rotor model.

Key words: Nonlinear, rotor, clearance, chaos.

1. Introduction

Many rotor dynamic systems exhibit nonlinear behavior due to bearing clearances, squeeze film dampers, seals and fluid dynamics effects. Nonlinear rotor systems involving bearing clearances were studied by several investigators. Bently [1] used a simple horizontal rotor model with a bearing clearance to explain the occurrence of subharmonics in his experimental results. Childs [2] used a perturbation technique to study the occurrence of subharmonics, assuming small nonlinearity for the bearing clearance. Saito [3] utilized a harmonic balance method (HBM) along with a fast Fourier transform (FFT) procedure, which was originally used by Yamauchi [4], to explain some nonlinear characteristics in a Jeffcott rotor on nonlinear supports. Choi and Noah [5] also used the HBM with FFT to show the occurrence of super and subharmonics in a rotor in presence of a bearing clearance. In [3] and [5], numerical differentiation was used within each iterative cycle. This did frequently lead to difficulties in getting consistent convergence in all parameter ranges. A numerical approach based on a collocation technique was adopted by Nataraj and Nelson [6] and used to obtain periodic whirling motions in nonlinear rotor systems. In their approach, the calculation of eigenvalues and eigenvectors is required to obtain steady-state rotor whirling motions. This could have the disadvantage of making the numerical process more elaborate and lengthy. Nevertheless, the method appears to be versatile and effective. Ehrich [7] used numerical integration to show the occurrence of higher subharmonics (up to 9th order) in a high speed rotor system with a bearing clearance.

Simulations revealing aperiodic whirling motion were reported by Childs [8]. Day [9] proposed an interpretation involving a 'nonlinear natural frequency' to explain the occurrence of aperiodic motion obtained using the multiple scales method.

Nonlinear Dynamics 1: 221-241, 1990

Few analysts have addressed the stability of periodic or subharmonic responses of nonlinear rotor systems despite its considerable significance in the development and analysis of modern high performance rotor systems. Most of the stability or bifurcation analyses were concentrated on one dimensional problems where motion patterns are assumed apriori (Shaw and Holmes [10] and Natsiavas [11]). These approaches could be proved unfeasible to extend to two dimensional nonlinear rotor problems in which, say, whirling motion involving intermittent contact with a bearing clearance would occur.

This paper addresses the response and stability of a modified Jeffcott rotor system with a discontinuous nonlinearity (bearing clearances). The paper consists of two parts. First, a modified HBM is developed which combines an exact Jacobian matrix and a Galerkin procedure to formulate a robust iterative procedure for determining the periodic solutions. Second, a new approach for the stability analysis of the periodic whirling is developed and applied to conduct bifurcation analysis of the rotor system and search for possible chaotic responses.

Equations of Motion

The equations of motion for a horizontal Jeffcott rotor with bearing clearances (refer to Figure 1) can be written as

$$mX'' + cX' + k_s X + Q_s Y + \Phi k_b X\left(1 - \frac{\delta}{\sqrt{X^2 + Y^2}}\right) - \mu \Phi k_b Y\left(1 - \frac{\delta}{\sqrt{X^2 + Y^2}}\right) = me\omega^2 \cos \omega t\,, \tag{1a}$$

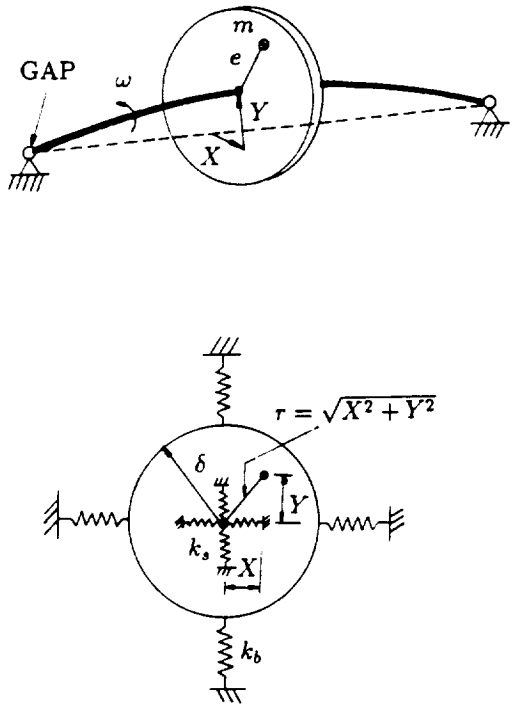

Fig. 1. Jeffcott rotor model with bearing clearances (refer to [7]).

$$mY'' + cY' + k_s Y - Q_s X + \Phi k_b Y\left(1 - \frac{\delta}{\sqrt{X^2 + Y^2}}\right) + \mu \Phi k_b X\left(1 - \frac{\delta}{\sqrt{X^2 + Y^2}}\right)$$
$$= me\omega^2 \sin \omega t - mg \,, \tag{1b}$$

where k_s is the shaft stiffness, Q_s is the cross coupling stiffness, c is the system damping, μ is the friction coefficient, δ is the radial clearance of the bearing. A prime represents a derivative with respect to time t and

$$\Phi = \begin{cases} 1, & \sqrt{X^2 + Y^2} > \delta \,, \\ 0, & \sqrt{X^2 + Y^2} \leq \delta \,. \end{cases}$$

To study the effect of the parameters on the behavior of the system, the following nondimensional groups are introduced: $\omega_n = \sqrt{K/m}$, $K = 4k_s k_b/(\sqrt{k_s} + \sqrt{k_b})^2$, $x = X/e$, $y = Y/e$, $\Omega = \omega/\omega_n$, $\zeta = c/2m\omega_n$, $\gamma = Q_s/K$, $\alpha = k_b/k_s$, $\delta^* = \delta/e$, $\phi = g/\omega_n^2 e$, $r^* = \sqrt{x^2 + y^2}$, and $\nu\theta = \omega t$. Here ν represents the subharmonic ratios. ($\nu = 1$ for harmonic and superharmonic cases, and $\nu = n$ for an nth subharmonic case.) Equation (1) can now be written as

$$\ddot{x} + \frac{2\zeta\nu}{\Omega}\dot{x} + \frac{\nu^2}{\Omega^2}\frac{(1+\sqrt{\alpha})^2}{4\alpha}x + \gamma\frac{\nu^2}{\Omega^2}y + T(\theta) - \mu F(\theta) = \nu^2 \cos \nu\theta \,, \tag{2a}$$

$$\ddot{y} + \frac{2\zeta\nu}{\Omega}\dot{y} + \frac{\nu^2}{\Omega^2}\frac{(1+\sqrt{\alpha})^2}{4\alpha}y - \gamma\frac{\nu^2}{\Omega^2}x + F(\theta) + \mu T(\theta) = \nu^2 \sin \nu\theta - \phi\frac{\nu^2}{\Omega^2} \,, \tag{2b}$$

where a dot represents a derivative with respect to the nondimensional time θ and Φ is unity if r^* is greater than δ^*, otherwise it is zero. $T(\theta)$ and $F(\theta)$ are given by the following expressions.

$$T(\theta) = \Phi\frac{\nu^2}{\Omega^2}\frac{(1+\sqrt{\alpha})^2}{4}x\left(1 - \frac{\delta^*}{\sqrt{x^2 + y^2}}\right),$$

$$F(\theta) = \Phi\frac{\nu^2}{\Omega^2}\frac{(1+\sqrt{\alpha})^2}{4}y\left(1 - \frac{\delta^*}{\sqrt{x^2 + y^2}}\right),$$

where

$$\Phi = \begin{cases} 1, & \sqrt{x^2 + y^2} > \delta^* \,, \\ 0, & \sqrt{x^2 + y^2} \leq \delta^* \,. \end{cases}$$

After reaching the steady-state, and assuming periodic whirl, the solution forms of x and y can be represented as

$$x(\theta) = a_{x0} + \sum_{n=1}^{N} (a_{xn} \cos n\theta - b_{xn} \sin n\theta) \,, \tag{3a}$$

$$y(\theta) = a_{y0} + \sum_{n=1}^{N} (a_{yn} \cos n\theta - b_{yn} \sin n\theta) \,. \tag{3b}$$

The nonlinear restoring forces of $T(\theta)$ and $F(\theta)$ are also expressed as

$$T(\theta) = c_{x0} + \sum_{n=1}^{N} (c_{xn} \cos n\theta - d_{xn} \sin n\theta) , \tag{4a}$$

$$F(\theta) = c_{y0} + \sum_{n=1}^{N} (c_{yn} \cos n\theta - d_{xn} \sin n\theta) . \tag{4b}$$

In equations (3) and (4), N represents the maximum number of harmonic terms considered. Inserting equations (3) and (4) into (2), and equating the coefficients of $\sin(n\theta)$ and $\cos(n\theta)$ on both sides of the equations, one arrives at the following implicitly nonlinear algebraic equations

for the constant series terms

$$g(1) = \frac{\nu^2}{\Omega^2} \frac{(1+\sqrt{\alpha})^2}{4\alpha} a_{x0} + \gamma \frac{\nu^2}{\Omega^2} a_{y0} + c_{x0} - \mu c_{y0} = 0 \tag{5}$$

$$g(2) = \frac{\nu^2}{\Omega^2} \frac{(1+\sqrt{\alpha})^2}{4\alpha} a_{y0} - \gamma \frac{\nu^2}{\Omega^2} a_{x0} + c_{y0} + \mu c_{x0} + \phi \frac{\nu^2}{\Omega^2} = 0 , \tag{6}$$

for the trigonometric series terms

$$g(4n-1) = -n^2 a_{xn} - \frac{2\zeta\nu n}{\Omega} b_{xn} + \frac{\nu^2}{\Omega^2} \frac{(1+\sqrt{\alpha})^2}{4\alpha} a_{xn} + \gamma \frac{\nu^2}{\Omega^2} a_{yn} + c_{xn} - \mu c_{yn} - \Psi(n)\nu^2 = 0 \tag{7}$$

$$g(4n) = n^2 b_{xn} - \frac{2\zeta\nu n}{\Omega} a_{xn} - \frac{\nu^2}{\Omega^2} \frac{(1+\sqrt{\alpha})^2}{4\alpha} b_{xn} - \gamma \frac{\nu^2}{\Omega^2} b_{yn} - d_{xn} + \mu d_{yn} = 0 \tag{8}$$

$$g(4n+1) = -n^2 a_{yn} - \frac{2\zeta\nu n}{\Omega} b_{yn} + \frac{\nu^2}{\Omega^2} \frac{(1+\sqrt{\alpha})^2}{4\alpha} a_{yn} - \gamma \frac{\nu^2}{\Omega^2} a_{xn} + c_{yn} + \mu c_{xn} = 0 \tag{9}$$

$$g(4n+2) = n^2 b_{yn} - \frac{2\zeta\nu n}{\Omega} a_{yn} + \frac{\nu^2}{\Omega^2} \frac{(1+\sqrt{\alpha})^2}{4\alpha} b_{yn} + \gamma \frac{\nu^2}{\Omega^2} b_{xn} - d_{yn} - \mu d_{xn} - \Psi(n)\nu^2 = 0 . \tag{10}$$

In the above equations, $\Psi(n)$ is unity if $n = \nu$, otherwise $\Psi(n)$ has zero value, and $n = 1, 2, \ldots, N$.

Let the unknown vector $\mathbf{P}$ of the displacement coefficients be defined as

$$\mathbf{P} = [a_{x0}, a_{y0}, a_{x1}, b_{x1}, a_{y1}, b_{y1}, \ldots, a_{yN}, b_{yN}]^T \tag{11a}$$

and the unknown restoring vector $\mathbf{Q}$ of the force coefficients be expressed as

$$\mathbf{Q} = [c_{x0}, c_{y0}, c_{x1}, d_{x1}, c_{y1}, d_{y1}, \ldots, c_{yN}, d_{yN}]^T , \tag{11b}$$

where T stands for the transpose. The Newton–Raphson method can be used for this two-dimensional rotor problem to solve for the unknown vectors $\mathbf{P}$ and $\mathbf{Q}$. Alternatively, using equations (5)–(10) another iterative scheme such as the Broyden method [12] can be used to obtain the steady-state solutions in which calculation of the Jacobian matrix would be avoided. Broyden method converges more slowly (usually it requires more iteration steps) but possesses

larger radii of convergence for initial guesses. In this study, Newton–Raphson method is used, since an explicit form of the Jacobian was made available.

Newton–Raphson Approach

Equations (5)–(10) are nonlinear algebraic equations whose solutions yield **P**. A system of linear equations for the correction increments $\Delta\mathbf{P}$ of the unknown coefficients can be written as

$$[J]\Delta\mathbf{P} + \mathbf{G} = 0\,, \tag{12}$$

where $[J] = [\partial\mathbf{G}/\partial\mathbf{P}]$ is the associated Jacobian (matrix of first order derivatives) whose elements are listed in Appendix A, and **G** is a $(4N + 2)$ column vector whose element $g(1), \ldots, g(4n + 2)$ are given by equations (5)–(10).

Using an AFT method [13], the nonlinear force vector **Q** can readily be obtained from the unknown vector **P**. An IDFT is first employed to obtain discrete displacements of x and y from **P** which in turn are used to calculate corresponding discrete values of the nonlinear forces. A DFT procedure is then used to calculate the **Q** vector from these discrete nonlinear forces. As **Q** is a function of **P**, the Jacobian matrix, $[J]$, has the components of $\partial\mathbf{Q}/\partial\mathbf{P}$ which are expressed as

$$\frac{\partial c_{xn}}{\partial a_{xl}} = \frac{1}{M}\sum_{r=0}^{M-1} A_r \cos\frac{2\pi lr}{M}\cos\frac{2\pi nr}{M}\,, \qquad \frac{\partial c_{xn}}{\partial b_{xl}} = -\frac{1}{M}\sum_{r=0}^{M-1} A_r \sin\frac{2\pi lr}{M}\cos\frac{2\pi nr}{M}\,,$$

$$\frac{\partial c_{xn}}{\partial a_{yl}} = -\frac{1}{M}\sum_{r=0}^{M-1} B_r \cos\frac{2\pi lr}{M}\cos\frac{2\pi nr}{M}\,, \qquad \frac{\partial c_{xn}}{\partial b_{yl}} = \frac{1}{M}\sum_{r=0}^{M-1} B_r \sin\frac{2\pi lr}{M}\cos\frac{2\pi nr}{M}\,,$$

$$\frac{\partial d_{xn}}{\partial a_{xl}} = -\frac{1}{M}\sum_{r=0}^{M-1} A_r \cos\frac{2\pi lr}{M}\sin\frac{2\pi nr}{M}\,, \qquad \frac{\partial d_{xn}}{\partial b_{xl}} = \frac{1}{M}\sum_{r=0}^{M-1} A_r \sin\frac{2\pi lr}{M}\sin\frac{2\pi nr}{M}\,,$$

$$\frac{\partial d_{xn}}{\partial a_{yl}} = \frac{1}{M}\sum_{r=0}^{M-1} B_r \cos\frac{2\pi lr}{M}\sin\frac{2\pi nr}{M}\,, \qquad \frac{\partial d_{xn}}{\partial b_{yl}} = -\frac{1}{M}\sum_{r=0}^{M-1} B_r \sin\frac{2\pi lr}{M}\sin\frac{2\pi nr}{M}\,,$$

$$\frac{\partial c_{yn}}{\partial a_{xl}} = -\frac{1}{M}\sum_{r=0}^{M-1} C_r \cos\frac{2\pi lr}{M}\cos\frac{2\pi nr}{M}\,, \qquad \frac{\partial c_{yn}}{\partial b_{xl}} = \frac{1}{M}\sum_{r=0}^{M-1} C_r \sin\frac{2\pi lr}{M}\cos\frac{2\pi nr}{M}\,,$$

$$\frac{\partial c_{yn}}{\partial a_{yl}} = \frac{1}{M}\sum_{r=0}^{M-1} D_r \cos\frac{2\pi lr}{M}\cos\frac{2\pi nr}{M}\,, \qquad \frac{\partial c_{yn}}{\partial b_{yl}} = -\frac{1}{M}\sum_{r=0}^{M-1} D_r \sin\frac{2\pi lr}{M}\cos\frac{2\pi nr}{M}\,,$$

$$\frac{\partial d_{yn}}{\partial a_{xl}} = \frac{1}{M}\sum_{r=0}^{M-1} C_r \cos\frac{2\pi lr}{M}\sin\frac{2\pi nr}{M}\,, \qquad \frac{\partial d_{yn}}{\partial b_{xl}} = -\frac{1}{M}\sum_{r=0}^{M-1} C_r \sin\frac{2\pi lr}{M}\sin\frac{2\pi nr}{M}\,,$$

$$\frac{\partial d_{yn}}{\partial a_{yl}} = -\frac{1}{M}\sum_{r=0}^{M-1} D_r \cos\frac{2\pi lr}{M}\sin\frac{2\pi nr}{M}\,, \qquad \frac{\partial d_{yn}}{\partial b_{yl}} = \frac{1}{M}\sum_{r=0}^{M-1} D_r \sin\frac{2\pi lr}{M}\sin\frac{2\pi nr}{M}\,; \tag{13}$$

$n, l = 1, 2, \ldots, N$, where

$$A_r = \left[\frac{\nu^2}{\Omega^2}\,\frac{(1+\sqrt{\alpha})^2}{4\alpha} - \frac{\nu^2}{\Omega^2}\,\frac{(1+\sqrt{\alpha})^2}{4\alpha}\,\delta^*(x^2+y^2)^{(-3/2)}y^2\right]_r\,,$$

$$B_r = \left[-\frac{\nu^2}{\Omega^2} \frac{(1+\sqrt{\alpha})^2}{4\alpha} \delta^*(x^2+y^2)^{(-3/2)}xy \right]_r ,$$

$$C_r = \left[-\frac{\nu^2}{\Omega^2} \frac{(1+\sqrt{\alpha})^2}{4\alpha} \delta^*(x^2+y^2)^{(-3/2)}xy \right]_r ,$$

$$D_r = \left[\frac{\nu^2}{\Omega^2} \frac{(1+\sqrt{\alpha})^2}{4\alpha} - \frac{\nu^2}{\Omega^2} \frac{(1+\sqrt{\alpha})^2}{4\alpha} \delta^*(x^2+y^2)^{(-3/2)}x^2 \right]_r$$

and M is the total number of discrete data points in the time domain. More details about the calculation procedure can be found in Appendix B.

The procedure of using the Newton–Raphson method to determine a periodic solution can be summed up as follows:

(1) Assume an initial value, $\mathbf{P}^{(0)}$, of the coefficient vector $\mathbf{P}$.
(2) At a given iteration step, evaluate $\mathbf{Q}^{(k)}$ from $\mathbf{P}^{(k)}$ by using the AFT method.
(3) Calculate $[J]$ and $\mathbf{G}$.
(4) Solve equation (12) to determine the correction vector $\Delta\mathbf{P}$.
(5) End iteration if $(\Delta\mathbf{P}^{(k)} - \Delta\mathbf{P}^{(k-1)})$ is within a specified error bound, otherwise set $\mathbf{P}^{(k+1)} = \mathbf{P}^{(k)} + \Delta\mathbf{P}^{(k)}$ and return to step (2). For obtaining possible multiple solutions, different initial guesses could be selected at step (1).

Stability Analysis

One of the advantages of the HBM with an AFT procedure is that it readily provides stability criteria as well as information concerning bifurcation behavior. In rotor systems, stability and bifurcation analysis of a given periodic solution can offer valuable design inputs to avoid sudden change of behavior, irregular (chaotic) motion, and dangerous subsynchronous or supersynchronous vibrations. To investigate the stability behavior of a 2π-periodic solution, eigenvalues of the associated monodromy matrix are utilized [14].

For the stability analysis, the second order nonlinear ordinary differential equations of the present two dimensional problem are perturbed about the determined periodic solution under consideration. This leads to the following perturbed equations

$$\Delta\ddot{x} + \frac{2\zeta\nu}{\Omega}\Delta\dot{x} + \frac{\nu^2}{\Omega^2}\frac{(1+\sqrt{\alpha})^2}{4\alpha}\Delta x + \gamma\frac{\nu^2}{\Omega^2}\Delta y + A\Delta x - B\Delta y + \mu C\Delta x - \mu D\Delta y = 0 , \qquad (14a)$$

$$\Delta\ddot{y} + \frac{2\zeta\nu}{\Omega}\Delta\dot{y} + \frac{\nu^2}{\Omega^2}\frac{(1+\sqrt{\alpha})^2}{4\alpha}\Delta y - \gamma\frac{\nu^2}{\Omega^2}\Delta x - C\Delta x + D\Delta y + \mu A\Delta x - \mu B\Delta y = 0 , \qquad (14b)$$

where A, B, C, and D have the same expressions as given previously. Equations (14) are ordinary differential equations with periodic coefficients, since A, B, C, and D are 2π-*periodic*. Equations (14a) and (14b) are cast in first order form, or

$$\dot{\mathbf{p}} = [u(\theta)]\mathbf{p} , \qquad (15)$$

where $\mathbf{p} = [\Delta x, \Delta y, \Delta\dot{x}, \Delta\dot{y}]^T$, and $[u(\theta)]$ is the matrix defined as

$$[u(\theta)] = \begin{pmatrix} 0 & 0 & 1 & 0 \\ 0 & 0 & 0 & 1 \\ -q_1(\theta) & -q_2(\theta) & \dfrac{-2\zeta\nu}{\Omega} & 0 \\ -q_3(\theta) & -q_4(\theta) & 0 & \dfrac{-2\zeta\nu}{\Omega} \end{pmatrix} \tag{16}$$

and

$$q_1(\theta) = \frac{\nu^2}{\Omega^2}\,\frac{(1+\sqrt{\alpha})^2}{4\alpha} + A + \mu C$$

$$q_2(\theta) = \gamma\,\frac{\nu^2}{\Omega^2} - B - \mu D$$

$$q_3(\theta) = -\gamma\,\frac{\nu^2}{\Omega^2} - C + \mu A$$

$$q_4(\theta) = \frac{\nu^2}{\Omega^2}\,\frac{(1+\sqrt{\alpha})^2}{4\alpha} + D - \mu B\,.$$

Let the monodromy matrix be denoted by $[R]$, and satisfy the following ordinary differential matrix equation

$$[\dot{R}] = [u(\theta)][R]\,; \qquad [R(0)] = [I]\,, \tag{17}$$

where $[I]$ is the identity matrix. Without loss of generality, the initial conditions are assumed as the identity matrix. The monodromy matrix can be calculated by integrating equation (17) numerically from time 0 to one period, 2π. The eigenvalues of the monodromy matrix are the Floquet multipliers which are used to determine the stability of the 2π-periodic solutions as follows, [15],

1. If all the multipliers are located within the unit circle, the system is stable.
2. If one of the multipliers leave the unit circle through -1, this indicates period multiplying bifurcations.
3. If one of the multipliers leaves the unit circle through $+1$, this could indicate bifurcations, possibly including a saddle node.
4. If a pair of complex conjugate multipliers is leaving the unit circle, a Hopf, or a secondary Hopf bifurcation could occur.

Numerical Results and Discussion

Among the seven nondimensional parameters (Ω, ζ, γ, α, δ^*, ϕ, μ), the magnitudes of $\delta^* = 30$ and $\phi = 30 \times$ stiffness $(=(1+\sqrt{\alpha})^2/4\alpha)$ were selected so as to satisfy the condition that the rotor center offset equals to the clearance (normal tightening condition [2]). The other five parameters were varied. The normal tightening condition not only reduces the number of parameter variation effects to be studied, but also fulfills the same whirling motions which were reported experimentally. This condition is necessary for intermittent rotor/bearing contacts to occur, constituting the

main nonlinearity of the system in the y direction. Figures 2, 3, and 4 display the same whirling shapes as obtained by Ehrich [7] within the same parameter ranges, as will be discussed below.

Periodic Response

The accuracy of the HBM/AFT utilizing a Newton–Raphson algorithm (hereafter the HBM/AFT is used to indicate the HBM/AFT with Newton–Raphson for convenience) is compared with numerical integration (4th order Runge–Kutta) as shown in Figures 2, 3 and 4. Figure 2 shows a period-1 whirling orbit at $\Omega = 1.1$. The figure shows very good accuracy of the HBM/AFT. Figures 3, 4 show a period-2 (2nd subharmonic) and a period-3 (3rd subharmonic) whirling response at $\Omega = 2.2$ and $\Omega = 3.2$, respectively. Again, these figures show the HBM/AFT method to be very accurate. Note that small discrepancies in higher subharmonic orbits are due to truncation of higher harmonic terms in the assumed steady state solutions. For the results presented herein, up to 4 harmonic terms were considered which combined good accuracy with high computational efficiency. The other iterative scheme of Broyden also converges to the same orbits as shown in Figures 2, 3, and 4 with comparable accuracy. The major difference between these two methods is that the HBM/AFT converges much faster than the Broyden but requires more narrow domain of

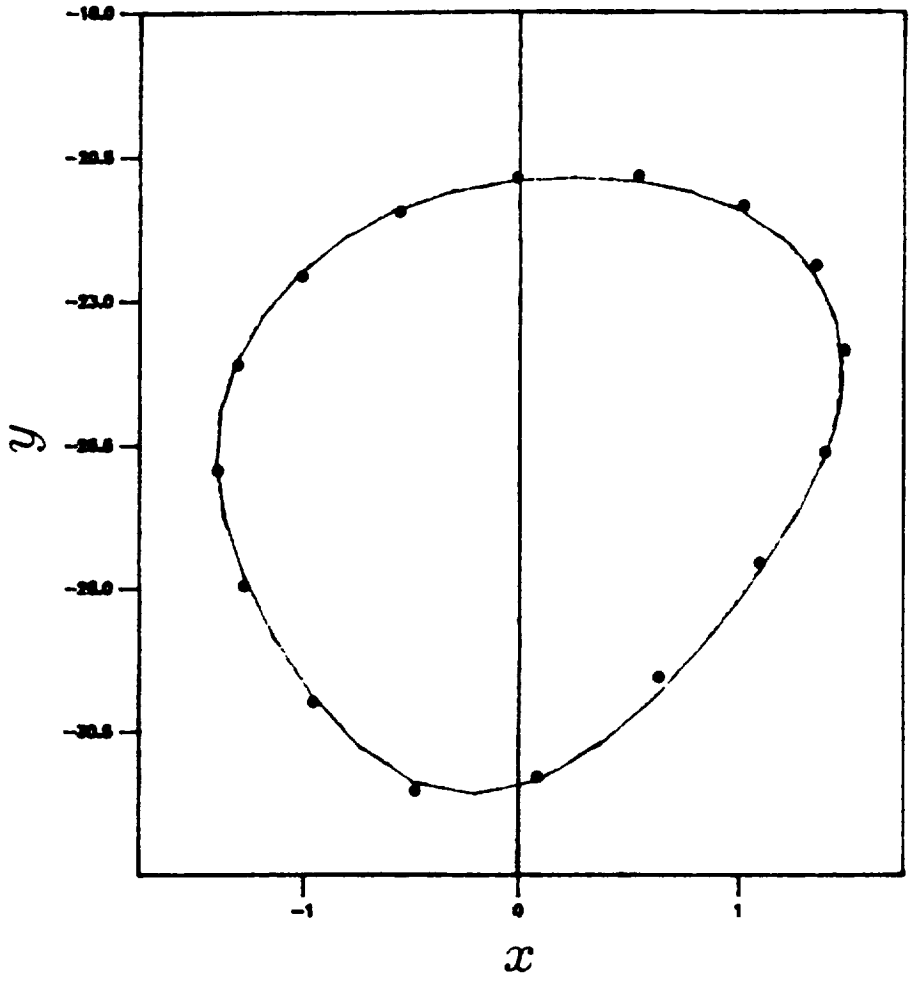

Fig. 2. Orbit-1 whirling motion ($\alpha = 25$, $\zeta = 0.02$, $\Omega = 1.1$, $\gamma = 0$, $\mu = 0$) —HBM; . . . Runge–Kutta.

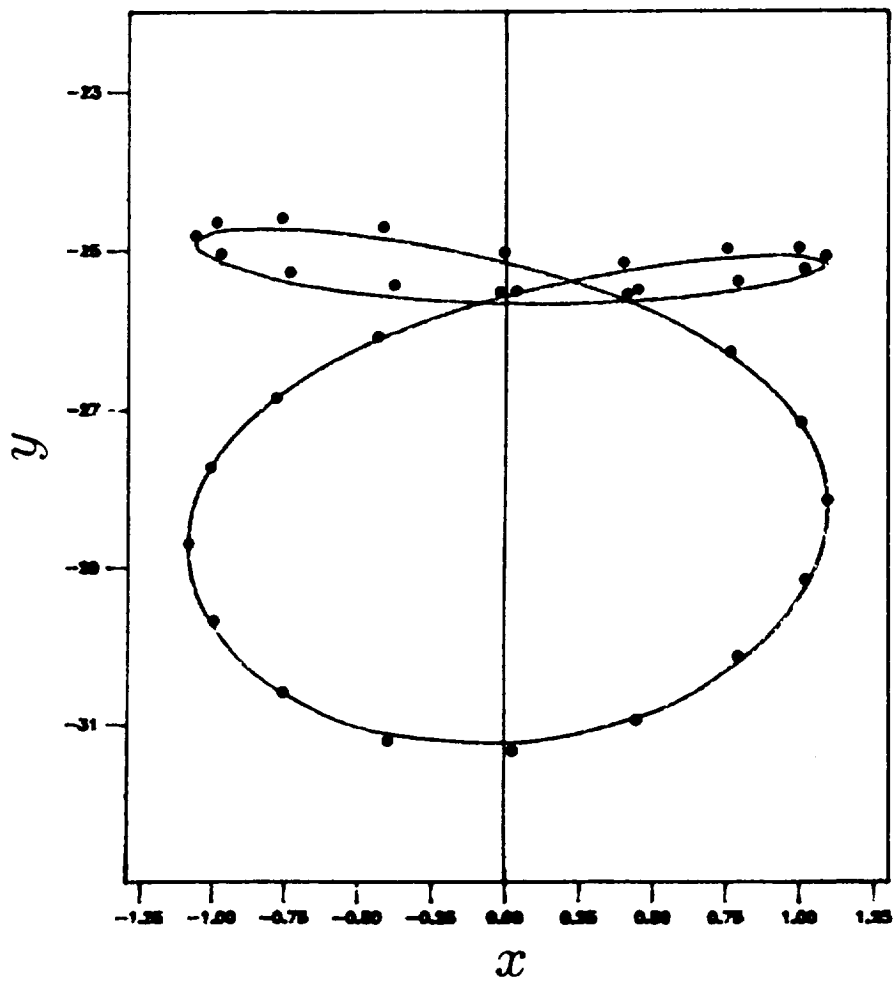

Fig. 3. Orbit-2 whirling motion ($\alpha = 25$, $\zeta = 0.02$, $\Omega = 2.2$, $\gamma = 0$, $\mu = 0$) — HBM; . . . Runge–Kutta.

initial guesses and more complicated formulations involving Jacobian calculation. However, with the HBM/AFT previously calculated results can be used to guess next initial starts for consecutive calculation. It was therefore concluded that the HBM/AFT method constitutes more effective means of obtaining bifurcation boundaries.

Bifurcation Behavior

One of the major advantages of implementing the HBM/AFT method is that it can readily lead to a procedure which yields stability and bifurcation boundaries at which qualitative changes in rotor whirling occur.

First, effects of the magnitudes of the stiffness ratio α and critical damping ζ were investigated. The results show that an increase in α causes period doubling through flip bifurcation. Boundaries between stable period-1 whirling motion and stable period-2 orbits are shown in Figure 5. In this figure, a stable period-1 orbit exists outside of each curve and period-2 orbits exist inside of each curve. This figure also reveals that higher ζ may eliminate dangerous period-2 orbits with the same frequency. This result well agree with previous results [16].

Figure 6 shows the same α and ζ influence on flip bifurcation with $\Omega = 1.6$–3.0. The figure

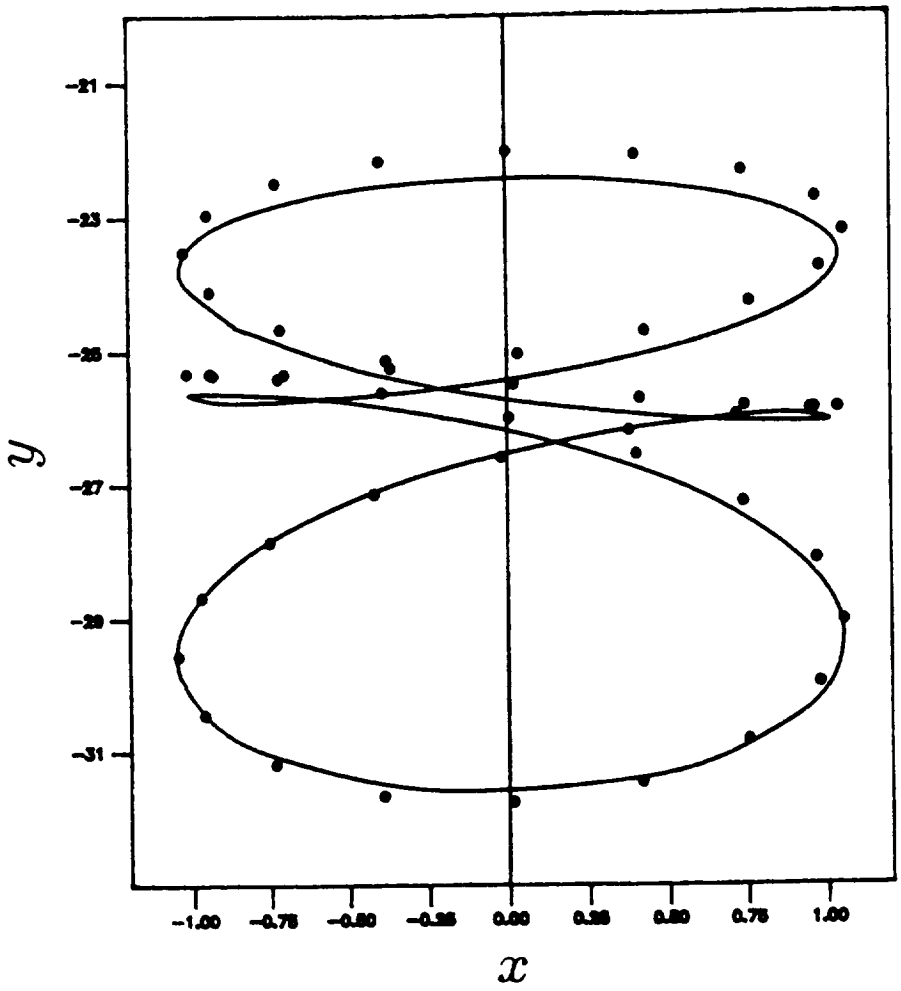

Fig. 4. Orbit-3 whirling motion ($\alpha = 25$, $\zeta = 0.02$, $\Omega = 3.2$, $\gamma = 0$, $\mu = 0$) — HBM; . . . Runge–Kutta.

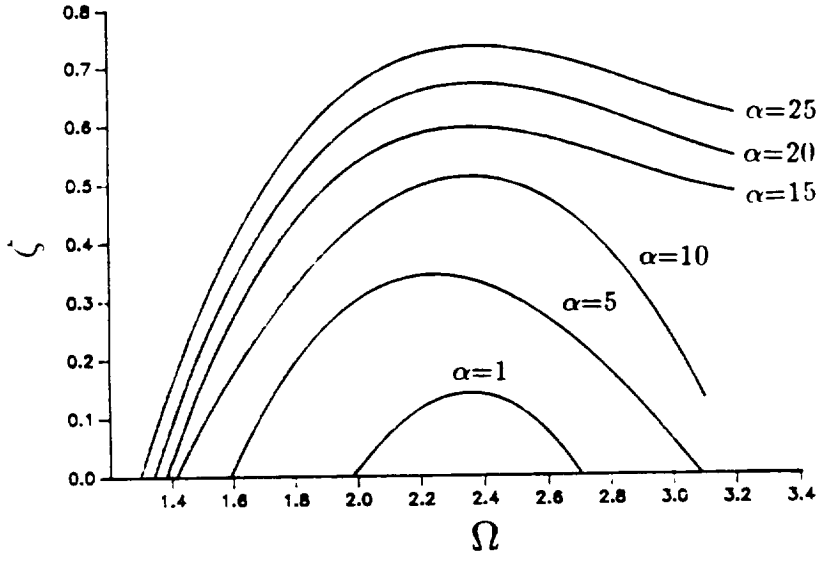

Fig. 5. First flip bifurcation boundaries in $\zeta - \Omega$ plane ($\gamma = 0$, $\mu = 0$).

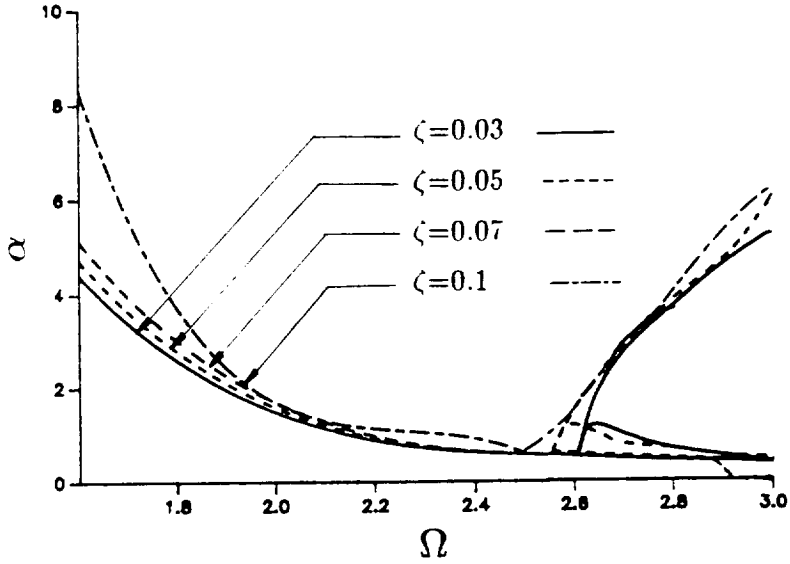

Fig. 6(a). First flip bifurcation boundaries in $\alpha - \Omega$ plane ($\Omega = 1.6$–3.0, $\gamma = 0$, $\mu = 0$).

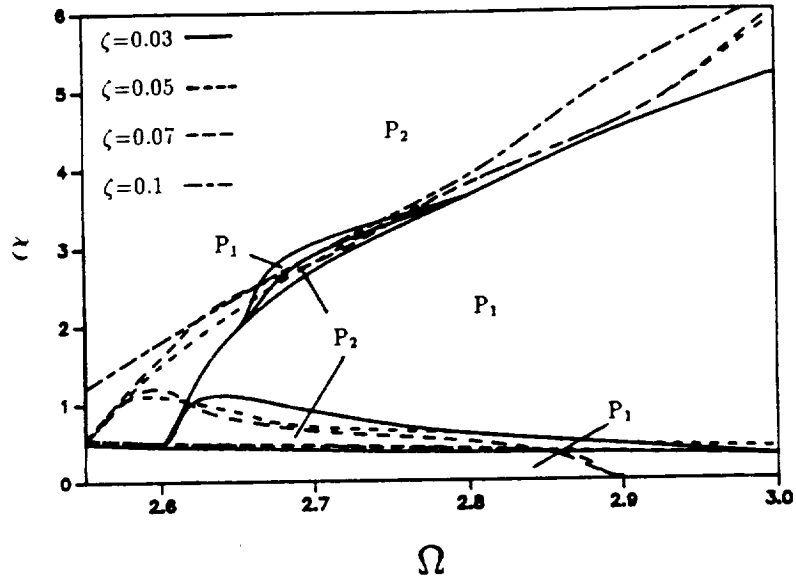

Fig. 6(b). First flip bifurcation boundaries in $\alpha - \Omega$ plane ($\Omega = 2.55$–3.0, $\gamma = 0$, $\mu = 0$); P_1 = period-1 whirling; P_2 = period-2 whirling.

reveals that there are two types of period-2 orbits possible in the range of $\Omega = 2.5$–3.0, since there are two flip boundary branches with fixed Ω. Next, the maximum magnitudes of Floquet multipliers are calculated for $\Omega = 2.7$ for different values of α and ζ as shown in Figure 7. In this figure, there are two types of period-2 orbits (denoted as type A and type B) which are possible with ζ less than 0.1. These two types of period-2 whirling motions are confirmed by numerical integration as shown in Figure 8. Type A response could be considered to be more dangerous since it has larger amplitude. Further increase of α leads to another flip bifurcation (2nd flip bifurcation) as shown in Figure 9. This figure shows a similar ζ effect as that observed in Figure 5. In this figure period-4 orbit exists outside of each curve and period-2 orbit is located inside of each curve. It is interesting to note that at the range of $\Omega = 1.8$–2.2, higher subharmonics are difficult

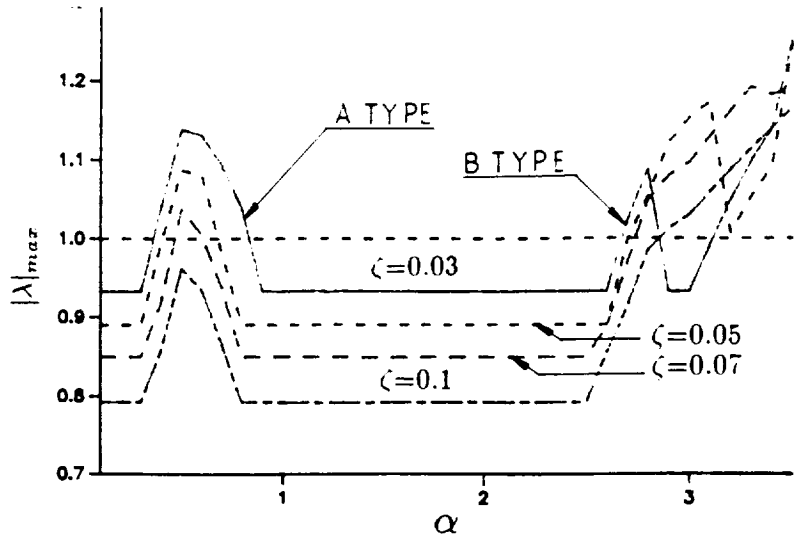

Fig. 7. Maximum magnitude of Floquet mutipliers near 1st flip bifurcation boundaries ($\Omega = 2.7$, $\gamma = 0$, $\mu = 0$).

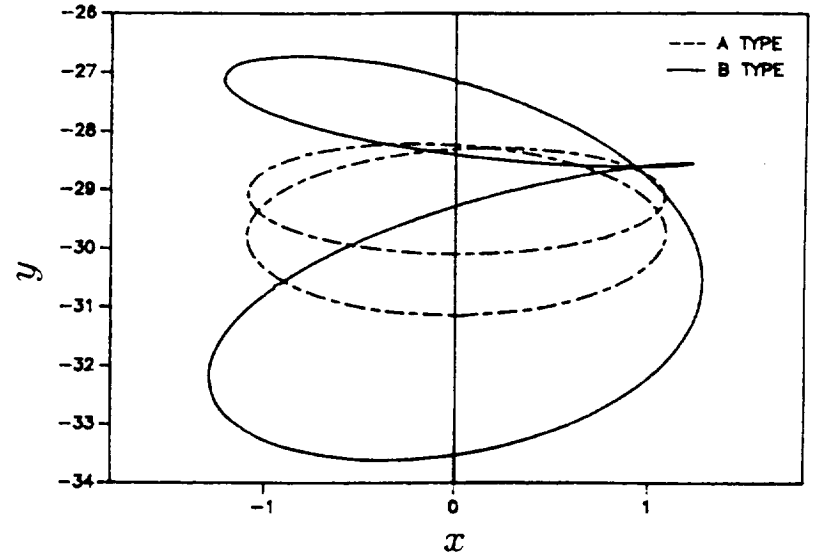

Fig. 8. Two type orbit-2 whiring motion ($\Omega = 2.7$, $\zeta = 0.03$, $\gamma = 0$, $\mu = 0$).

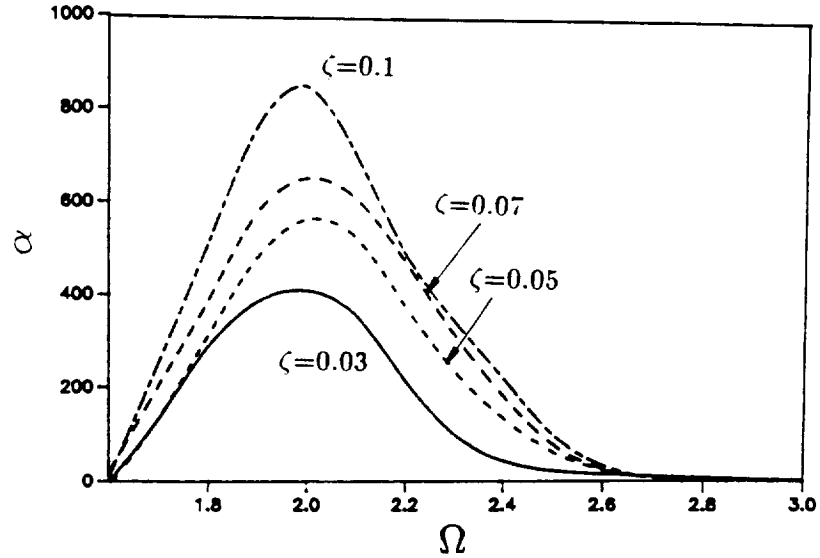

Fig. 9. 2nd flip bifurcation boundaries ($\gamma = 0$, $\mu = 0$).

to obtain unless α has very high value, which approaches an impact condition. From Figure 9 it is predicted that by increasing α, further sequences of period doubling occur leading to irregular (or chaotic) whirling motion of the nonlinear rotor system studied herein. Figures 10 (a)–(c) show this period doubling process at $\Omega = 1.6$. Figure 10 (d) shows chaotic whirling with a high α value. This chaotic motion is quite different from aperiodic whirling motion (which is discussed later). The occurrence of both types of motion is confirmed by stroboscopic snap plots at every forcing period, which is similar to the Poincaré maps in one dimensional problems.

The important characteristics of chaotic motion in the present rotor system are associated with its violent vibration which might cause severe rotor-stator interaction. Chaotic motion is also characterized by a wide-band, continuous frequency content which might lead to adverse conditions of fatigue or excitation of other coupled structures to the rotor. A remedy of this

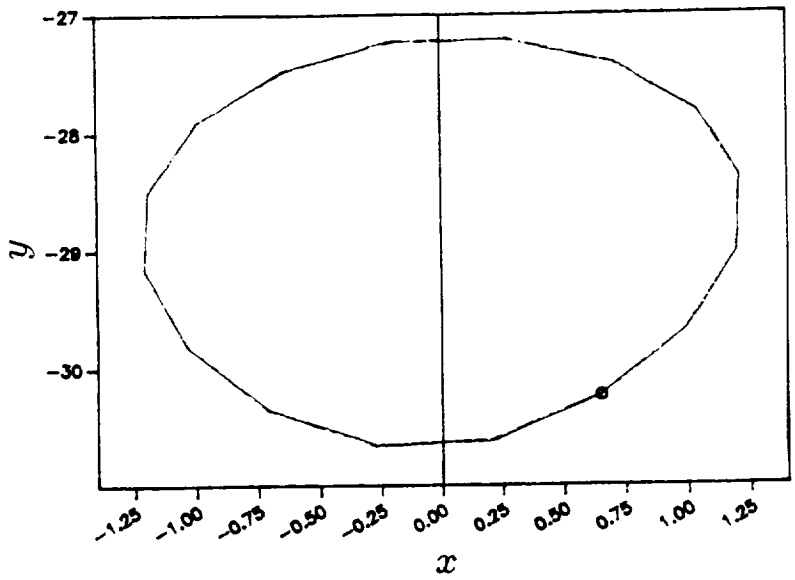

Fig. 10(a). Orbit-1 whirling motion ($\Omega = 1.6$, $\alpha = 10$, $\zeta = 0.1$, $\gamma = 0$, $\mu = 0$).

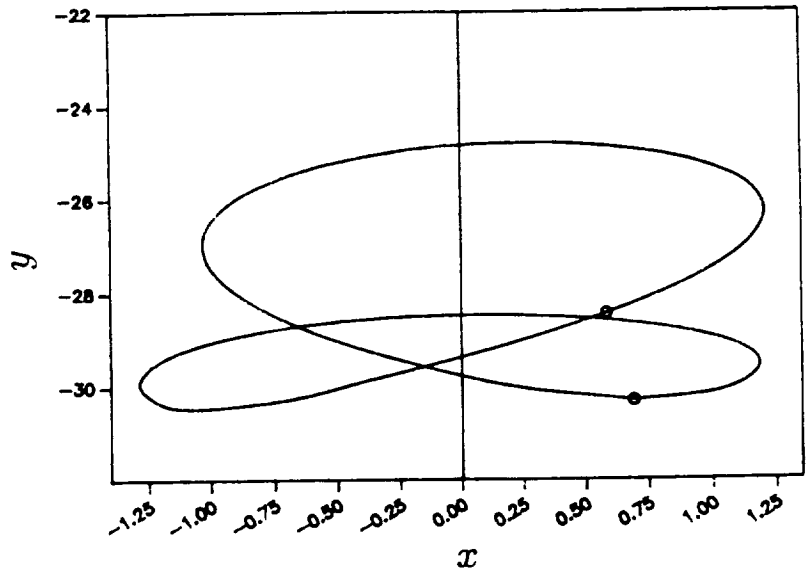

Fig. 10(b). Orbit-2 whirling motion ($\Omega = 1.6$, $\alpha = 40$, $\zeta = 0.1$, $\gamma = 0$, $\mu = 0$).

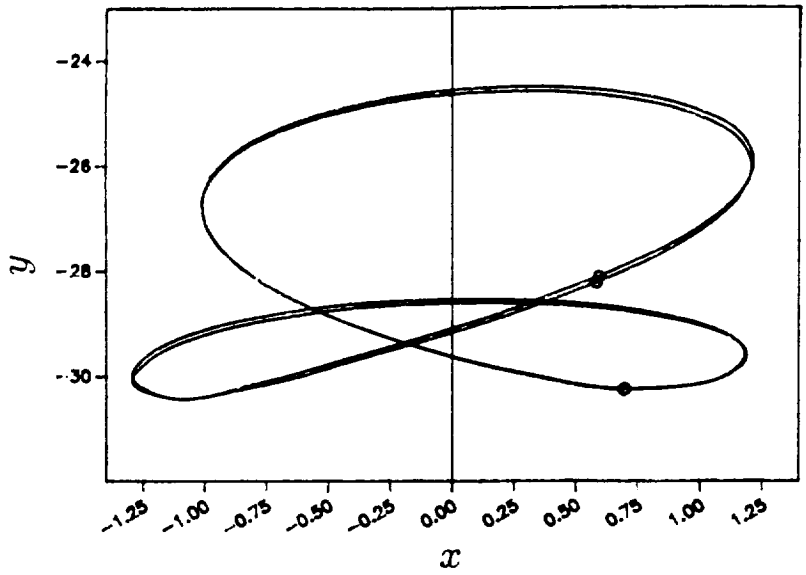

Fig. 10(c). Orbit-4 whirling motion ($\Omega = 1.6$, $\alpha = 50$, $\zeta = 0.1$, $\gamma = 0$, $\mu = 0$).

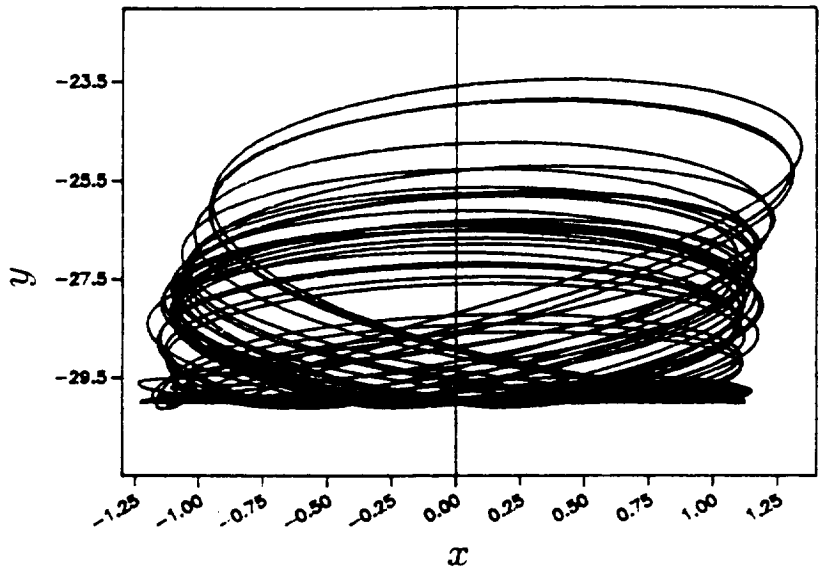

Fig. 10(d). Chaotic whirling motion ($\Omega = 1.6$, $\alpha = 100$, $\zeta = 0.1$, $\gamma = 0$, $\mu = 0$).

situation could be to increase the critical damping or to decrease the shaft-to-support stiffness ratio.

The effect of the friction coefficient, μ, between rotor and stator, is investigated and the results are shown in Figure 11 for $\Omega = 1.5$. The figure shows that higher μ tends to stabilize whirling near the flip bifurcation boundary. However, it is apparent that μ has little effect on the whirling magnitude or stability within stable orbit regions. Figure 12 shows a critical example revealing how μ affects the whirling motion near the first flip bifurcation boundary region. The figure shows that by increasing μ the period-2 orbit becomes period-1 orbit but the whirling amplitude does not change. Therefore, in critical situations, subharmonic vibration could be eliminated by increasing the magnitude of μ.

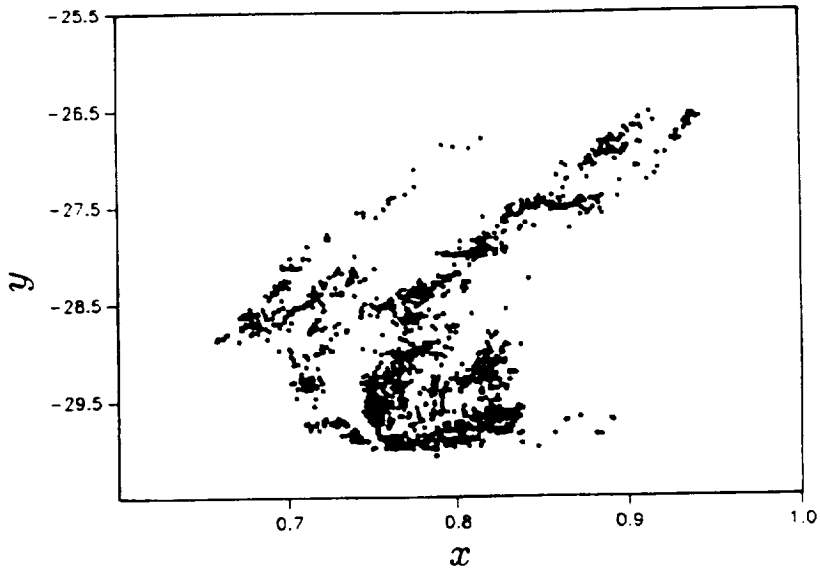

Fig. 10(e). A stroboscopic snap shot of chaotic whirling motion ($\Omega = 1.6$, $\alpha = 100$, $\zeta = 0.1$, $\gamma = 0$, $\mu = 0$).

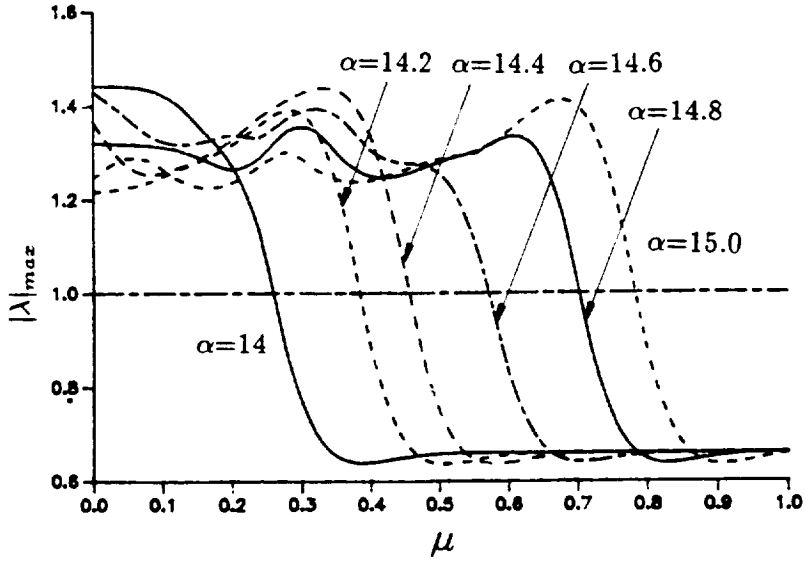

Fig. 11. Maximum magnitude of Floquet multipliers near 1st flip bifurcation boundaries ($\Omega = 1.5$, $\zeta = 0.11$, $\gamma = 0$).

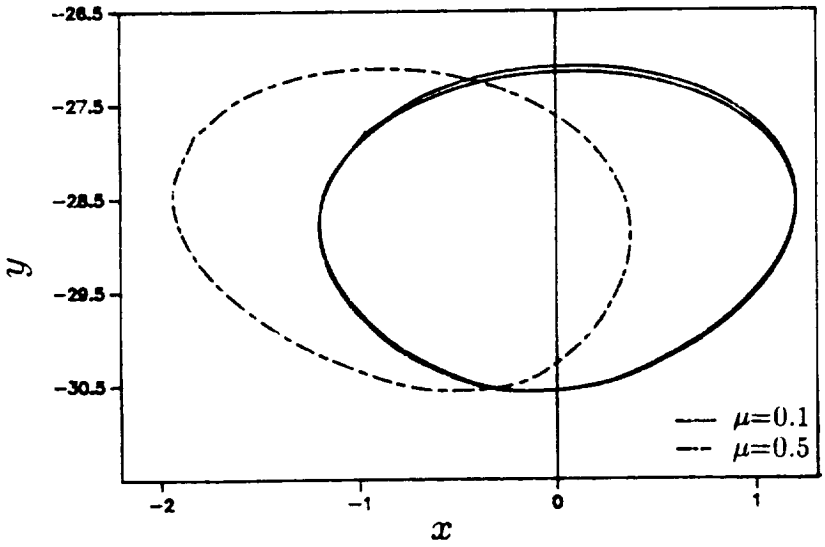

Fig. 12. Effect of μ ($\Omega = 1.5$, $\zeta = 0.11$, $\alpha = 14.4$, $\gamma = 0$) — $\mu = 0.1$; - - - $\mu = 0.5$.

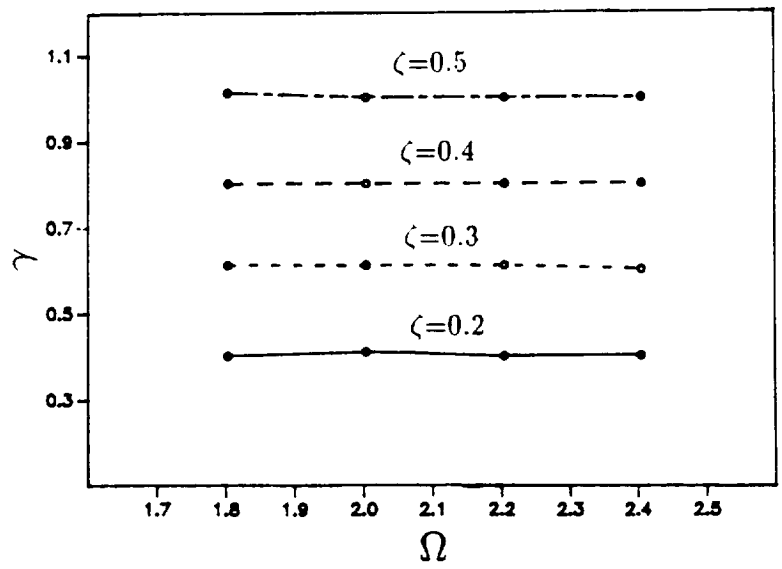

Fig. 13. Hopf bifurcation boundaries ($\alpha = 1$, $\mu = 0$).

Finally the effect of the cross coupling stiffness, γ, is investigated and the results are shown in Figure 13. It is seen that the change in γ results in a different type of bifurcation. A Hopf bifurcation can exist in this case (two complex conjugate multipliers leave the unit circle while the other two remain inside of the unit circle). In Figure 13, the period-1 orbit exists below each line and a Hopf bifurcation occurs above that line. A Hopf bifurcation produces aperiodic (or quasi-periodic) motion as shown in Figure 14. The figure shows that the aperiodic motion has two different frequency components (which are incommensurate) and much larger whirling amplitude than the period-1 orbit.

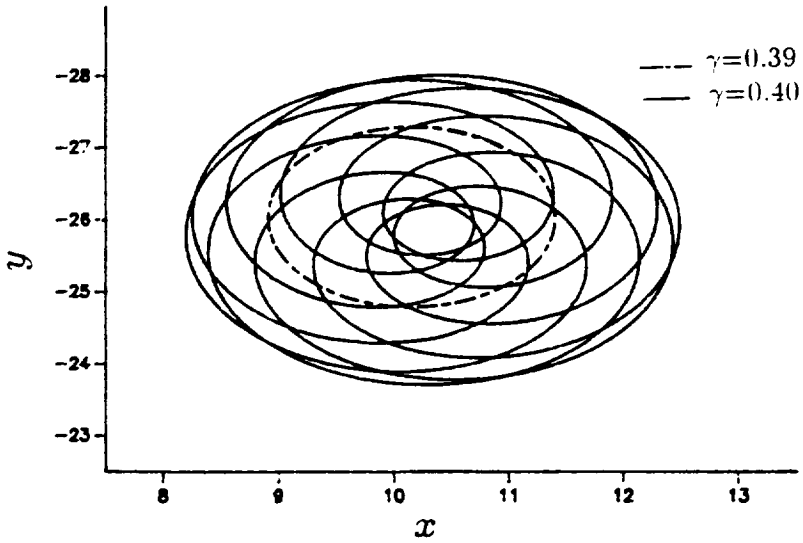

Fig. 14(a). Aperiodic whirling motion due to Hopf bifurcation ($\alpha = 1$, $\mu = 0$) --- $\gamma = 0.39$; — $\gamma = 0.40$.

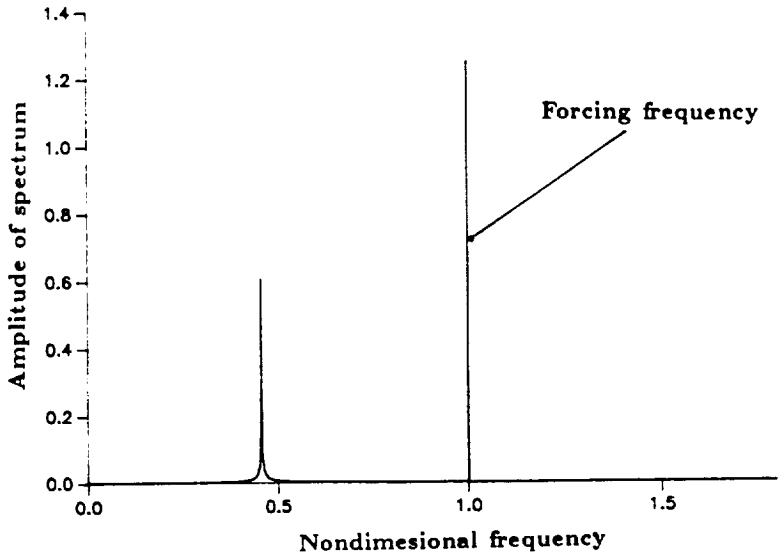

Fig. 14(b). Power spectrum of aperiodic whirling motion ($\alpha = 1$, $\mu = 0$, $\gamma = 0.40$).

Conclusion

A robust iterative numerical procedure based on the HBM/AFT method has been presented for obtaining the periodic responses of a rotor system on nonlinear supports. Modern bifurcation theory is utilized to characterize the dynamic behavior of the system. A bifurcation analysis method is developed which provides boundaries of parameter regions at which rotor whirling change its shape rapidly, resulting in the occurrence of subharmonic, aperiodic or possible chaotic motion.

The results of this study lead to the following observations concerning the dynamic behavior of the nonlinear, modified Jeffcott rotor model considered herein as function of its dimensionless parameters:

1. Increasing the bearing to shaft stiffness ratio, α, increases the degree of nonlinearity which makes it possible for a flip bifurcation to occur, possibly producing a sequence of period doubling motions.
2. For the same α and Ω, an increase in ζ leads to elimination of the subharmonic motion.
3. With high values of α, occurrence of chaotic whirling motion is possible. This follows from (1).
4. For the parameters considered herein, the coefficient of friction, μ, has little effect on the subharmonic response. However, higher μ could eliminate the subharmonics near existing flip bifurcation boundaries.
5. Increasing the cross coupling coefficient, γ, could cause a Hopf bifurcation to occur which may lead to aperiodic whirling. A more systematic investigation of the quasi-periodic response of nonlinear rotor systems is needed. A nonzero value of γ is necessary for the occurrence of aperiodic solution. This is since in this case a limit cycle can exist in absence of imbalance forces. A quasi-periodic response then occurs in presence of an imbalance force involving a frequency related to that of the limit cycle and the forcing frequency, or rotational speed of the shaft.

Acknowledgement

This work was carried out as part of a research project supported by NASA, Marshall Flight Center under contract No. NAS8-37465. The authors are grateful to Thomas Fox, the technical monitor, for his enthusiastic support and interest.

Appendix A

Elements of the Jacobian matrix, $[J]$

$$J_{4n-1,4n-1} = \frac{\partial g_{4n-1}}{\partial a_{xn}} = -n^2 + t_1 + \frac{\partial c_{xn}}{\partial a_{xn}} - \mu \frac{\partial c_{yn}}{\partial a_{xn}}$$

$$J_{4n-1,4n} = \frac{\partial g_{4n-1}}{\partial b_{xn}} = -nt_2 + \frac{\partial c_{xn}}{\partial b_{xn}} - \mu \frac{\partial c_{yn}}{\partial b_{xn}}$$

$$J_{4n-1,4n+1} = \frac{\partial g_{4n-1}}{\partial a_{yn}} = t_3 + \frac{\partial c_{xn}}{\partial a_{yn}} - \mu \frac{\partial c_{yn}}{\partial a_{yn}}$$

$$J_{4n-1,4n+2} = \frac{\partial g_{4n-1}}{\partial b_{yn}} = \frac{\partial c_{xn}}{\partial b_{yn}} - \mu \frac{\partial c_{yn}}{\partial b_{yn}}$$

$$J_{4n,4n-1} = \frac{\partial g_{4n}}{\partial a_{xn}} = -nt_2 - \frac{\partial d_{xn}}{\partial a_{xn}} + \mu \frac{\partial d_{yn}}{\partial a_{xn}}$$

$$J_{4n,4n} = \frac{\partial g_{4n}}{\partial b_{xn}} = n^2 - t_1 - \frac{\partial d_{xn}}{\partial b_{xn}} + \mu \frac{\partial d_{yn}}{\partial b_{xn}}$$

$$J_{4n,4n+1} = \frac{\partial g_{4n}}{\partial a_{yn}} = -\frac{\partial d_{xn}}{\partial a_{yn}} + \mu \frac{\partial d_{yn}}{\partial a_{yn}}$$

$$J_{4n,4n+2} = \frac{\partial g_{4n}}{\partial b_{yn}} = -t_3 - \frac{\partial d_{xn}}{\partial b_{yn}} + \mu \frac{\partial d_{yn}}{\partial b_{yn}}$$

$$J_{4n+1,4n-1} = \frac{\partial g_{4n+1}}{\partial a_{xn}} = -t_3 + \frac{\partial c_{yn}}{\partial a_{xn}} + \mu \frac{\partial c_{xn}}{\partial a_{xn}}$$

$$J_{4n+1,4n} = \frac{\partial g_{4n+1}}{\partial b_{xn}} = +\frac{\partial c_{yn}}{\partial b_{xn}} + \mu \frac{\partial c_{xn}}{\partial b_{xn}}$$

$$J_{4n+1,4n+1} = \frac{\partial g_{4n+1}}{\partial a_{yn}} = -n^2 + t_1 + \frac{\partial c_{yn}}{\partial a_{yn}} + \mu \frac{\partial c_{xn}}{\partial a_{yn}}$$

$$J_{4n+1,4n+2} = \frac{\partial g_{4n+1}}{\partial b_{yn}} = -nt_2 + \frac{\partial c_{yn}}{\partial b_{yn}} + \mu \frac{\partial c_{xn}}{\partial b_{yn}}$$

$$J_{4n+2,4n-1} = \frac{\partial g_{4n+2}}{\partial a_{xn}} = -\frac{\partial d_{yn}}{\partial a_{xn}} - \mu \frac{\partial d_{xn}}{\partial a_{xn}}$$

$$J_{4n+2,4n} = \frac{\partial g_{4n+2}}{\partial b_{xn}} = t_3 - \frac{\partial d_{yn}}{\partial b_{xn}} - \mu \frac{\partial d_{xn}}{\partial b_{xn}}$$

$$J_{4n+2,4n+1} = \frac{\partial g_{4n+2}}{\partial a_{yn}} = -nt_2 - \frac{\partial d_{yn}}{\partial a_{yn}} - \mu \frac{\partial d_{xn}}{\partial a_{yn}}$$

$$J_{4n+2,4n+2} = \frac{\partial g_{4n+2}}{\partial b_{yn}} = n^2 - t_1 - \frac{\partial d_{yn}}{\partial b_{yn}} - \mu \frac{\partial d_{xn}}{\partial b_{yn}}$$

where

$$t_1 = \frac{\nu^2}{\Omega^2} \frac{(1+\sqrt{\alpha})^2}{4\alpha}, \qquad t_2 = \frac{2\zeta\nu}{\Omega}, \qquad t_3 = \gamma \frac{\nu^2}{\Omega^2}.$$

Appendix B

Calculation of elements of $[J]$

Using

$$T(x, y) = \Phi \frac{\nu^2}{\Omega^2} \frac{(1+\sqrt{\alpha})^2}{4} x\left(1 - \frac{\delta^*}{\sqrt{x^2+y^2}}\right) \tag{B1}$$

$$F(x, y) = \Phi \frac{\nu^2}{\Omega^2} \frac{(1+\sqrt{\alpha})^2}{4} y\left(1 - \frac{\delta^*}{\sqrt{x^2+y^2}}\right) \tag{B2}$$

the incremental form is expressed as

$$\Delta T(x, y) = \left(\frac{\partial T}{\partial x}\Delta x + \frac{\partial T}{\partial y}\Delta y\right) = A\Delta x - B\Delta y \tag{B3}$$

$$\Delta F(x, y) = \left(\frac{\partial N}{\partial x}\Delta x + \frac{\partial N}{\partial y}\Delta y\right) = -C\Delta x + D\Delta y \tag{B4}$$

where

$$A = \Phi \frac{\nu^2}{\Phi^2}\left\{\frac{(1+\sqrt{\alpha})^2}{4} - \frac{(1+\sqrt{\alpha})^2}{4}\delta^*(x^2+y^2)^{-3/2}y^2\right\}$$

$$B = -\Phi \frac{\nu^2}{\Omega^2}\left\{\frac{(1+\sqrt{\alpha})^2}{4}\delta^*(x^2+y^2)^{-3/2}xy\right\}$$

$$C = -\Phi \frac{\nu^2}{\Omega^2}\left\{\frac{(1+\sqrt{\alpha})^2}{4}\delta^*(x^2+y^2)^{-3/2}xy\right\}$$

$$D = \Phi \frac{\nu^2}{\Omega^2}\left\{\frac{(1+\sqrt{\alpha})^2}{4} - \frac{(1+\sqrt{\alpha})^2}{4}\delta^*(x^2+y^2)^{-3/2}x^2\right\}.$$

Also, the Δx and Δy are

$$\Delta x = \frac{\partial x}{\partial a_{x0}}\Delta a_{x0} + \sum_{n=1}^{N}\left(\frac{\partial x}{\partial a_{xn}}\Delta a_{xn} - \frac{\partial x}{\partial b_{xn}}\Delta b_{xn}\right) = \Delta a_{x0} + \sum_{n=1}^{N}(\Delta a_{xn}\cos n\theta - \Delta b_{xn}\sin n\theta), \tag{B5}$$

$$\Delta y = \frac{\partial y}{\partial a_{x0}} \Delta a_{y0} + \sum_{n=1}^{N} \left(\frac{\partial y}{\partial a_{yn}} \Delta a_{yn} - \frac{\partial y}{\partial b_{yn}} \Delta b_{yn} \right) = \Delta a_{y0} + \sum_{n=1}^{N} (\Delta a_{yn} \cos n\theta - \Delta b_{yn} \sin n\theta) . \tag{B6}$$

Similarly, from equation (4), ΔT and ΔF can be expressed as

$$\Delta T = \Delta c_{x0} + \sum_{n=1}^{N} (\Delta c_{xn} \cos n\theta - \Delta d_{xn} \sin n\theta) , \tag{B7}$$

$$\Delta F = \Delta c_{y0} + \sum_{n=1}^{N} (\Delta c_{yn} \cos n\theta - \Delta d_{yn} \sin n\theta) , \tag{B8}$$

From equations (B3), (B4), (B7) and (B8), and using Galerkin's method, one can get the following expressions for determining the elements of $[J]$. (The utilization of Galerkin's method rather than DFT and IDFT makes it much easier to obtain the $\partial \mathbf{Q}/\partial \mathbf{P}$ for the present two dimensional system.)

$$\begin{aligned}
&\int_0^T A\left\{\Delta a_{x0} + \sum_{n=1}^{N} (\Delta a_{xn} \cos n\theta - \Delta b_{xn} \sin n\theta)\right\}\{\cos\theta, \ldots, \sin\theta\}^T \, d\theta \\
&- \int_0^T B\left\{\Delta a_{y0} + \sum_{n=1}^{N} (\Delta a_{yn} \cos n\theta - \Delta b_{yn} \sin n\theta)\right\}\{\cos\theta, \ldots, \sin n\theta\}^T \, d\theta = \\
&\int_0^T A\left\{\Delta c_{x0} + \sum_{n=1}^{N} (\Delta c_{xn} \cos n\theta - \Delta d_{xn} \sin n\theta)\right\}\{\cos\theta, \ldots, \sin n\theta\}^T \, d\theta ,
\end{aligned} \tag{B9}$$

$$\begin{aligned}
&- \int_0^T C\left\{\Delta a_{x0} + \sum_{n=1}^{N} (\Delta a_{xn} \cos n\theta - \Delta b_{xn} \sin n\theta)\right\}\{\cos\theta, \ldots, \sin n\theta\}^T \, d\theta \\
&+ \int_0^T D\left\{\Delta a_{y0} + \sum_{n=1}^{N} (\Delta a_{yn} \cos n\theta - \Delta b_{yn} \sin n\theta)\right\}\{\cos\theta, \ldots, \sin n\theta\}^T \, d\theta = \\
&\int_0^T A\left\{\Delta c_{y0} + \sum_{n=1}^{N} (\Delta c_{yn} \cos n\theta - \Delta d_{yn} \sin n\theta)\right\}\{\cos\theta, \ldots, \sin n\theta\}^T \, d\theta ,
\end{aligned} \tag{B10}$$

where the upper limit of integration, T, is 2π. Using equations (B9), (B10), the first derivatives, $\partial \mathbf{Q}/\partial \mathbf{P}$, for the Jacobian matrix are obtained as listed in equations (13) in text.

References

1. Bently, D., 'Forced subrotative speed dynamic action of rotating machinery', *ASME* paper No. 74-PET-16; *Petroleum Mechanical Engineering Conference*, Dallas, Texas, 1974.
2. Childs, D. W., 'Fractional-frequency rotor motion due to nonsymmetric clearance effects', *ASME Journal of Energy and Power* **104**, 1982, 533–541.
3. Saito, S., 'Calculation of nonlinear unbalance response of horizontal Jeffcott rotors supported by ball bearings with radial clearances', *ASME paper No. 85-DET-33*, 1985.
4. Yamauchi, S., 'The nonlinear vibration of flexible rotors, 1st report, Development of a new analysis technique', *JSME* **49**, No. 446, Series C, 1983, 1862–1868.
5. Choi, Y. S. and S. T. Noah, 'Nonlinear steady-state response of a rotor-support system', *ASME Journal of Vibration, Acoustics, Stress, and Reliability in Design* **109**, 1987, 255–261.

6. Nataraj, C. and H. D. Nelson, 'Periodic solutions in rotor dynamic systems with nonlinear supports: A general approach', *ASME Design Conference*, Oct. 1987.
7. Ehrich, F. F., High order subharmonic response of high speed rotors in bearing clearance', *ASME Journal of Vibration, Acoustics, Stress, and Reliability in Design* **110**, 1988, 9–16.
8. Childs, D. W., 'Rotordynamic characteristics of the HPOTP (High Pressure Oxygen Turbopump) of the SSME (Space Shuttle Main Engine)', Turbomachinery Laboratories Report (Texas A&M Univ.) FD-1-84, 1984.
9. Day, W.B., 'Asymptotic expansions in nonlinear rotordynamics', *Quarterly of Applied Mathematics* **44**, 1987, 779–792.
10. Shaw, S. W. and J. P. Holmes, 'A periodically forced piecewise-linear oscillator', *Journal of Sound and Vibration* **108**, 1983, 129–155.
11. Natsiavas, S., 'Periodic response and stability of oscillators with symmetric trilinear restoring force', *Journal of Sound and Vibration* **134**, 1989, 315–331.
12. Dennis, Jr., J. E., and J. J. More, 'Quasi-Newton method, motivation and theory', *SIAM Review* **19**, 1977, 46–88.
13. Kim, Y. B. and Noah, S. T., 'Stability and bifurcation analysis of oscillators with piecewise-smooth characteristics: A general approach', accepted for publication in ASME *J. of Applied Mechanics*, 1990.
14. Hale, J. K., *Oscillators in Nonlinear Systems*, McGraw-Hill, New York, 1963.
15. Guckenheimer J and J. P. Holmes, *Nonlinear Oscillations, Dynamical Systems, and Bifurcation of Vector Fields*, Springer-Verlag, 1983.
16. Kim, Y. B. and Noah, S. T., 'Steady-state analysis of a nonlinear rotor-housing system', to appear in ASME *Journal of Turbomachinery*, 1989. Also ASME paper No. 90-GT-328.

APPENDIX B

"Response and Bifurcation Analysis of MDOF Rotor System with a Strong Nonlinearity," Kim, Y.B. and Noah, S.T., to appear in Nonlinear Dynamics, 1991.

ABSTRACT

A new HB (harmonic Balance)/AFT (Alternating Frequency Time) method is further developed to obtain synchronous and subsynchronous whirling response of nonlinear MDOF rotor systems. Using the HBM, the nonlinear differential equations of a rotor system can be transformed to algebraic equations with unknown harmonic coefficients. A technique is applied to reduce the algebraic equations to only those of the nonlinear coordinates. Stability analysis of the periodic solutions is performed via perturbation of the solutions. To further reduce the computational time for the stability analysis, the reduced system parameters (mass, damping, and stiffness) are calculated in terms of the already known harmonic coefficients. For illustration, a simple MDOF rotor system with a piecewise-linear bearing clearance is used to demonstrate the accuracy of the calculated steady-state solutions and their bifurcation boundaries. Employing ideas from modern dynamics theory, the example MDOF nonlinear rotor system is shown to exhibit subsynchronous, quasi-periodic and chaotic whirling motions.

INTRODUCTION

There has recently been a tendency to increase the power and efficiency of rotating machinery. Smooth running of such machinery is often of great importance both for mechanical reliability and for user satisfaction. Consequently various rotordynamic effects, which in some cases may be due to existing nonlinearities, become increasingly important in the design and operation of such machinery.

A nonlinearity such as due to bearing clearances or rotor/stator rubs may sig-

nificantly alter the vibrational response. In the past, some aspects of the associated phenomena have been considered for simple rotor systems [1,2,3], experimentally [4] or analytically [5,6,7]. Day [2] and Neilson and Barr [3] showed possible occurrence of quasi-periodic whirling of rotors in presence of bearing clearances. Other investigators [1,4,5,6,7] also showed subsynchronous whirling motion occurring with nonlinear rotors. Very few studies were performed however for *multi-degree of freedom* (MDOF) nonlinear rotor systems.

Nataraj and Nelson [8] adopted a collocation approach and the Guyan reduction technique to obtain the steady-state whirling motion of a MDOF rotor system with squeeze film dampers. Despite of the complex calculation involved and lack of any stability analysis, their method is one of few existing approaches for determining the steady-state motion of MDOF nonlinear rotor systems. Ehrich [9] demonstrated experimentally that "chaotic" motion does occur in a high speed MDOF turbomachinery.

The present study consists of two main parts : i) First, the new harmonic balance method (HBM), with alternating DFT(Discrete Fourier Transform)/IDFT(Inverse Discrete Fourier Transform), is adapted for obtaining the periodic steady-state whirling motion of a MDOF rotor with bearing clearances. This approach has the advantage of offering robust convergent solution algorithms during the iteration process. Stability analysis using the present HBM can yield parameter ranges for which quasi-periodic whirling motion would occur. ii) Secondly, the stability analysis for nonlinear MDOF rotor systems is performed based on perturbation involving the harmonic coefficients of the periodic solutions. Through application of modern dynamic theory, all possible parameter ranges for the sud-

den change of whirling motion (i.e. bifurcation) can be obtained. This stability approach can be extended for any MDOF rotor systems with piecewise-smooth or polynomial-type nonlinearities. Another advantage of this approach is that it enables predicting parameter ranges in which chaotic rotor whirling would occur.

SYSTEM REDUCTION

A typical multi-disk rotor system with nonlinear bearings is considered. For a finite element (FE) formulation of the nonlinear rotor system, the rotor shaft segments are modeled as Euler beam elements taking shaft rotation effects into account [10]. An assumed axisymmetric geometry of the rotor shaft elements leads to the same mass and stiffness matrices in the X-Y and X-Z planes. If internal damping is neglected, the system equations of motion can be expressed in terms of the assembled mass, damping and stiffness matrices [M], [C] and [K] as

$$[M]\ddot{\mathbf{q}} + [C]\dot{\mathbf{q}} + [K]\mathbf{q} = \mathbf{f_u} + \mathbf{f_n} \tag{1}$$

where $\mathbf{q} = [y, z]^T$ and y, z denote the 2L×1 assembled state vectors in the X-Y and X-Z planes, where L is the total number of nodes. [C] has nonzero off-diagonal elements including damping opposing the motion of the disks and gyroscopic terms which couple the motion in the two planes. [K] has also nonzero off-diagonal elements due to rubbing and other coupling forces between rotor and stator. The vector $\mathbf{f_u}$ represents the vector of the disks' mass imbalances and side forces on the disks, while the vector $\mathbf{f_n}$ denotes the force vector at the nonlinear bearing. In particular, the nonlinear restoring forces in the y, z-directions on the bearing with

clearances, at the node j, are expressed as

$$f_{y_j} = k_b y_j (1 - \frac{\delta}{\sqrt{{y_j}^2 + {z_j}^2}}) \qquad (2-a)$$

$$f_{z_j} = k_b z_j (1 - \frac{\delta}{\sqrt{{y_j}^2 + {z_j}^2}}) \qquad (2-b)$$

where k_b is the bearing stiffness and δ is the clearance between bearing outer race and stator. The bearing forces f_{y_j} or f_{z_j} will vanish if δ is larger than the radial displacement, otherwise the bearing forces will be as given by equation (2).

In equation (1), the matrix size becomes 4L×4L, where L is the total number of nodes. This may require a very large core size and much computation time to calculate the dynamics of the nonlinear rotor-bearing system. In linear rotor dynamics, system matrix reduction techniques, such as the component mode method [11] or the Guyan reduction technique, could give a reduced form of the dynamic equation of motion. As an another approach, the impedance method [12] can reduce the number of equations of motion to obtain forced responses at specific locations of the system from those of "master", (kept) degrees of freedom. This reduction is exact and does not involve any approximation. In a similar fashion, large nonlinear rotor dynamical equations can be reduced to obtain steady-state response at bearing location using the HBM. This is achieved by using a version of an impedance formulation in which the system is reduced to its displacements at the bearing clearances. (see [12] and [20]). In the present study, the impedance method is applied to each of the harmonic components of the assumed periodic solution.

Extending the procedure developed by Kim and Noah [14], a periodic solution for the motion of the rotor is represented by a finite Fourier series expansion. For

the displacement of the i^{th} node (i=1,2,...,L), one can write

$$y_i = a^i_{0y} + \sum_{n=1}^{N}(a^i_{ny}\cos\frac{n\omega t}{\nu} - b^i_{ny}\sin\frac{n\omega t}{\nu}) \qquad (3-a)$$

$$z_i = a^i_{0z} + \sum_{n=1}^{N}(a^i_{nz}\cos\frac{n\omega t}{\nu} - b^i_{nz}\sin\frac{n\omega t}{\nu}) \qquad (3-b)$$

where ν is the subharmonic ratio, which is unity for harmonic and superharmonic cases, or an integer other than unity for subharmonic cases, and ω is the shaft rotational frequency. Since the motion is periodic, the nonlinear restoring force can be written as

$$f_{yj} = c^j_{0y} + \sum_{n=1}^{N}(c^j_{ny}\cos\frac{n\omega t}{\nu} - d^j_{ny}\sin\frac{n\omega t}{\nu}) \qquad (4-a)$$

$$f_{zj} = c^j_{0z} + \sum_{n=1}^{N}(c^j_{nz}\cos\frac{n\omega t}{\nu} - d^j_{nz}\sin\frac{n\omega t}{\nu}) \qquad (4-b)$$

where j denotes the j^{th} bearing node (j=1,2,...,m). The advantage of introducing equation (4) is to avoid the difficulties which would arise if standard harmonic balance procedure is directly applied to equation (2). The denominator term of equation (2) would not then be easily expressed in harmonic terms resulting from using equations (3-a) and (3-b).

Substituting equations (3) and (4) into equation (1) and equating the coefficients of similar harmonic terms lead to the following algebraic relationships :

constant terms

$$[K]\mathbf{A^0} = \mathbf{C^0} \qquad (5)$$

where $\mathbf{A^0}$ and $\mathbf{C^0}$ represent the constant Fourier coefficients of equations (3) and (4), respectively, and both are of size 4L×1.

cosine terms

$$-(\frac{n\omega^2}{\nu})[M]\mathbf{A^n}-(\frac{n\omega}{\nu})[C]\mathbf{B^n}+[K]\mathbf{A^n}=\mathbf{C^n}+\mathbf{F_{uc}} \qquad (n=1,2,...,N) \quad (6)$$

where $\mathbf{A^n}$ and $\mathbf{B^n}$ represent the n^{th} cosine and sine coefficient vectors, respectively, both of 4×1 dimension, $\mathbf{C^n}$ denotes the n^{th} cosine coefficient vector of $\mathbf{f_n}$, while $\mathbf{F_{uc}}$ represents the cosine coefficient of the imbalance and side force vector $\mathbf{F_u}$.

sine terms

$$(\frac{n\omega^2}{\nu})[M]\mathbf{B^n}-(\frac{n\omega}{\nu})[C]\mathbf{A^n}-[K]\mathbf{A^n}=\mathbf{D^n}+\mathbf{F_{us}} \qquad (n=1,2,...,N) \quad (7)$$

where vectors $\mathbf{A},\mathbf{B}$ are the same in equation (6), $\mathbf{D^n}$ denotes the n^{th} sine coefficient vector of $\mathbf{f_n}$, and $\mathbf{F_{us}}$ is the sine term of the imbalance and side force vector $\mathbf{F_u}$.

At this stage, one can reduce equations (5),(6) and (7) using the impedance reduction technique, only retaining the coordinates at the bearing nodes. For the constant terms, equation (5) can be partitioned as

$$\begin{pmatrix}[K_{kk}] & [K_{kr}]\\ [K_{rk}] & [K_{rr}]\end{pmatrix}\begin{pmatrix}\mathbf{A_k^0}\\ \mathbf{A_r^0}\end{pmatrix}=\begin{pmatrix}\mathbf{C_k^0}\\ \mathbf{C_r^0}\end{pmatrix} \qquad (8)$$

where the subscripts "r" and "k" denote *reduced out* and *kept* coordinates, respectively. By applying the elimination procedure, the constant terms can be represented in the reduced form

$$[K'_{kk}]\mathbf{A_k^0}=\mathbf{C_k^0} \qquad (9)$$

where $[K'_{kk}]$ is the reduced stiffness matrix of the rotor and $\mathbf{A_k^0}$, $\mathbf{C_k^0}$ are both 2m×1 vectors, where m is the total number of bearings. The n^{th} cosine and sine harmonic

terms can be reduced in a similar fashion to yield

$$[S'_{kk}]_n \mathbf{A_k^n} = \mathbf{C_k^n} + \mathbf{U^n} \tag{10}$$

where $[S'_{kk}]_n$ is the reduced matrix involving system mass, damping and stiffness matrices, $\mathbf{A_k^n}$ is the n^{th} Fourier coefficient vector of equation (3) at the bearing, $\mathbf{C_k^n}$ is the n^{th} Fourier coefficient vector of equation (4) and $\mathbf{U^n}$ is the reduced vector involving imbalance and side forces. Here $\mathbf{A_k^n}$, $\mathbf{C_k^n}$, $\mathbf{U^n}$ are all 4×1 vectors for each n.

Combining equations (9) and (10), the following assembled matrix is obtained

$$[T]\mathbf{A_k} = \mathbf{C_k} + \mathbf{V} \tag{11}$$

where $[T]$ is a 2m(2N+1)×2m(2N+1) matrix, $\mathbf{A_k}$, and $\mathbf{C_k}$ are 2m(2N+1) vectors which represent the trigonometric Fourier coefficients of equations (3) and (4) at the bearing node, respectively, and $\mathbf{V}$ is the total sum of the reduced imbalance force vector. It is noted here that the total dimension of the system equations is reduced from 4L to 4mN+2m. For a multi-degree of freedom rotor, L is very large in comparison with m (number of bearing nodes) and N (number of retained harmonic terms), so the system is significantly reduced for obtaining the steady-state response of the nonlinear rotor system. Another advantage of the reduction technique using the HBM is that stability analysis of the periodic response of multi-degree of freedom rotor systems can be made highly efficient by considering only truncated harmonic terms. This is discussed in the section further below on stability analysis.

In equation (11), the only unknown vector is $\mathbf{A_k}$. The vector $\mathbf{C_k}$ can be calculated using DFT and IDFT relations since $\mathbf{C_k}$ is a nonlinear function of $\mathbf{A_k}$. This procedure is described next.

Calculation of $\mathbf{C_k}$ from $\mathbf{A_k}$

To determine $\mathbf{C_k}$ from $\mathbf{A_k}$, it is necessary to first calculate the discrete y and z values of $\mathbf{y_\Delta} = [y(\Delta t), \quad y(2\Delta t), ..., y((M+1)\Delta t)]^T$ and $\mathbf{z_\Delta} = [z(\Delta t), \quad z(2\Delta t), ..., z((M+1)\Delta t)]^T$, where Δt is any discrete time steps, M+1 is the total number of discrete points, and superscript T denotes the transpose. Using IDFT, the discrete displacements, $\mathbf{y_\Delta}$ and $\mathbf{z_\Delta}$, can be obtained as

$$\mathbf{y_\Delta} = [V_\Delta]\mathbf{A_{yk}} \tag{12-a}$$

$$\mathbf{z_\Delta} = [V_\Delta]\mathbf{A_{zk}} \tag{12-b}$$

where

$$[V_\Delta] = \begin{pmatrix} 1 & 1 & 0 & ... & 1 & 0 \\ 1 & \cos\Delta t/\nu & -\sin\Delta t/\nu & ... & \cos\Delta t/\nu & -\sin\Delta t/\nu \\ \vdots & \vdots & \vdots & \ddots & \vdots & \vdots \\ 1 & \cos M\Delta t/\nu & -\sin M\Delta t/\nu & ... & \cos M\Delta t/\nu & -\sin M\Delta t/\nu \end{pmatrix} \tag{13}$$

and in which $\mathbf{A_{yk}}$, $\mathbf{A_{zk}}$ denote the cosine and sine parts of $\mathbf{A_k}$, respectively. The discrete nonlinear restoring force $\mathbf{f_{y\Delta}}$, $\mathbf{f_{z\Delta}}$ can be obtained using equations (2) and (12) as

$$\mathbf{f_{y\Delta}} = \mathbf{f_y}(\mathbf{y_\Delta}, \mathbf{z_\Delta}) \tag{14-a}$$

$$\mathbf{f_{z\Delta}} = \mathbf{f_z}(\mathbf{y_\Delta}, \mathbf{z_\Delta}) \tag{14-b}$$

where

$$\mathbf{f_{y\Delta}} = [f_y(\Delta t), f_y(2\Delta t), ..., f_y((M+1)\Delta t)]^T \tag{15-a}$$

$$\mathbf{f_{z\Delta}} = [f_z(\Delta t), f_z(2\Delta t), ..., f_z((M+1)\Delta t)]^T \tag{15-b}$$

As $\mathbf{C_k}$ is the Fourier coefficients of $\mathbf{f_{y\Delta}}$ and $\mathbf{f_{z\Delta}}$, DFT offers the following expression

$$\mathbf{C_k} = \frac{2}{M+1}[Z_\Delta]\mathbf{f}(\mathbf{V_\Delta A_k}) \tag{16}$$

where

$$[Z_\Delta] = \begin{pmatrix} 0.5 & 0.5 & 0.5 & \cdots & 0.5 \\ 1 & \cos \Delta t/\nu & \cos 2\Delta t/\nu & \cdots & \cos (M+1)\Delta t/\nu \\ 1 & -\sin \Delta t/\nu & -\sin 2\Delta t/\nu & \cdots & -\sin (M+1)\Delta t/\nu \\ \vdots & \vdots & \vdots & \ddots & \vdots \\ 1 & -\sin N\Delta t/\nu & -\sin 2N\Delta t/\nu & \cdots & -\sin (M+1)N\Delta t/\nu \end{pmatrix} \quad (17)$$

and $\mathbf{f}$ is the sum of $\mathbf{f_y}$ and $\mathbf{f_z}$.

From equation (11), one can solve the nonlinear algebraic equation by a successive iteration procedure. Newton-Raphson scheme is one of the favorable techniques for obtaining steady-state solutions since it has rank two convergence. The disadvantage of this method is that it requires calculation of an explicit form of the Jacobian which is not simply obtainable in multi-degree of freedom systems. However, since the problem only involves nonlinear bearing coordinates, the explicit form of the Jacobian can be obtained using the DFT and IDFT procedure. One of the techniques to avoid calculation of the Jacobian is to utilize the forward differentiation [6] which replaces the use of the Jacobian [14]. From the authors experience, forward differentiation poses the difficulty of requiring control of the differentiation length for each parameter and obtaining the probable convergence values near the resonance responses. Moreover, forward differentiation convergence rate is much slower than when directly using the explicit Jacobian formulation. Therefore, in this study an explicit Jacobian formulation is utilized to enhance the computational efficiency and to guarantee convergence for all parameter ranges. Another iterative scheme, where calculation of a Jacobian is not required, is to use the quasi-Newton method [15]. Although this method avoids calculation of the Jacobian, its convergence is much slower when applied to nonlinear multi-degree of freedom rotor systems.

Newton-Raphson Method

To apply the Newton-Raphson method to determine the unknown vector $\mathbf{A_k}$, equation (11) can be put in the form

$$\mathbf{G} = [T]\mathbf{A_k} - \mathbf{C_k} - \mathbf{V} = \mathbf{0} \tag{18}$$

In using the Newton-Raphson algorithm, the following derivative is needed (using equation (16))

$$\frac{\partial \mathbf{C_k}}{\partial \mathbf{A_k}} = \frac{2}{M+1}[Z_\Delta]\frac{\partial \mathbf{f}(\mathbf{V_\Delta A_k})}{\partial \mathbf{A_k}} \tag{19}$$

It follows from equations (16) and (18) that the Jacobian column vector of $\mathbf{G}$ is given explicitly by the relation

$$[J] = [T] + \frac{\partial \mathbf{C_k}}{\partial \mathbf{A_k}} \tag{20}$$

since $[J] = \frac{\partial \mathbf{G}}{\partial \mathbf{A_k}}$ and $\mathbf{A_k}$ is the only unknown vector. The Newton-Raphson algorithm for the unknown vector $\mathbf{A_k}$ with an initial guess $\mathbf{A_k^{(0)}}$ can be described as

$$[J]\Delta \mathbf{A_k}^{(p)} + \mathbf{G}^{(p)} = \mathbf{0} \tag{21}$$

where the superscript, p, denotes the p^{th} iteration number. The above algorithm terminates after r iterations, so that

$$|\mathbf{G}^{(r)}| < \epsilon \tag{22}$$

where ϵ is small number, and $\mathbf{A_k^{(r)}}$ is a final solution.

STABILITY ANALYSIS

From the previous section, the steady-state, harmonic or subharmonic whirling responses, are obtained utilizing the present HBM formulation. As the steady-state whirling responses are calculated using Newton-Raphson technique, a stability analysis is necessary to check whether the obtained responses are stable. Multiple solutions could exist for a given set of parameters. Some of these solutions could become unstable and bifurcate to other forms of solutions.

If the nonlinear rotor system is of small number of degrees of freedom, it is straightforward to perform a stability analysis through perturbation of the periodic solution obtained [13]. However, if the nonlinear rotor system possesses large number of degrees of freedom, excessive computational time would be required to check the stability or to obtain bifurcation information. This is since for the stability analysis, the procedure would involve integration of a large matrix in order to calculate the monodromy matrix for the perturbed equations with periodic coefficients. In the present paper, a more efficient stability analysis method for MDOF nonlinear rotor systems is presented.

From equation (10), the reduced system matrix with the n^{th} harmonic terms is rewritten as

$$[S'_{kk}]_n \mathbf{A}_\mathbf{k}^\mathbf{n} = \mathbf{C}_\mathbf{k}^\mathbf{n} + \mathbf{U}^\mathbf{n} \tag{23}$$

where $[S'_{kk}]_n$ is the reduced system matrix, $\mathbf{A}_\mathbf{k}^\mathbf{n}$ is the vector which represents the Fourier coefficients of displacement at the nonlinear bearing node, $\mathbf{C}_\mathbf{k}^\mathbf{n}$ is the vector of Fourier coefficients of the nonlinear restoring forces and $\mathbf{U}^\mathbf{n}$ is the reduced vector involving the imbalance and side forces. The unknown vectors $\mathbf{A}_\mathbf{k}^\mathbf{n}$ and $\mathbf{C}_\mathbf{k}^\mathbf{n}$ in equation (23), which were already obtained by the HBM method, have the following

elements

$$\mathbf{A_k^n} = \left[\sum_{j=1}^{m} a_{ny}^j, \sum_{j=1}^{m} b_{ny}^j, \sum_{j=1}^{m} a_{nz}^j, \sum_{j=1}^{m} b_{nz}^j\right]^T \tag{24}$$

$$\mathbf{C_k^n} = \left[\sum_{j=1}^{m} c_{ny}^j, \sum_{j=1}^{m} d_{ny}^j, \sum_{j=1}^{m} c_{nz}^j, \sum_{j=1}^{m} d_{nz}^j\right]^T \tag{25}$$

where T denotes a transpose, j represents all the j^{th} bearing nodes, and m is the total number of bearings. As equation (23) represents the reduced system matrix involving only the nodes at the nonlinear bearings, all the coefficients of $\mathbf{A_k^n}$ are in general coupled, i.e. the off-diagonal terms of $[S'_{kk}]_n$ matrix have non-zero elements. At j^{th} nonlinear bearing node, the damping and restoring force are affected by all the damping and stiffness coefficients, C_{ij}, K_{ij}, $(i, j = 1, 2, ..., m)$, respectively. Therefore, coupled terms in damping and stiffness coefficients can lead to the following equations

$$M_{yj}\ddot{y}_j + \sum_{i=1}^{m} C_{yji}\dot{y}_i + \sum_{i=1}^{m} K_{yji}y_i = f_{yj} + U_y^j \tag{26}$$

$$M_{zj}\ddot{z}_j + \sum_{i=1}^{m} C_{zji}\dot{z}_i + \sum_{i=1}^{m} K_{zji}z_i = f_{zj} + U_z^j \tag{27}$$

where M, C and K represent reduced mass, damping and stiffness coefficients matrix, respectively, f_{yj}, f_{zj} denote nonlinear restoring forces in the y, z-direction and subscript j represents the j^{th} nonlinear bearing node. It is noted here that the Fourier coefficients of f_y and f_y are represented by $\mathbf{C_k^n}$ in equation (23). The next step is to calculate each reduced mass, damping and stiffness coefficients from the reduced system matrix $[S'_{kk}]_n$.

From the previous section, the displacement of the j^{th} bearing node can be represented by only the n^{th} harmonic component as

$$y^j = a_{ny}^j \cos n\frac{\omega t}{\nu} - b_{ny}^j \sin n\frac{\omega t}{\nu} \tag{28 - a}$$

$$z^j = a^j_{nz}\cos n\frac{\omega t}{\nu} - b^j_{nz}\sin n\frac{\omega t}{\nu} \qquad (28-a)$$

where j=1,2,...,m. Inserting equations (28) into equation (26) and (27), the following relations can be arrived at :

$$\begin{pmatrix} -(\frac{n\omega}{\nu})^2 M_{y1} + K_{y1} & -C_{y1}\frac{n\omega}{\nu} & \cdots & 0 & 0 \\ -C_{y1}\frac{n\omega}{\nu} & (\frac{n\omega}{\nu})^2 M_{y1} - K_{y1} & \cdots & 0 & 0 \\ \vdots & \vdots & \ddots & \vdots & \vdots \\ 0 & 0 & \cdots & -(\frac{n\omega}{\nu})^2 M_{zm} + K_{zm} & -C_{zm}\frac{n\omega}{\nu} \\ 0 & 0 & \cdots & -C_{zm}\frac{n\omega}{\nu} & (\frac{n\omega}{\nu})^2 M_{zm} - K_{zm} \end{pmatrix}$$

$$\times \begin{pmatrix} a^1_{ny} \\ b^1_{ny} \\ \vdots \\ a^m_{nz} \\ b^m_{nz} \end{pmatrix} = \begin{pmatrix} c^1_{ny} \\ d^1_{ny} \\ \vdots \\ c^m_{nz} \\ d^m_{nz} \end{pmatrix} + \mathbf{U^n} \qquad (29)$$

As equation (23) and (29) are the same, all reduced mass, damping and stiffness coefficients of equations (26) and (27) can be calculated from the matrix $[S'_{kk}]_n$ in equation (23).

Equations (26) and (27) can now be rewritten as

$$h_{yj} = \ddot{y}_j + \sum_{i=1}^{m}\frac{C_{yj}}{M_{yj}}\dot{y}_i + \sum_{i=1}^{m}\frac{K_{yj}}{M_{yj}}y_i - \frac{f_{yj}}{M_{yj}} - \frac{U_y}{M_{yj}} = 0 \qquad (30)$$

$$h_{zj} = \ddot{z}_j + \sum_{i=1}^{m}\frac{C_{zj}}{M_{zj}}\dot{z}_i + \sum_{i=1}^{m}\frac{K_{zj}}{M_{zj}}z_i - \frac{f_{zj}}{M_{zj}} - \frac{U_z}{M_{zj}} = 0 \qquad (31)$$

Equations (30) and (31) are the reduced system equations to be utilized for the stability analysis of the steady-state whirling motion. It is noted here that the system equations are reduced from 2L to 2m where L is the total number of nodes, including the number of bearing nodes, m. Therefore, for MDOF nonlinear rotor systems, the reduction of system equations has the effect of rendering the stability analysis significantly more efficient.

Perturbation of equations (30) and (31) can be obtained using Taylor expansion as

$$\Delta h_{yj} = \frac{\partial h_{yj}}{\partial \ddot{y}_j}\Delta\ddot{y}_j + \sum_{i=1}^{m}\frac{\partial h_{yj}}{\partial \dot{y}_i}\Delta\dot{y}_i + \sum_{i=1}^{m}\frac{\partial h_{yj}}{\partial y_i}\Delta\dot{z}_i + \frac{\partial f_{yj}}{\partial y_j}\Delta y_i + \frac{\partial f_{yj}}{\partial z_j}\Delta z_i = 0 \quad (32)$$

$$\Delta h_{zj} = \frac{\partial h_{zj}}{\partial \ddot{z}_j}\Delta\ddot{z}_j + \sum_{i=1}^{m}\frac{\partial h_{zj}}{\partial \dot{y}_i}\Delta\dot{y}_i + \sum_{i=1}^{m}\frac{\partial h_{zj}}{\partial \dot{z}_i}\Delta\dot{z}_i + \frac{\partial f_{zj}}{\partial y_j}\Delta y_i + \frac{\partial f_{zj}}{\partial z_j}\Delta z_i = 0 \quad (33)$$

where j=1,2,...,m.

Equations (32) and (33) are transformed into a system of first order equations with

$$\mathbf{u} = [\Delta y_j,\ \Delta z_j,\ \Delta\dot{y}_j,\ \Delta\dot{z}_j]^T \qquad (j = 1, 2, ..., m) \quad (34)$$

The resulting variational equations can be written in the following form :

$$\dot{\mathbf{u}} = [W(t)]\ \mathbf{u} \quad (35)$$

where $\mathbf{u} \in \mathbf{R}^{4m}$ and $W(t)$ is a 4m×4m matrix. The stability problem of the prescribed motion can be formulated as the local stability analysis for $\mathbf{u} = \mathbf{0}$. The fundamental matrix $[Z(t)]$ for the ordinary differential equation (35) with periodic coefficients is related to $[Z(t+T)]$, which is also a fundamental matrix by [18]

$$[Z(t+T)] = [Z(t)][S] \quad (36)$$

where $[S]$ is referred to as the monodromy matrix for the system. The monodromy matrix $[S]$ can be produced by evaluating the matrix $[Z]$ at the end of one period for the system. The Floquet multipliers, or the eigenvalues, μ, of S determine the stability of the system. When all the multipliers are of absolute value less than unity except for some with absolute value of unity, then the system is located at the

stability boundary. Three different types of loss of stability of a periodic solution can occur [19] for the system considered when one or more μ are given by

i) μ=1, saddle-node or transcritical

ii) μ=-1, period multiplying

iii) $\mu = \alpha + i\beta$ $|\mu_3|$=1, secondary Hopf bifurcation

The bifurcation can be super- or subcritical.

AN EXAMPLE MDOF ROTOR SYSTEM

To demonstrate the application and computational efficiency of the new HBM/AFT, the method is applied to a simple MDOF model shown in Figure 1. The equations of motion of the rotor are formulated using the finite element method (FEM), employing Euler beam elements. The rotor is supported on a linear bearing at the left and by a nonlinear bearing with a gap at the middle. The rotor is subjected to imbalance forces and a constant direction side force. The detailed rotor configuration is shown in Table 1.

First, the whirling orbit at the nonlinear bearing is obtained for a rotor with 2000 rad/sec rotational speed, as shown in Figure 2. The solid line in this figure represents the HBM solution which is seen to be accurate. The minor discrepancies between the numerical integration and the HBM solutions are due to : i) truncation errors in assuming a finite number of harmonics for the steady-state solution and for the nonlinear restoring force. This error can be reduced by retaining larger number of harmonic terms. ii) errors introduced by the Guyan reduction.

A more complicated subsynchronous whirling motion at a rotor spinning speed

of 1600 rad/sec is shown in Figure 3. The solid line represents the response obtained by the HBM, while the dotted line stands for the solution of direct numerical integration. The results show good agreement between the HBM and the numerical integration methods. In most of the simulations, only four harmonic terms were considered in obtaining the whirling response. This results in drastic reduction in the computational time in comparison with direct numerical integration.

Another characteristic of the behavior of the nonlinear rotor is the sudden change of its whirling shape with small changes of certain parameters. This is due to bifurcation whose study is very important since it can lead to a sudden change from synchronous to subsynchronous motion (including subharmonic or quasi-periodic motion) or vice versa. To better understand the nonlinear MDOF rotor characteristics with bearing clearances, stability charts, or bifurcation boundary plots, are utilized. Figure 4-a shows the effects of the gap (clearance) and mass eccentricity on Hopf bifurcation boundaries. The regions marked by "A" indicates quasi-periodic whirling motion. These regions were obtained using present stability analysis method which indicated a Hopf bifurcation at their boundaries. Region B indicates a stable harmonic whirling motion, i.e. all the roots of the monodromy matrix are located within the unit disk. To confirm these stability boundaries, numerical integration was performed for a selected set of parameter values, and the results are displayed in Figure 4-b and 4-c. These results show that the stability analysis developed here is quite accurate. The figure shows that for the range of parameters utilized, a complicated quasi-periodic whirling motion can be eliminated by decreasing the bearing clearance, while changing the bearing stiffness does not affect the motion.

Figure 5-a shows effects of the rotational speed and side force on the flip (period multiplying) bifurcation boundaries. Region A of this figure represents the *primary* stable whirling motion (i.e. the stable whirling when the rotor does not contact the gap), region B is the subsynchronous whirling of order 1/4 which can cause violent whirling motion, region C is the subsynchronous whirling with order 1/3, and region D shows the *secondary* stable synchronous whirling motion (i.e. the stable whirling when the rotor stays in contact with the supports through the gap). Numerical integrations for the orbits in each regions are also performed to confirm the bifurcation boundaries as shown in Figures 5-b-e. Since the MDOF rotor system displays a 550 rad/sec critical speed with the rotational speeds around 3 or 4 times this critical speed, the subsynchronous whirling motions might, therfore, occur. Another interesting phenomenon emerging from the results in regions B and C is that the motions can bifurcate further by increasing the side force (i.e. by period doubling or tripling according to the side force variation). As the HBM can handle only finite number of low order subharmonic terms (so that chaotic whirling motion, which possesses a large number of low order subharmonics, can not be obtained using the HB/AFT method), numerical integration is used to study further flip bifurcation in the region C, as shown in Figures 6-a-e. Since region B has similar flip bifurcation pattern, the results of this region is not included here. Shown in Figure 6-a is the *primary* stable whirling motion. By increasing the side force, the shape of whirling orbits continue to change until subsynchronous motion with order 1/3 is achieved. This is shown in Figure 6-b. Further increase of the side force results in bifurcation to subsynchronous motions of order 1/9 and 1/27, as shown in Figures 6-c and d, respectively. With a small increase of the side force beyond these subsynchronous regions, whirling can become almost non-periodic ("chaotic") as

shown in Figure 6-e. Figure 6-f, which shows the response spectra of that in Figure 6-e, clearly indicates chaotic motion. The reversed bifurcation (i.e. inverse process of above bifurcation from *primary* stable whirling to chaos) begins to occur suddenly ("crisis") by changing from chaotic motion to *secondary* stable whirling when the side force is increased, as shown in Figure 7.

Figure 8 shows the effects of the mass eccentricity and side force on the flip bifurcation boundaries. The region marked by A has a *primary* stable harmonic whirling, while region B has a subsynchronous whirling shape. The figure shows that the *primary* whirling shape does not change its motion very rapidly with the eccentricity or with the amount of imbalance. However, the *secondary* stable whirling becomes unstable for the same side force. All bifurcation regions were confirmed using numerical integration. The results of the comparisons are not included here since they display similar whirling shapes as those of Figure 5. Figure 9 shows the effects of clearance and the side force on the flip bifurcation boundaries. The regions A,B, and C of this figure have the same whirling motions as those in Figure 7. The figure shows that larger side force is needed to cause *primary* or *secondary* stable harmonic whirling when the gap size is increased.

CONCLUDING REMARKS

A further developed HBM, using DFT/IDFT, is employed to obtain the steady-state periodic response for MDOF rotor systems with bearing clearances (piecewise-linear nonlinearity). The Guyan reduction technique is utilized to reduce the system to the nonlinear coordinates. The stability analysis is performed via perturbation of the obtained periodic solutions. The reduced and approximated system param-

eters (mass, damping, and stiffness) are calculated from the determined harmonic coefficients.

A simple MDOF rotor system with a bearing clearance is used for illustration of the method. The results obtained show that i) the HBM method, as developed here, is robust and efficient. ii) the method leads to accurate bifurcation boundaries for nonlinear MDOF rotor systems. Furthermore, the method can in general be applied to MDOF rotor systems with piecewise-smooth or polynomial type nonlinearities at the bearing supports.

If the system possesses quasi-periodic response for a given set of parameters, the present HB/AFT approach cannot be used to obtain the corresponding whirling motion. However, a modified DFT, which is now under study, is believed to be able to produce quasi-periodic whirling motions.

ACKNOWLEDGMENT

This work was carried out as part of a research project supported by NASA, Marshall Flight Center under contract No. NAS8-37465. The authors are grateful to Thomas Fox, the technical monitor, for his enthusiastic support and interest.

REFERENCES

1. Ehrich, F.F., 1966, "Subharmonic Vibration of Motors in Bearing Clearance," ASME paper 66-MD-1.

2. Day, W.B., 1985, "Nonlinear Rotordynamics Analysis," NASA report CR

171425.

3. Neilson, R.D. and Barr, A.D.S., 1984, "Spectral Features of the Response of a Rigid Rotor Mounted on Discontinuously Nonlinear Supports," 7th world congress on the theory of machines and mechanics, Seville, pp. 1799-1803.

4. Bently, D.E., 1974, "Forced Subrotative Speed Dynamic Action of Rotating Machinery," ASME paper 74-PET-16. Clearance," ASME paper 66-MD-1.

5. Childs, D.W., 1982, "Fractional Frequency Rotor Motion Due to Nonsymmetric Clearance Effects," ASME *J. of Eng. Power*, Vol. 104., pp. 533-541.

6. Choi, Y.S. and Noah, S.T., 1987, " Nonlinear Steady-state Response of a Rotor-support System," ASME *Journal of Vibration, Acoustics, Stress, And Reliability in Design* Vol. 109, pp. 255-261.

7. Kim, Y.B. and Noah, S.T., 1989, "Bifurcation Analysis for a Modified Jeffcott Rotor with a Bearing Clearance," accepted for publication in *Journal of Nonlinear Dynamics.*

8. Nataraj, C. and Nelson, H.D., "Periodic Solutions in Rotor Dynamic Systems with Nonlinear Supports : A General Support," ASME *Design Conference*, Oct. 1987.

9. Ehrich, F.F., 1989, "High Order Subharmonic Response of High Speed Rotors in Bearing Clearance," ASME *J. of Vibration, Acoustics, Stress, and Reliability in Design*, Vol. 110, pp.9-16.

10. Nelson, H.D. and McVaugh, 1976, "The dynamics of Rotor-Bearing Systems

Using Finite Elements," ASME *J. of Engineering for Industry*, Vol. 98, pp.593-600.

11. Rouch, K.E. and Kao, J.S., 1980, "Dynamic Reduction in Rotor Dynamics by the Finite Element Method," ASME *J. of Mechanical Design*, Vol. 102, pp.360-368.

12. Fan, U.J. and Noah, S.T., 1989, "Vibration Analysis of Rotor Systems Using Reduced Subsystem Models," AIAA *J. of Propulsion and Power*, Vol. 5, number 5, pp. 602-609.

13. Kim, Y.B. and Noah, S.T., 1989, "Stability and Bifurcation Analysis of Oscillators with Piecewise-linear Characteristics : A General Approach," accepted for publication in ASME *Journal of Applied Mechanics*.

14. Kim Y.B. and Noah S.T., 1989, "Steady-State Analysis of a Nonlinear Rotor-Housing System," to appear in ASME *J. of Turbomachinery*.

15. Dennis, Jr., J.E. and More, J.J., 1977, "Quasi-Newton Methods, Motivation and Theory," *SIAM Review*, Vol. 19, pp.46-88.

16. Davis, L.B., Wolfe, E.A. and Betty, R.F., 1984, "Housing Flexibility Effects on Rotor Stability," MSFC Advanced High Pressure O_2/H_2 Technology Conference Proceedings, G.M. Space Flight Center ; Huntsville, Alabama, June 27-29.

17. Muszynska, A., 1984, "Partial Lateral Rotor to Stator Rubs," Proceedings in Rotating Machinery, Univ. of York, Sept., pp.327-335.

18. Meirovitch, L., 1979, Methods of Analytical Dynamics, McGraw-Hill, New York.

19. Guckenheimer, J. and Holmes, P., 1983, Nonlinear Oscillations, Dynamical Systems and Bifurcations of Vector Fields, Springer-Verlag, New York.

20. Noah, S.T., 1984, "Rotordynamic Analysis of the SSME Turbopumps Using Reduced Models," Report on NASA Contract NAS8-34505, Texas A&M University, Sept.

Figure 1. MDOF rotor model with a piecewise-linear bearing clearance

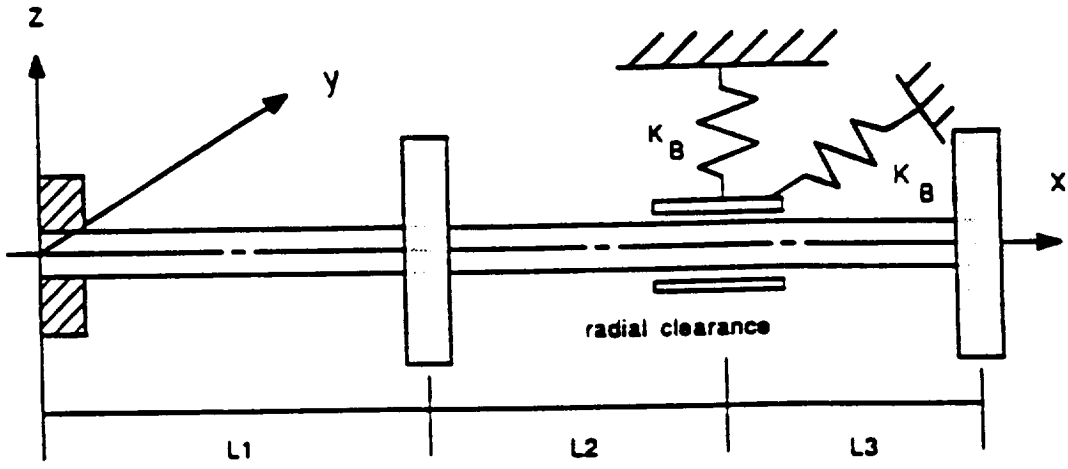

Figure 2. Comparison between HBM and numerical integration

(speed=2000 rad/sec. gap=3 mm, side force=1400 N,

eccentricity=1 mm, damping=10 N-sec/m, bearing stiff.=1E+06 N/m)

— HBM ; ... Numerical integration

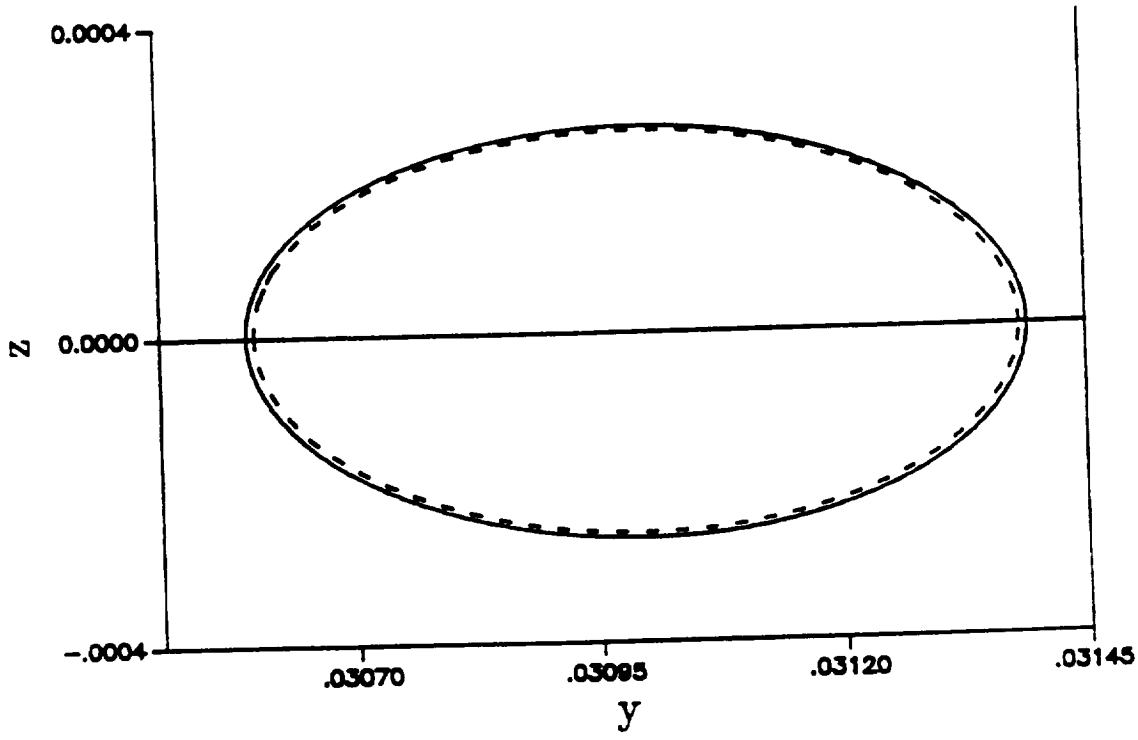

Figure 3. Comparison between HBM and numerical integration

(speed=1600 rad/sec, gap=3 mm, side force=1400 N,

eccentricity=23 mm, damping=10 N-sec/m, bearing stiff.=1E+06 N/m)

— HBM ; ... Numerical integration

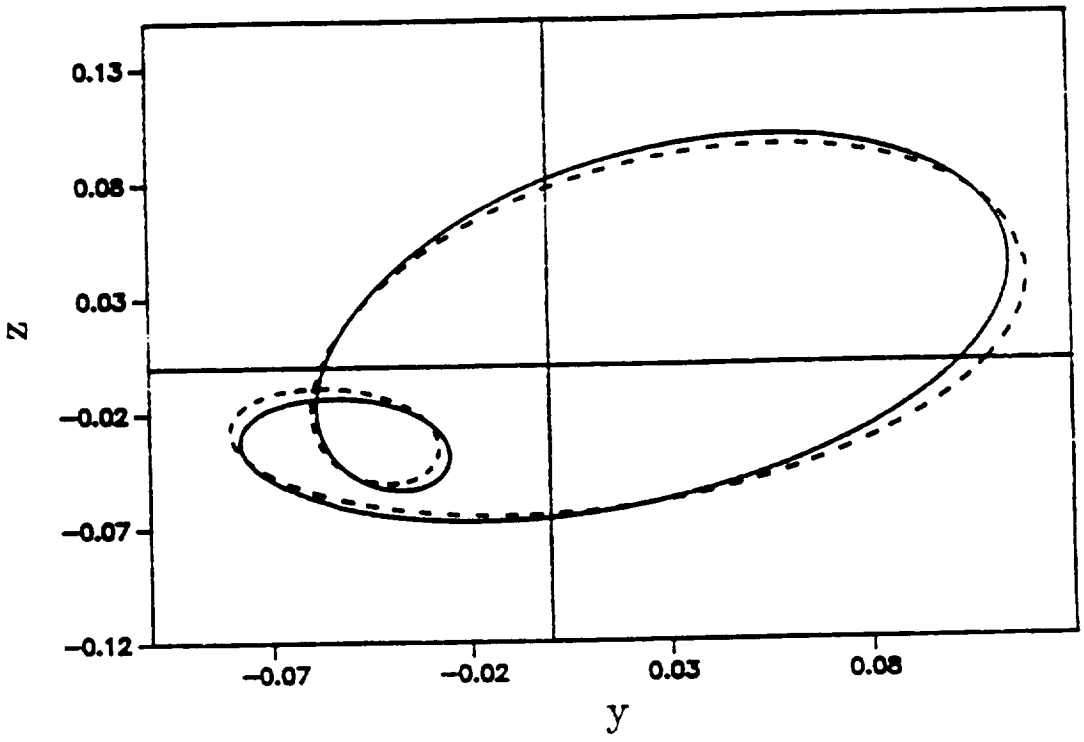

Figure 4. Effect of gap and eccentricity on Hopf bifurcation boundaries

(speed=2300 rad/sec, side force=2800 N, damping=10 N-m/sec)

(b) - Region A (gap=3 mm, ecc.=20 mm) ;

(c) - Region B (gap=3 mm, ecc.=40 mm)

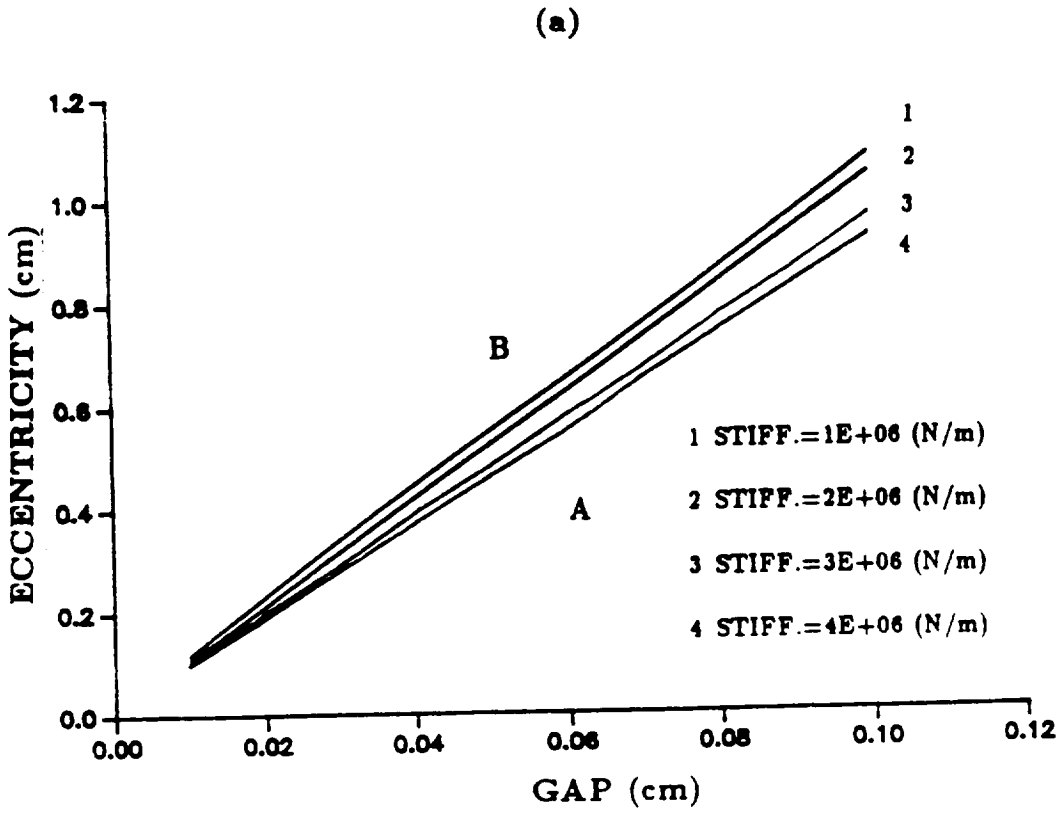

Figure 5. Effect of side force and speed on flip bifurcation boundaries (gap=3 mm, damping=10 N-m/sec. stiff.=1E+06 N/m)

(b) - Region A (speed=2100 rad/sec, side f.=400 N) ;

(c) - Region B (speed=2100 rad/sec, side f.=500 N) ;

(d) - Region C (speed=1600 rad/sec, side f.=500 N) ;

(e) - Region D (speed=2100 rad/sec, side f.=600 N)

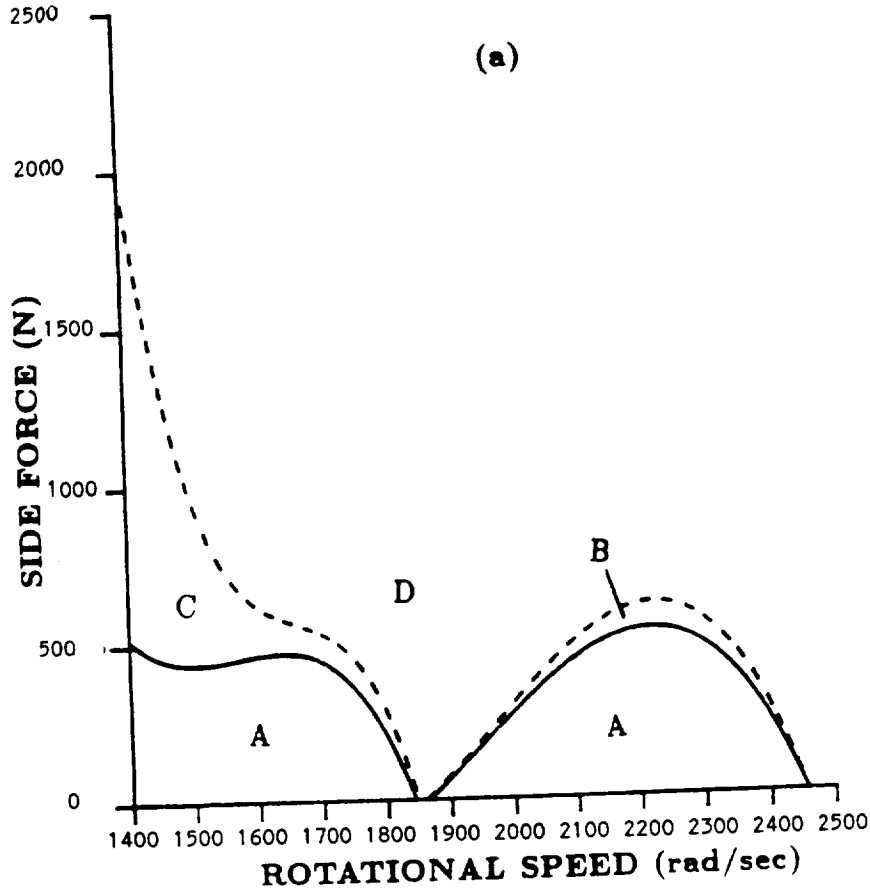

(b)

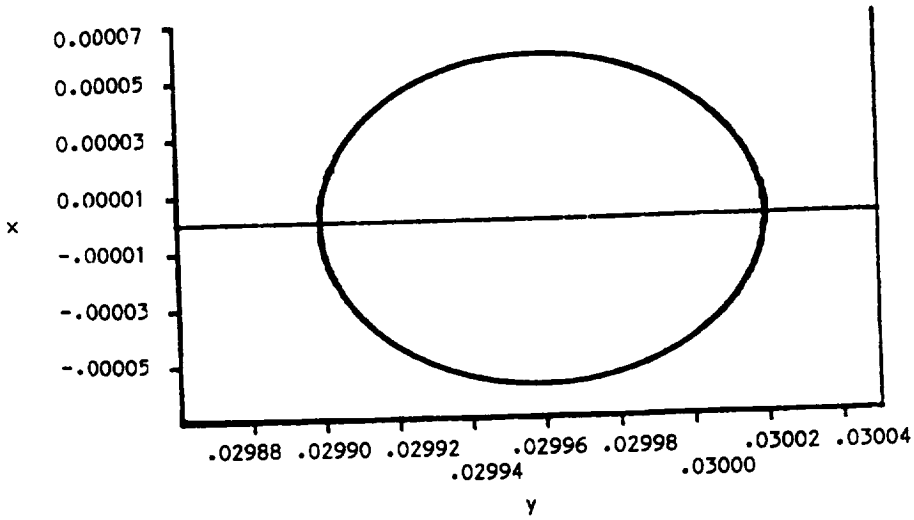

(c)

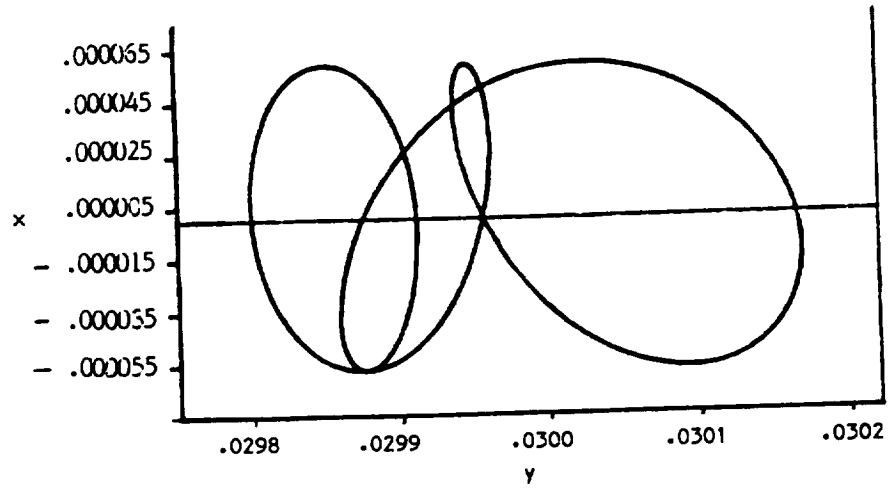

Figure 5, Continued

(d)

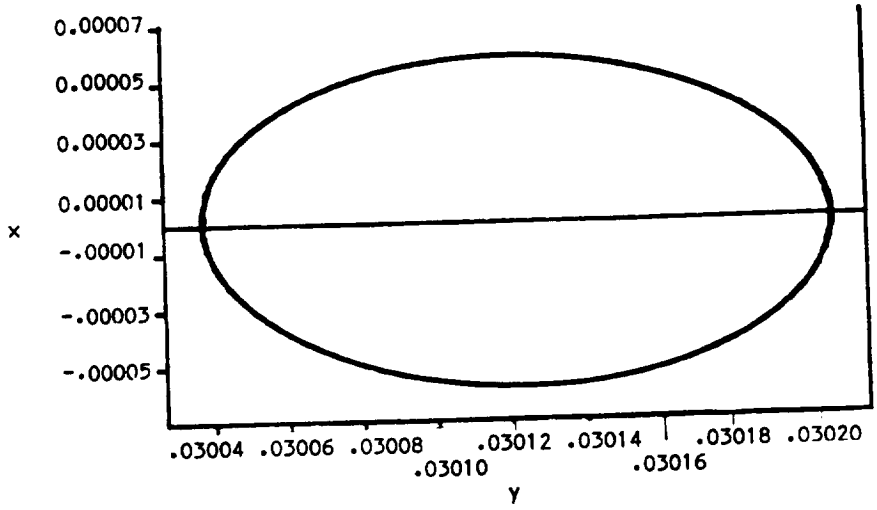

(e)

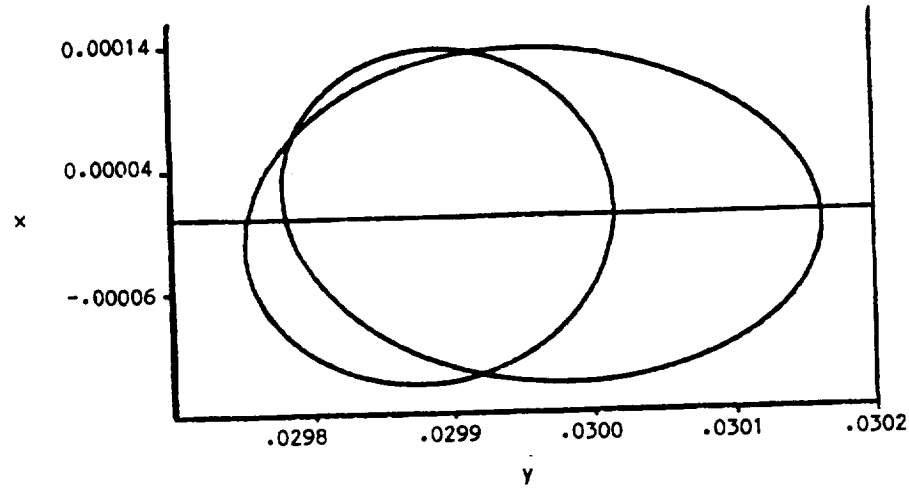

Figure 5, Continued

Figure 6. Flip bifurcation process with speed of 1600 rad/sec

(a) - *primary* stable whirling motion (side f.=450 N) ;

(b) - subsynchronous whirling motion with order 1/3 (side f.=500 N) ;

(c) - subsynchronous whirling motion with order 1/9 (side f.=527 N) ;

(d) - subsynchronous whirling motion with order 1/27 (side f.=535 N) ;

(e) - chaotic whirling motion (side f.=550 N) ;

(f) - power spectrum of chaotic motion (side f.=550 N)

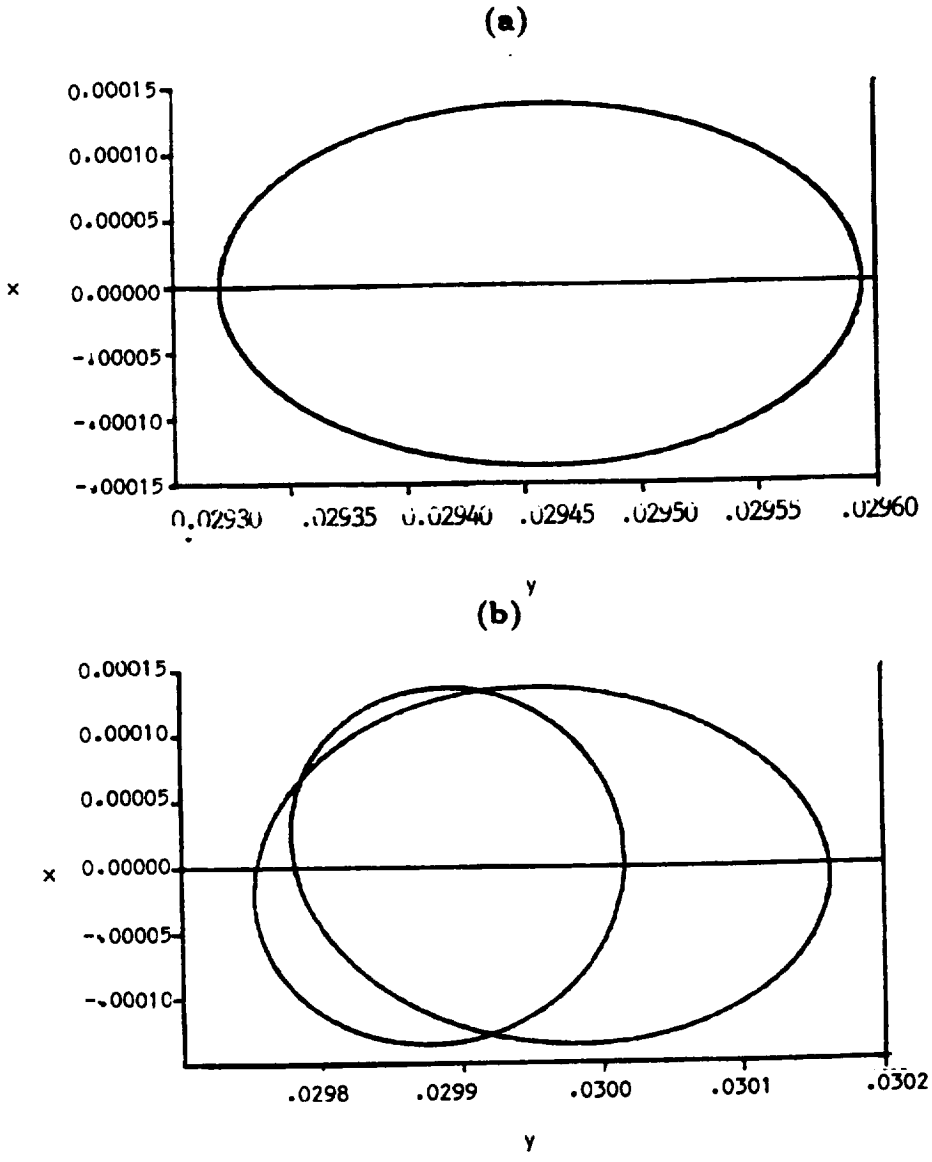

(c)

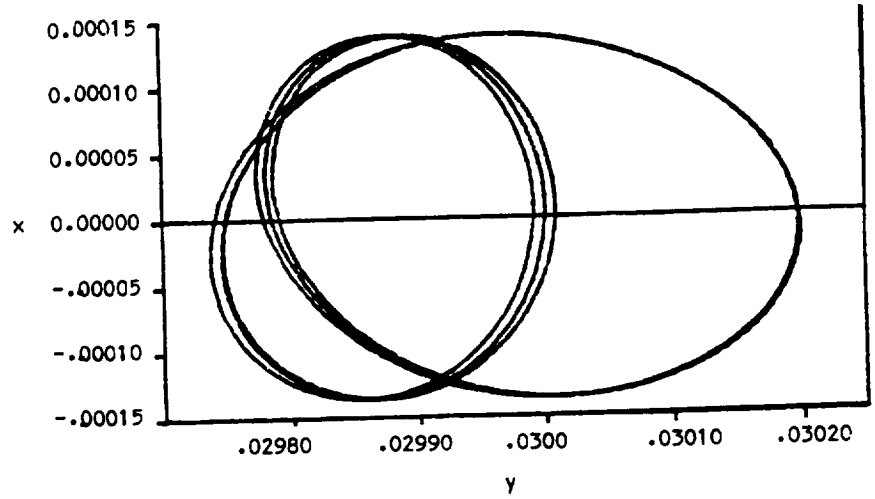

(d)

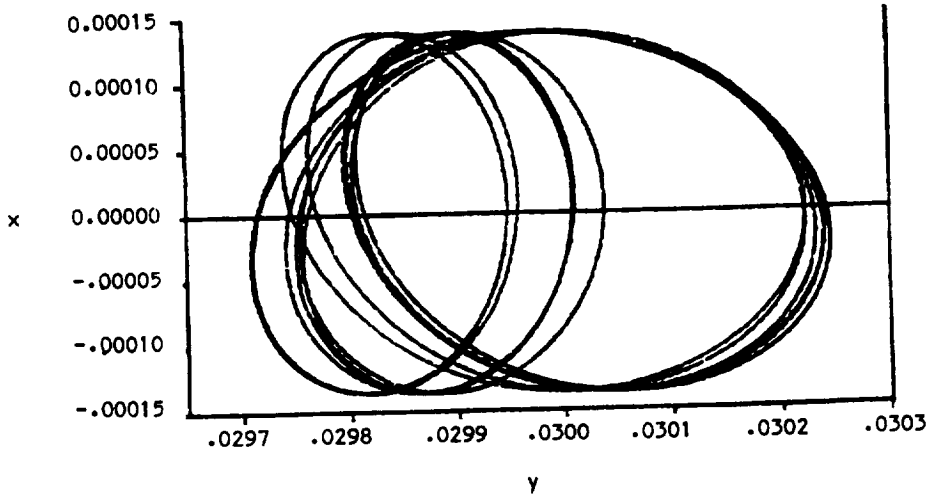

Figure 6, Continued

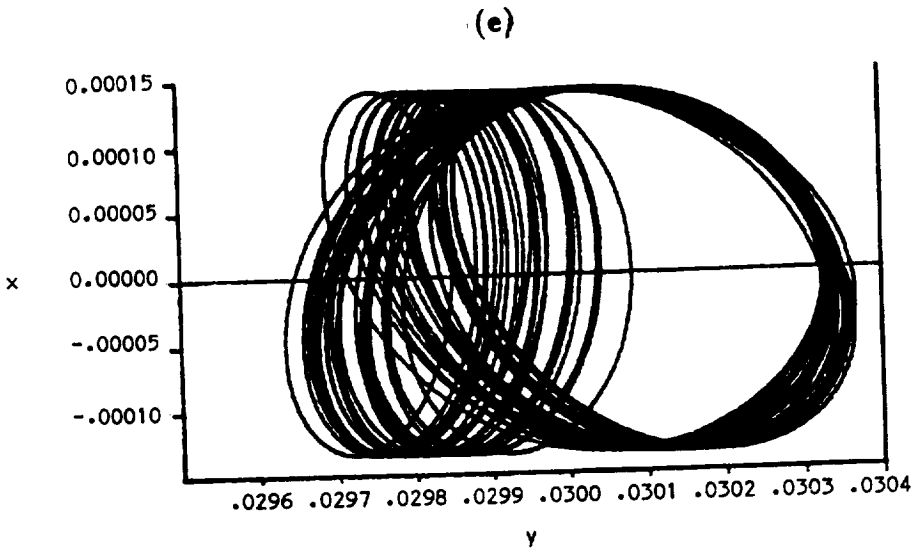

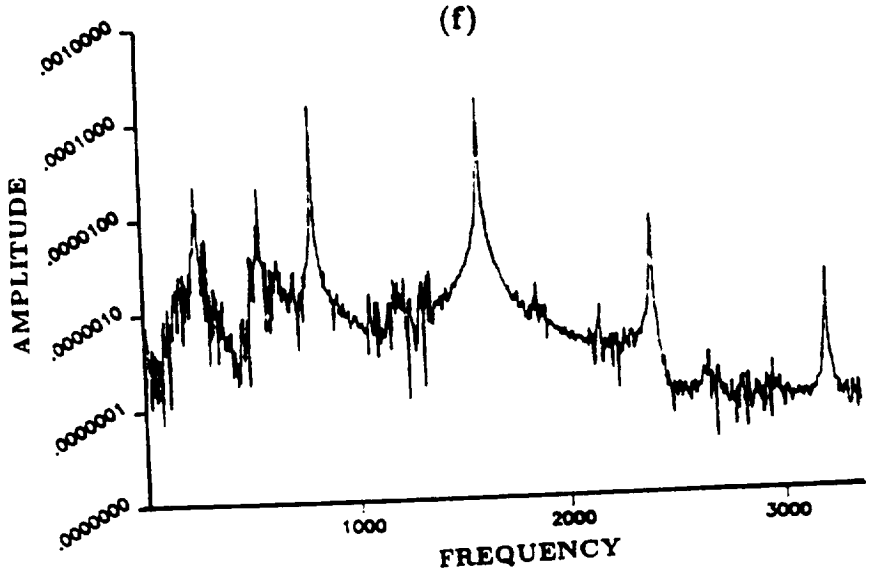

Figure 6, Continued

Figure 7. Bifurcation plot due to side force

(gap=0.03 cm, damping 10 N-sec/m. stiff.=1E+06 N/m, speed=1600 rad/sec)

P_1 primary synchronous whirling motion

P_3 subsynchronous whirling motion with order 1/3

P_9 subsynchronous whirling motion with order 1/9

P_1' secondary synchronous whirling motion

— HBM(stable solution) ; .... HBM(unstable solution); o numerical integration

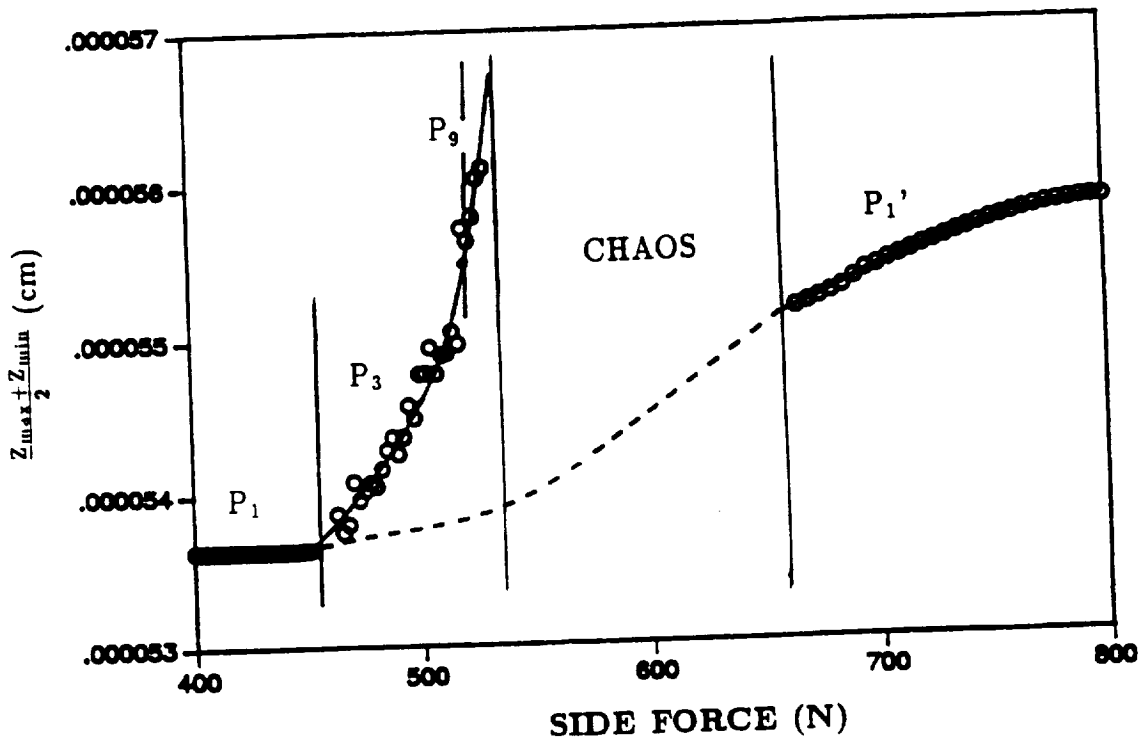

Figure 8. Effect of side force and eccentricity on flip bifurcation boundaries (speed=2100 rad/sec, gap=0.03 cm. damping=10 N-sec/m, stiff.=1E+06 N/m) A *primary* whirling ; B subsynchronous whirling ; C *secondary* whirling

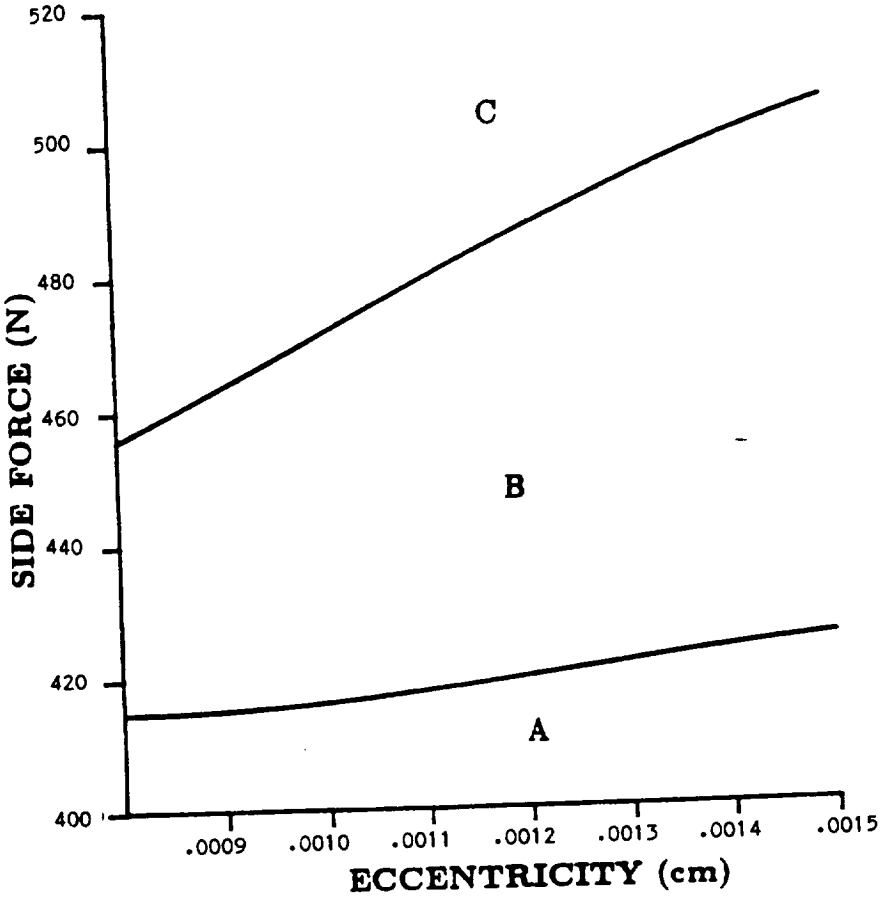

Figure 9. Effect of side force and gap on flip bifurcation boundaries (speed=2100 rad/sec, eccentricity=0.001 cm, damping=10 N-sec/m, stiff.=1E+06 N/m)

A *primary* whirling ; B subsynchronous whirling ; C *secondary* whirling

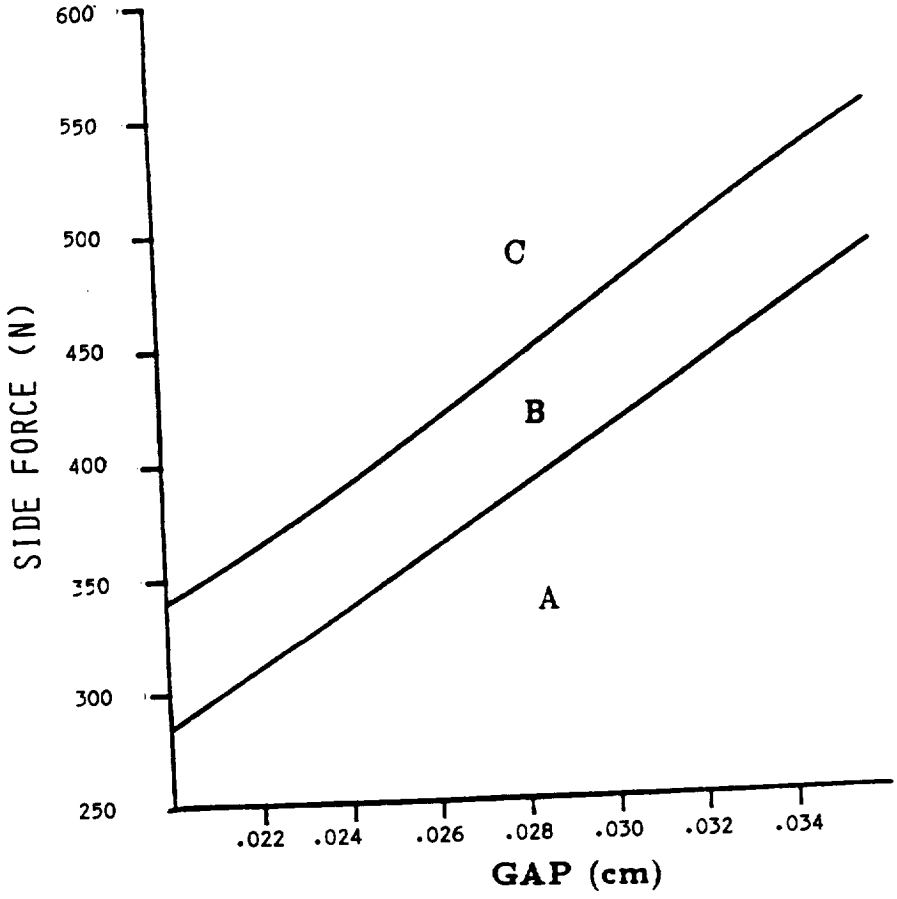

APPENDIX C

"A Convolution Approach for the Transient Analysis of Locally Nonlinear Rotor Systems," ASME Journal of Applied Mechanics, Vol. 57, pp. 731-737, 1990.

A Convolution Approach for the Transient Analysis of Locally Nonlinear Rotor Systems

I. F. Chiang
Graduate Student.

S. T. Noah
Associate Professor.
Mem. ASME.

Mechanical Engineering Department,
Texas A&M University,
College Station, TX 77843

A computationally efficient convolution method, based on discretized impulse response and transition matrix integral formulations, is developed for the transient analysis of complex linear structures interacting through strong local nonlinearities. In the formulation, the coupling forces due to the nonlinearities are treated as external forces acting on the coupled subsystems. Iteration is utilized to determine their magnitudes at each time increment. The method is applied to a generic rotor-housing model representing a turbopump of a space shuttle main engine (SSME). In that model, the local nonlinearity is due to clearances between the rotor bearing outer races and the carrier attached to the housing. As compared to the fourth-order Runge-Kutta numerical integration methods, the convolution approach proved more efficient and robust for the same accuracy requirement. This is due to the closed-form formulation of the convolution approach which allows for the use of relatively larger time increments and for a reduction in the roundoff errors.

Introduction

The use of a direct numerical integration for determining the transient response of coupled nonlinear rotor-flexible housing systems may require excessive computational time and involve unacceptable computational roundoff errors. To remedy these problems, different procedures have been developed by analysts to determine the transient response of large order rotor systems. The procedures can be recognized as falling under one of two basic approaches: those using physical or modal coordinates of the complete system and those using the coordinates of the individuals components of the system. The methods also differ in the numerical integration methods selected for the analysis.

Rouch and Kao (1980) employed Guyan (static) reduction method to arrive at a reduced size model in terms of the remaining physical coordinates. Accuracy of the results could be expected to be acceptable, since the rotor is basically a train of mass-stiffness subsystems. Nordmann (1975) attempted to minimize the inaccuracy of static condensation by applying the static reduction technique to an arbitrarily substructured rotor system and then assembling the reduced substructures to form a reduced system. The procedure is very laborious and no guarantees of accuracy are apparent.

Childs (1978) utilized free-interface modes of the various system components to represent the assembled turbopumps of a space shuttle main engine (SSME). The method, using fourth-order Runge-Kutta integration, does not allow for size reduction of the housing model while maintaining sufficient modal coordinates for accurate representation of the housing. Nelson et al. (1982), on the other hand, uses fixed-interface complex component modes to assemble a reduced size model. For systems with a large number of coupling points among the components, the approach suffers from an introduction of higher frequencies resulting from an excessive number of constraints imposed at the coupling (or boundary) points. In a transient analysis, this will necessitate employing much smaller time increments and consequently will lead to excessive computational time.

Only a few analysts have presented techniques for the general transient analysis of large nonlinear rotor systems. Adams (1980) used a normal mode representation for the rotor in terms of its undamped, free symmetric modes and treated gyroscopic and nonlinear terms as pseudo-external loads. The method presented by Childs (1978) makes use of a similar procedure to couple the rotor to its flexible housing. Nelson et al. (1982) developed a general computer code for the transient analysis of large rotor systems. The user may utilize time-step integration in the constrained-rotor (fixed-interface) modal space. Again, all connection points, including those at the nonlinearities, must be constrained, leading to the same shortcomings described previously.

Spanos et al. (1988) considered linear systems analyzed as decoupled subsystems. The accelerations at the interface are predicted at the beginning of each time step. The accelerations of the interface and interior nodes are then calculated and

Contributed by the Applied Mechanics Division of THE AMERICAN SOCIETY OF MECHANICAL ENGINEERS for presentation at the Winter Annual Meeting, Dallas, Texas, Nov. 25-30, 1990.

Discussion on this paper should be addressed to the Technical Editor, Leon M. Keer, The Technological Institute, Northwestern University, Evanston, IL 60208, and will be accepted until two months after final publication of the paper itself in the JOURNAL OF APPLIED MECHANICS. Manuscript received by the ASME Applied Mechanics Division, Oct. 10, 1988; final revision, Sept. 27, 1989.

Paper No. 90-WA/APM-21.

corrected through iterations. The decoupling makes the modeling of the assembled system more efficient. Hagedorn (1988) proposed a method for the analysis of a large linear subsystem coupled to one or more nonlinear subsystems. The dynamics of the system is represented by an integral equation of the convolution type containing the transfer matrix of the linear subsystem, and by the functional relation describing the nonlinearities. It appears that since no iterative technique was used, the method would require a very small integration step.

A method which proves to be highly efficient in determining the transient response of linear systems under specified general excitations is to utilize the convolution integral, or the transition matrix (Meirovitch, 1980) of the system. Von Pragenau (1981) utilized the transition matrix, stating that it offers the simplicity of the Euler method without requiring small steps. Von Pragenau maintained that for systems with constant coefficients, the stability and accuracy of the method are acquired through the closed-form solution of the transition matrix.

In the present study, the convolution methods (impulse response and transition integrals) are shown to be very effective when extended for application to linear systems with *local nonlinearities*. The forces at the nonlinear locations are treated as the external forces on the systems or subsystems and iteration is used at each time increment to determine the magnitude of the forces for subsequent increments.

The technique presented in this paper can also be applied in terms of the modes of subsystems calculated separately. However, system equations of motion will be formed as in a component mode synthesis approach. The response of each substructure is solved separately by treating the interface forces of the system as external forces to the subsystems. The convolution approach can also be applied to the generalized second-order system equations developed from component mode synthesis. In contrast to the convolution approach, if local nonlinearities occur at the interface, standard free interface, component mode synthesis methods fail.

The convolution approach is applied to a general rotor-housing system with rotor imbalance during startup or shutdown. In the present work, eigencoordinates are used to represent both housing and rotor. The local nonlinearities were taken as deadband clearances at the rolling element bearings which support the rotor in its housing. The integral formulation of the rotor motion is represented by its transition matrix and that of the housing by a convolution integral (based on the housing's impulse response).

The convoluted impulse response can only be applied to a system of uncoupled equations while the transition matrix formulation, in addition, can be applied to coupled equations. The transition matrix can therefore be applied to coupled dynamical systems represented by their physical coordinates or, in case of rotors, coupled by the gyroscopic terms in otherwise decoupled modal representation. Kubomura (1985) used a convolution integration method to achieve dynamic condensation of a substructure to its coupling points to other structures. Convolution was also used by Tongue and Dowell (1983), and Clough and Wilson (1979) to reduce system coordinates to that at the nonlinearities.

Modeling of a Rotor-Housing System

A representative complex rotor system with a flexible housing is shown in Fig. 1. The particular model shown in which the present method can be readily applied, represents the high pressure oxygen turbopump (HPOTP) of the SSME. The interaction forces between rotor and housing include various seal, impeller, turbine tip clearance, bearing clearance, and fluid side forces.

(a) Rotor. The equations of small transverse motion, (Noah, 1986), $\{S\}$ of the rotor under transient external and imbalance forces may be written as

$$[M]_R\{\ddot{S}\} - \dot{\phi}[G]\{\dot{S}\} + [K]_R\{S\} = \{F_I\}_R + \{F_E\}_R. \quad (1)$$

In equation (1), $\{S\}$ represents the translational and rotational displacements and only includes those displacements which are associated with masses and rotary inertias. Other displacements are reduced out using static condensation. The spinning speed of the rotor is denoted by $\dot{\phi}$, $[G]$ is the gyroscopic matrix corresponding to the attached disks, $\{F\}_R$ represents the coupling forces on the rotor due to coupling to the housing while $\{F_E\}_R$ represents the external forces including the imbalance forces. Let

$$\{S\} = [\Phi]_R\{q\}_R \quad (2)$$

in which $[\Phi]_R$ is the modal matrix, normalized with respect to the mass matrix of the nonspinning rotor and $\{q\}_R$ are the associated modal coordinates.

Nomenclature

$[C]$ = structural damping matrix
$[C]_I$ = coupling damping matrix
$[CM]$ = convergent matrix
$[D]$ = generalized damping matrix of rotor model
e = imbalance of disk
$\{F\}$ = physical force
$[G]$ = gyroscopic matrix
$\{H\}$ = physical coordinates of housing
$[I]$ = identity matrix
$[K]$ = structural stiffness matrix
$[K]_I$ = coupling stiffness matrix
$[M]$ = mass matrix
$\{P\}$ = generalized force (modal force)
$\{q\}$ = generalized displacement (modal displacement)
$[Q]$ = transition matrix
S = physical displacement of rotor in bearing
$\{S\}$ = physical coordinates of rotor
t = time
T = time increment
t_i = time at iT
$\{u\} = \begin{pmatrix} q \\ \dot{q} \end{pmatrix}$, generalized coordinates of rotor
ω_n, ω_d = natural and damped natural frequencies
$[0]$ = null matrix
$[\alpha]$ = the rotor state matrix
$[\Lambda]$ = diagonal eigenvalue matrix
$\dot{\phi}$ = spinning speed of rotor
$[\Phi]$ = normalized modal matrix
ζ = damping ratio

Brackets and Symbols

$[\ ]$ = square matrix
$[\ ]$ = diagonal matrix
$\{\ \}$ = column matrix
$[\ ]^{-1}$ = inverse of a matrix
$[\ ]^T$ = transpose of a matrix

Subscripts

R = rotor
H = housing
E = external
I = coupling
X, Y, Z = X, Y, Z direction
i = ith time increment

Using the modal transformation (2), equation (1) is written in the form

$$\{\ddot{q}\}_R - [\Phi]_R^T\dot{\phi}[G]_R[\Phi]_R\{\dot{q}\}_R + [\Lambda]_R\{q\}_R = [\Phi]_R^T(\{F_I\}_R + \{F_E\}_R) \quad (3)$$

where

$$[\Lambda]_R = [\omega_n^2]_R.$$

ω_n is the natural frequency of the nonspinning of the rotor. Adding a modal damping matrix $[C]$ to equation (3) yields

$$\{\ddot{q}\}_R + [D]_R\{\dot{q}\}_R + [\Lambda]_R\{q\}_R = [\Phi]_R^T(\{F_I\}_R + \{F_E\}_R) \quad (4)$$

where

$$[D]_R = [C]_R - [\Phi]_R^T\dot{\phi}[G]_R[\Phi]_R \quad (5)$$

$$[C]_R = [2\zeta\omega_n]_R. \quad (6)$$

(b) Housing. The equation of motion of the housing may be expressed as

$$[M]_H\{\ddot{H}\} + [K]_H\{H\} = \{F_I\}_H + \{F_E\}_H \quad (7)$$

where $\{H\}$ represents the transverse displacement in the Y and Z-directions. In terms of the modal coordinates of the housing while uncoupled to the rotor, equation (7) takes the form (after adding a modal damping matrix)

$$\{\ddot{q}\}_H + [D]_H\{\dot{q}\}_H + [\Lambda]_H\{q\}_H = [\Phi]_H^T(\{F_I\}_H + \{F_E\}_H) \quad (8)$$

where

$$[D]_H = [C]_H = [2\zeta\omega_n]_H \quad (9)$$

and

$$[\Lambda]_H = [\omega_n^2]_H. \quad (10)$$

(c) Coupling Forces. Forces due to linear coupling between rotor and housing may include the direct and cross-coupling forces due to seals, impeller, and turbine forces. The nonlinear coupling forces are taken as those due to the clearance between the rolling element bearing outer race and the housing. Figure 2 shows a model for the gap at each of the loosely supported bearings.

The bearing force acting on the housing in the Y-direction is

$$(F_G)_Y = K_G(R-\delta)\frac{S_Y - H_Y}{R} + C_G(\dot{S}_Y - \dot{H}_Y) \quad R \geq \delta$$

$$(F_G)_Y = C_G(\dot{S}_Y - \dot{H}_Y) \quad R \leq \delta$$

where the bearing support stiffness, K_G, is shown in Fig. 3 and C_G is the damping in bearing. Analogous equations hold for the Z-direction, and

$$R = \sqrt{(S_Y - H_Y)^2 + (S_Z - H_Z)^2}$$

where

S_Y, S_Z are the physical displacements of rotor in the Y and Z directions, respectively, at the bearing location.

H_Y, H_Z are the physical displacements of housing in the Y and Z directions, respectively, at the bearing location.

The bearing forces can further be written as

$$(F_G)_Y = \bar{K}_G(S_Y - H_Y) + C_G(\dot{S}_Y - \dot{H}_Y) \quad (11)$$

$$(F_G)_Z = \bar{K}_G(S_Z - H_Z) + C_G(\dot{S}_Z - \dot{H}_Z) \quad (12)$$

where

$$\bar{K}_G = K_G\left(1 - \frac{\delta}{R}\right) \quad R \geq \delta \quad (13)$$

$$\bar{K}_G = 0 \quad R \leq \delta. \quad (14)$$

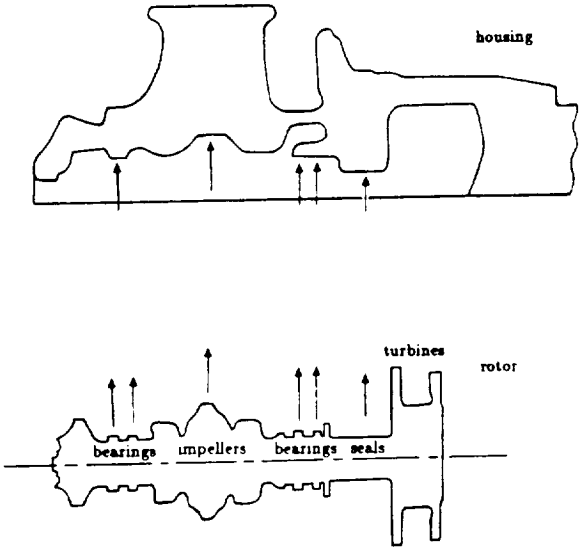

Fig. 1 Complex rotor system with flexible housing

Method of Analysis

A hybrid convolution method proposed by Noah et al., (1986) and (1988), is utilized here for the analysis of the coupled rotor-housing system. The displacements of the housing are best represented by a convolution integral due to its accuracy advantage over the transition matrix formulation. Due to the presence of the unsymmetric gyroscopic terms, the equations of motion for the rotor are transformed to first order. The displacements of the rotor are expressed in terms of transition matrix for the motion of the rotor.

The restriction of an impulse response convolution integral is that the equations of motion have to be decoupled. For a coupled subsystem, such as rotor with gyroscopic moments at the left-hand side of its equations, a transition matrix formulation has to be employed. However, the convolution integral is more computationally efficient than transition matrix formulation.

Transition Matrix for the Rotor. The equations of motion of the rotor, equation (4), are cast in first-order form,

$$\{\dot{u}\}_R = [\alpha]_R\{u\}_R + \{P\}_R \quad (15)$$

where

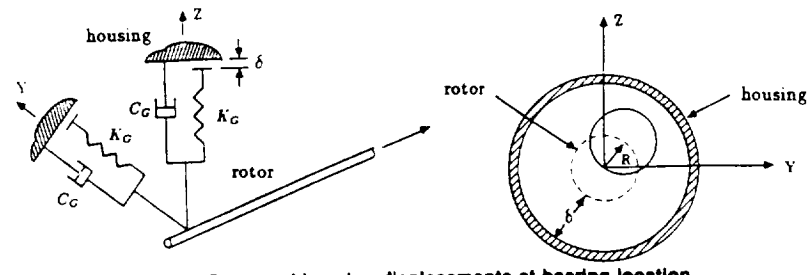

Fig. 2 Rotor and housing displacements at bearing location

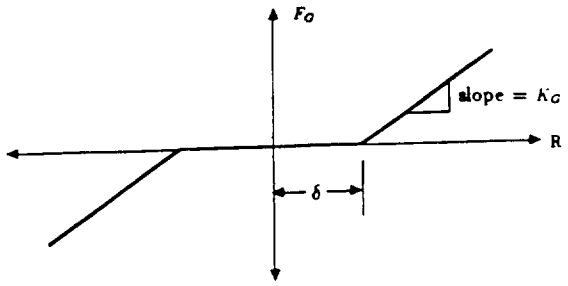

Fig. 3 Nonlinear bearing force, F_G, due to K_G

$$[\alpha]_R = \begin{pmatrix} [0] & [I] \\ -[\Lambda]_R & -[D]_R \end{pmatrix} \tag{16}$$

$$\{P\}_R = \begin{pmatrix} 0 \\ [\Phi]_R^T(\{F_I\}_R + \{F_E\}_R) \end{pmatrix}. \tag{17}$$

If the spinning speed is a function of time, the gyroscopic term of equation (5) can be moved to the right-hand side of equation (4) to avoid solving a new eigenproblem at each time step. In this case, the coefficient matrices, given by equations (16) and (17), are replaced by

$$[\alpha]_R = \begin{pmatrix} [0] & [I] \\ -[\Lambda]_R & -[C]_R \end{pmatrix} \tag{16'}$$

$$\{P\}_R = \begin{pmatrix} 0 \\ [\Phi]_R^T(\{F_I\}_R + \{F_E\}_R) \end{pmatrix} + \begin{pmatrix} 0 \\ [\Phi]_R^T\dot{\phi}[G]_R[\Phi]_R\{\dot{q}\}_R \end{pmatrix}. \tag{17'}$$

In this case, the equations of motion of the rotor becomes decoupled, and a convolution integral becomes a better selection because it is more efficient than the transition matrix method.

The solution of equation (15) can be written as

$$\{u(t)\}_R = e^{t[\alpha]_R}\{u_0\} + \int_0^t e^{(t-\tau)[\alpha]_R}\{P(\tau)\}_R d\tau \tag{18}$$

where

$$e^{t[\alpha]_R} = \sum_{k=0}^{\infty} \frac{t^k[\alpha]_R^k}{k!}. \tag{19}$$

Equation (19) is transition matrix and $\{u_0\}$ is the initial generalized coordinates.

Equation (18) can be cast in a discretized form in which the generalized forces, $\{P\}_R$, are taken as varying linearly between time t_i and t_{i+1} so that

$$\{P(t)\} = \{P(t_i)\} + \frac{t-t_i}{T}(\{P(t_{i+1})\} - \{P(t_i)\}) \quad t_i \le t \le t_{i+1}$$

where $t_{i+1} = t_i + T$ and T is a small increment in time. The discretized form of equation (18) can then be shown to take the form

$$\{u(t_{i+1})\}_R = [Q(T)]\{u(t_i)\}_R + ([Q(T)] - [I])[\alpha]_R^{-1}\left(\{P(t_i)\}_R + [\alpha]_R^{-1} \times \frac{\{P(t_{i+1})\}_R - \{P(t_i)\}_R}{T}\right) - [\alpha]_R^{-1}(\{P(t_{i+1})\}_R - \{P(t_i)\}_R) \tag{20}$$

where

$$[Q(T)] = e^{T[\alpha]_R}. \tag{21}$$

Convolution Integral for Housing. The decoupled form of the equations of motion of the housing allows expressing the nodal displacements of the housing by an integral. The integral formulation has the advantage of providing a closed-form expression as opposed to conventional numerical integration schemes. Also this representation allows dealing directly with diagonal modal matrices as opposed to coupled, first-order modal equations used with the Runge-Kutta method of the convolutional formulation matrices. This results in higher computational speed and accuracy of the convolution formulation.

Based on equation (8), the housing generalized coordinates can be expressed as

$$\{q(t)\}_H = [e^{-\zeta\omega_n t}\cos\omega_d t]\{q(0)\}_H + \left[\frac{1}{\omega_d}e^{-\zeta\omega_n t}\sin\omega_d t\right](\{\dot{q}(0)\}_H + \zeta\omega_n\{q(0)\}_H) + \int_0^t \left[\frac{1}{\omega_d}e^{-\zeta\omega_n(t-\tau)}\sin\omega_d(t-\tau)\right]\{P(\tau)\}_H d\tau \tag{22}$$

where $\{q(0)\}$, $\{\dot{q}(0)\}$ are initial solutions, ω_n, ω_d are undamped and damped natural frequencies of housing, ζ is damping ratio of housing, $\{P\}_H = [\Phi]_H^T(\{F_I\}_H + \{F_E\}_H)$, the generalized forces act on housing.

The expression (22) is next written in discretized form, with the generalized forces taken as before as varying linearly within each time step, or

$$\{q(t_{i+1})\}_H = [e^{-at_{i+1}}\cos bt_{i+1}]\{q(0)\}_H + \left[\frac{1}{b}e^{-at_{i+1}}\sin bt_{i+1}\right](\{\dot{q}(0)\}_H + a\{q(0)\}_H) + \left\{\frac{\sin bt_{i+1}}{b(a^2+b^2)}EA_{i+1} - \frac{\cos bt_{i+1}}{b(a^2+b^2)}EB_{i+1}\right\} \tag{23}$$

$$\{\dot{q}(t_{i+1})\}_H = [-e^{-at_{i+1}}(a\cos bt_{i+1} + b\sin bt_{i+1})]\{q(0)\}_H + \left[e^{-at_{i+1}}\left(-\frac{a}{b}\sin bt_{i+1} + \cos bt_{i+1}\right)\right](\{\dot{q}(0)\}_H + a\{q(0)\}_H) + \left\{\frac{-a\sin bt_{i+1} + b\cos bt_{i+1}}{b(a^2+b^2)}EA_{i+1} + \frac{a\cos bt_{i+1} + b\sin bt_{i+1}}{b(a^2+b^2)}EB_{i+1}\right\} \tag{24}$$

where

$$a = \zeta\omega_n \tag{25}$$

$$b = \omega_d \tag{26}$$

$$EA_{i+1} = e^{-aT}EA_i + A_{i+1} \tag{27}$$

$$EB_{i+1} = e^{-aT}EB_i + B_{i+1} \tag{28}$$

$$EA_i = e^{-at_{i-1}}A_1 + e^{-at_{i-2}}A_2 + \ldots + A_i \tag{29}$$

$$EB_i = e^{-at_{i-1}}B_1 + e^{-at_{i-2}}B_2 + \ldots + B_i \tag{30}$$

$$A_{i+1} = P_{i+1}(a\cos bt_{i+1} + b\sin bt_{i+1}) - \frac{P_{i+1}-P_i}{T(a^2+b^2)}(a^2\cos bt_{i+1} + 2ab\sin bt_{i+1} - b^2\cos bt_{i+1}) + \frac{P_{i+1}-P_i}{T(a^2+b^2)}e^{-aT}(a^2\cos bt_i + 2ab\sin bt_i - b^2\cos bt_i) - P_i e^{-aT}(a\cos bt_i + b\sin bt_i) \tag{31}$$

$$B_{i+1} = P_{i+1}(a \sin bt_{i+1} - b \cos bt_{i+1})$$
$$- \frac{P_{i+1} - P_i}{T(a^2+b^2)}(a^2 \sin bt_{i+1} - 2ab \cos bt_{i+1} - b^2 \sin bt_{i+1})$$
$$+ \frac{P_{i+1} - P_i}{T(a^2+b^2)} e^{-aT}(a^2 \sin bt_i - 2ab \cos bt_i - b^2 \sin bt_i)$$
$$- P_i e^{-aT}(a \sin bt_i - b \cos bt_i) \quad (32)$$

P is element of vector $\{P\}$.

The Coupling Forces. The coupling forces acting on the housing are given by

$$\{F_I\}_H = [K]_I(\{S\} - \{H\}) + [C]_I(\{\dot{S}\} - \{\dot{H}\}) \quad (33)$$

and those on the rotor are

$$\{F_I\}_R = -\{F_I\}_H$$

where $[K]_I$ and $[C]_I$ are the coupling stiffness and damping matrices, respectively. The coupling stiffness matrix includes the updated bilinear bearing stiffness at each iteration.

The Computational Procedure. For the responses at time $t = t_{i+1}$, the coupling forces between the housing and rotor are unknown. An iterative technique is used to calculate these forces. The following iterative loop is used in both the hybrid and Runge-Kutta methods:

If the responses at $t = t_i$ are known and responses at $t = t_{i+1}$ are desired, then:

(a) Set $\{F_I(t_{i+1})\} = \{F_I(t_i)\}$.

(b) Calculate $\{P\}_R$ and $\{P\}_H$.

(c) Solve $\{u(t_{i+1})\}_R$ and $\{q(t_{i+1})\}_H$, $\{\dot{q}(t_{i+1})\}_H$ by the hybrid method (or the Runge-Kutta method). Calculate the Euclidean norm of $\{u(t_{i+1})\}_R$ and $\{q(t_{i+1})\}_H$.

(d) Transfer $\{u(t_{i+1})\}_R$ and $\{q(t_{i+1})\}_H$, $\{\dot{q}(t_{i+1})\}_H$ back to physical coordinates, then a new connection force $\{F_I(t_{i+1})\}$ can be calculated.

(e) If the Euclidean norms of two consecutive iterations of both rotor and housing are close enough then stop the iteration and go to step (f), otherwise go to (b).

(f) Move a time increment and go to (a) until t reaches a specified time for terminating the run.

The Convergence of Hybrid Method. Rewrite the coupling forces as the function of the generalized coordinates, equations (20), (23), and (24) can be arranged as the following form:

$$\begin{pmatrix} u(t_{i+1})^{(k)} \\ \cdots \\ q(t_{i+1})^{(k)} \\ \dot{q}(t_{i+1})^{(k)} \end{pmatrix} = [CM] \times \begin{pmatrix} u(t_{i+1})^{(k-1)} \\ \cdots \\ q(t_{i+1})^{(k-1)} \\ \dot{q}(t_{i+1})^{(k-1)} \end{pmatrix} + \{c\} \quad (34)$$

where k stands for kth iteration at a given time t_{i+1}, $[CM]$ is the convergent matrix (Isaacson and Keller, 1966), $\{c\}$ is vector with known values, and

$$[CM] = \begin{pmatrix} [S1] & [S2] \\ [S3] & [S4] \end{pmatrix} \quad (35)$$

where

$$[S1] = [T1] \times \begin{pmatrix} 0 & 0 \\ -[\Phi]_R^T[K]_I[\Phi]_R & -[\Phi]_R^T[C]_I[\Phi]_R \end{pmatrix}$$

$$[S2] = [T1] \times \begin{pmatrix} 0 & 0 \\ [\Phi]_R^T[K]_I[\Phi]_H & [\Phi]_R^T[C]_I[\Phi]_H \end{pmatrix}$$

$$[S3] = \begin{pmatrix} [T2][\Phi]_H^T[K]_I[\Phi]_R & [T2][\Phi]_H^T[C]_I[\Phi]_R \\ [T3][\Phi]_H^T[K]_I[\Phi]_R & [T3][\Phi]_H^T[C]_I[\Phi]_R \end{pmatrix}$$

$$[S4] = \begin{pmatrix} -[T2][\Phi]_H^T[K]_I[\Phi]_H & -[T2][\Phi]_H^T[C]_I[\Phi]_H \\ -[T3][\Phi]_H^T[K]_I[\Phi]_H & -[T3][\Phi]_H^T[C]_I[\Phi]_H \end{pmatrix}$$

and

$$[T1] = [\alpha]_R^{-1}\left(([Q(T)] - [N])\frac{[\alpha]_R^{-1}}{T} - [N]\right)$$

$$[T2] = \begin{bmatrix} \frac{\sin bt_{i+1}}{b(a^2+b^2)} AC - \frac{\cos bt_{i+1}}{b(a^2+b^2)} AS \end{bmatrix}$$

$$[T3] = \begin{bmatrix} \frac{-a \sin bt_{i+1} + b \cos bt_{i+1}}{b(a^2+b^2)} AC \\ + \frac{a \cos bt_{i+1} + b \sin bt_{i+1}}{b(a^2+b^2)} AS \end{bmatrix}$$

where

$$AC = a \cos bt_{i+1} + b \sin bt_{i+1}$$
$$- \frac{1}{T(a^2+b^2)}(a^2 \cos bt_{i+1} + 2ab \sin bt_{i+1} - b^2 \cos bt_{i+1})$$
$$+ \frac{e^{-aT}}{T(a^2+b^2)}(a^2 \cos bt_i + 2ab \sin bt_i - b^2 \cos bt_i)$$

$$AS = a \sin bt_{i+1} - b \cos bt_{i+1}$$
$$- \frac{1}{T(a^2+b^2)}(a^2 \sin bt_{i+1} - 2ab \cos bt_{i+1} - b^2 \sin bt_{i+1})$$
$$+ \frac{e^{-aT}}{T(a^2+b^2)}(a^2 \sin bt_i - 2ab \cos bt_i - b^2 \sin bt_i).$$

Equation (34) is in the form of the Jacobi iterative method (simultaneous iterations), see (Isaacson and Keller, 1966). The convergent matrix, $[CM]$ may not be fixed at a given time $t = t_{i+1}$ as in an ordinary linear system because matrix $[K]_I$ may change during the iteration if the switch between two slope areas in Fig. 3 exists. $[K]_I$ will be updated because the nonlinear bearing stiffness, K_G, changes. In this case, there are two convergence rates during the iteration at that given time.

Equation (34) will converge if and only if all eigenvalues of $[CM]$ are less than one in absolute value. An alternative way to check the convergence is that the iterative method will converge if, for any matrix norm (Euclidean, maximum, etc.), $\|[CM]\| < 1$. Uncommon cases occur where convergence criteria are met within one region in Fig. 3 and not the other. In that case, overall convergence at a given time t_{i+1} might occur depending on the pattern of movement from one region to the other. In any case, the convergence rate and size of the increment T will determine the outcome for acceptable accuracy.

The rate of convergence, CR, is defined as the following:

$$CR \equiv -\log \rho([CM])$$

where $\rho([CM])$ is the spectral radius of $[CM]$ defined by

$$\rho([CM]) \equiv \max|\lambda_i|$$

where λ_i are the eigenvalues of $[CM]$.

Let the initial error be defined as the norm of the vector of the difference between the exact solution and an initial guess at the beginning of iteration. The number of iterations, ν, required to reduce the initial error by the factor 10^{-m} is inversely proportional to CR and is defined as

$$\nu \geq \frac{m}{CR}.$$

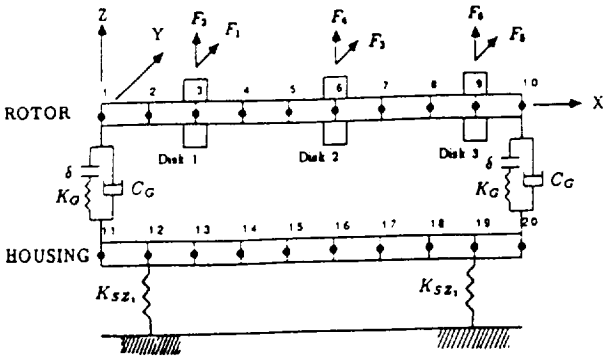

ROTOR: Shaft diameter: OD = 7.26×10^{-3}m, ID = 0.0m
Material: $E = 2.0684 \times 10^{10} N/m^2$
Joint length= 7.26×10^{-2}m
Rotor length= 6.858×10^{-1}m

HOUSING: Housing/rotor weight ratio = 6/1

$(EI)_R = 8.6947 \times 10^3 Nm^2$
$(EI)_H = 1.7494 \times 10^4 Nm^2$

$F_1(t) = m_1 e\phi^2 \cos\phi t$ $K_{SZ_1} = 7.005 \times 10^6 N/m$ $C_G = 0.0$
$F_2(t) = m_1 e\phi^2 \sin\phi t$ $K_{SY_1} = 8.7563 \times 10^6 N/m$
$F_3(t) = m_2 e\phi^2 \cos\phi t$ $K_{SZ_2} = 8.7563 \times 10^6 N/m$
$F_4(t) = m_2 e\phi^2 \sin\phi t$ $K_{SY_2} = 2.6269 \times 10^7 N/m$
$F_5(t) = m_3 e\phi^2 \cos\phi t$ $K_G = 8.7563 \times 10^7 N/m$
$F_6(t) = m_3 e\phi^2 \sin\phi t$ $\delta = 0.0127mm$

Fig. 4 The generic model

Application and Discussion

The present convolution method is applied to a modified version of a rotor model proposed by Davis et al. (1984). The model was proposed to represent a simplified generic model of the SSME turbopumps. The parameters and coefficients of the present generic model (shown in Fig. 4) are given in Tables 1 and 2. The imbalance forces are taken as shown on Fig. 4.

Response of the generic rotor-housing model at the bearing location is determined for the hypothetical startup-shutdown case shown in Fig. 5. For various time increments, Δt, a comparison is made of the errors and computer CPU time (on a VAX 8650) between the results obtained using Runge-Kutta fourth-order method and those using the present convolution method.

Comparisons of the CPU time, are made with comparable errors of the results of using both methods. The errors is measured at time $t = 0.01$ seconds and defined as the following

$$\text{Error} = \frac{\|V_{ex} - V\|}{\|V_{ex}\|}$$

where V_{ex} is the exact solution of the rotor and housing displacements in vector form and V represents the displacements of rotor and housing at the corresponding time in vector form.

The "exact" solution is calculated using the hybrid convolution method with a very small time increment, 2×10^{-7} seconds and tolerance = 1×10^{-12}. The tolerance is the absolute value of the difference of the displacement and velocity norms of rotor and housing described in step (e) of the computational procedure.

As shown in Figs. 6 and 7, with the tolerance equals to 1×10^{-8} seconds, the hybrid convolution method is faster and more accurate. For more meaningful comparison, the accuracies of the Runge-Kutta and convolution methods are made closer by reducing the allowable tolerance for the Runge-Kutta to 1×10^{-12} seconds and 1×10^{-14} seconds. The CPU time for the Runge-Kutta increases quickly from 1.42 times of the hybrid method's CPU to 4.23 times (with a time increment of 2×10^{-5}). For the closest accuracies, the CPU time of the Runge-Kutta is 4.23 times that of the hybrid method. The hybrid convolution method is also more robust than the Runge-Kutta method. The Runge-Kutta algorithm failed to converge for time increments greater than 2×10^{-5} seconds. However, the hybrid method will diverge when the increment used is larger than 3.3×10^{-5} seconds.

Table 1 Parameters of the generic model

Disk	Mass (Kg)	Imbalance (mm)	Moment of inertia ($Kg.m^2$) Polar	Diametrical
1	4.5358	0.0508	3.1635×10^{-3}	1.7964×10^{-3}
2	6.8124	0.0508	2.1806×10^{-2}	1.1411×10^{-2}
3	9.0175	0.0508	1.1363×10^{-1}	5.7373×10^{-2}

Table 2 Coefficients of the generic model

Disk	K_{YY}, K_{ZZ} (N/m)	K_{XY}, K_{YX} (N/m)	C_{YY}, C_{ZZ} (N sec/m)
1	1.7513×10^7	2.6269×10^6	1.1033×10^4
2	-1.5586×10^6	-7.0050×10^5	1.7513×10^2
3	1.5236×10^6	3.3274×10^5	4.0279×10^2

Disk	Side force (N) Y-direction	Z-direction
1	$2.2019 \times 10^{-5}\ \dot{\phi}^2$	$-1.2482 \times 10^{-4}\ \dot{\phi}^2$
2	$2.7210 \times 10^{-4}\ \dot{\phi}^2$	$3.2387 \times 10^{-4}\ \dot{\phi}^2$
3	$1.0582 \times 10^{-4}\ \dot{\phi}^2$	0

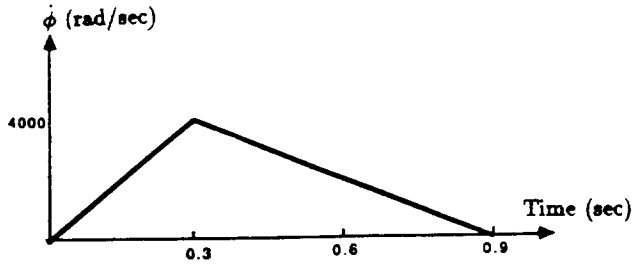

Fig. 5 Running speed of rotor

Concluding Remarks

The convolution integral and transition matrix methods are represented in closed form. They generate less roundoff errors and require less numerical computation time in comparison with the Runge-Kutta fourth-order method. Moreover, they are more robust than the Runge-Kutta method since they will converge for larger time-step size.

The hybrid convolution approach developed in this study is shown to provide an efficient and accurate closed-form integral formulation for determining the transient response of linear systems coupled through local nonlinearities. A typical application in which the present method proved quite effective is the determination of the transient response of a generic model of the high pressure oxygen turbopump (HPOTP) of a space shuttle main engine (SSME) in presence of bearing clearances, constituting the local nonlinearities. Substantial savings in computation time were achieved as compared with direct numerical integration techniques.

The use of the transition matrix allows the representation of rotors involving skew-symmetric matrices of gyroscopic loads or other nonconservative systems with general velocity coefficient matrices. A convolution integral would represent quite effectively other systems with classical modes, such as

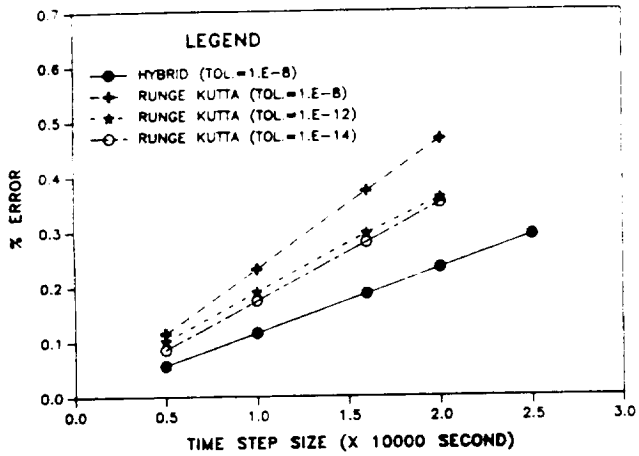

Fig. 6 Accuracy of hybrid method and Runge-Kutta methods

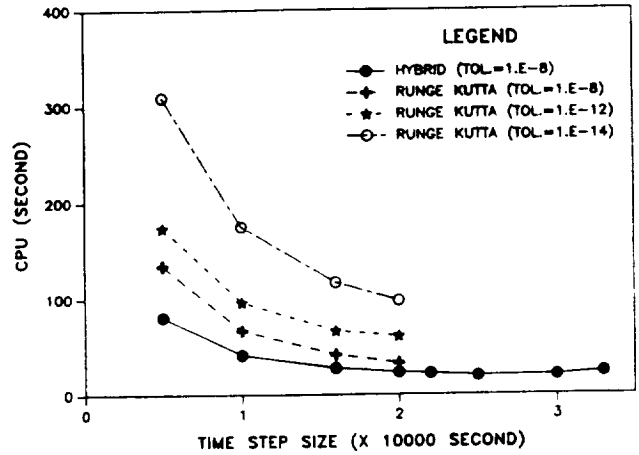

Fig. 7 CPU time of hybrid method and Runge-Kutta methods

the housing of the HPOTP or other nonrotating, proportionally damped structures. The convolution formulation allows accommodating with ease changes in the nonlinear or linear coupling parameters among the various linear subsystems involved.

Possible improvement of the method could be achieved through other alternative or optimization for the iteration procedure utilized in this study. The methods described in this study is believed to be capable of handling any type of local nonlinearity. For an impact case at the bearing, for example, iteration over the contact force could be replaced by iteration to establish contact/no-contact at each increment and then reverse the impact velocity. Applications of the present method to systems with various types of local nonlinearities could be worthwhile.

Acknowledgment

This work was carried out as part of a research project supported by NASA, Marshall Flight Center, under contract No. NAS8-36293. The authors are grateful to Thomas Fox, the technical monitor, for his enthusiastic support and interest.

References

Adams, M. L., 1980, "Non-linear Dynamics of Flexible Multi-Bearing Rotors," *Journal of Sound and Vibration*, Vol. 71, pp. 129–144.

Childs, D. W., 1978, "The Space Shuttle Main Engine High Pressure Fuel Turbopump-Rotordynamic Instability Problem," *ASME Journal of Engineering for Power*, Vol. 100, pp. 48–51.

Clough, R. W., and Wilson, E. L., 1979, "Dynamic Analysis of Large Structural Systems With Local Nonlinearities," *Computer Methods in Applied Mechanics and Engineering*, Vol. 17 18, pp. 107–129.

Davis, L. B., Wolfe, E. A., and Beatty, R. F., 1984, "Housing Flexibility Effects on Rotor Stability," MSFC Advanced High Pressure O_2/H_2 Technology Conference Proceedings, G. Marshall Space Flight Center, Huntsville, Ala.

Hagedorn, P., Schramm, W., 1988, "On the Dynamics of Large Systems With Localized Nonlinearities," ASME JOURNAL OF APPLIED MECHANICS, Vol. 55, pp. 946–951.

Isaacson, E., and Keller, H. B., 1966, *Analysis of Numerical Methods*, John Wiley and Sons, New York.

Kubomura, K., 1985, "Transient Loads Analysis by Dynamic Condensation," ASME JOURNAL OF APPLIED MECHANICS, Vol. 52, pp. 559–564.

Meirovitch, L., 1980, *Computational Methods in Structural Dynamics*, Sijthoff and Noordhoff.

Nelson, H. D., Meacham, W. L., Fleming, D. P., and Kascak, A. F., 1982, "Nonlinear Analysis of Rotor Bearing Systems Using Component Mode Synthesis, ASME Paper No. 82-GT-303.

Noah, S. T., 1986, "Hybrid Methods for Rotordynamic Analysis," Final NASA Report, G. C. Marshall Space Flight Center, Ala., under Contract No. NAS8-36182, Dec. 1986.

Noah, S. T., Chiang, I. F., and Kim, Y. B., 1988, "Dynamic Analysis of Nonlinear Rotor/Housing Systems," MSFC Advanced High Pressure O_2/H_2 Technology Conference Proceedings, G. Marshall Space Flight Center, Huntsville, Ala.

Noah, S. T., Fan, U. J., Choi, Y.-S., and Fox, T., 1986, "Efficient Transient Analysis Methods for the Space Shuttle Main Engine Turbopumps," NASA Conference on Advanced Earth-to-Orbits Propulsion Tech., G. Marshall Space Flight Center, Huntsville, Ala., May 13–15.

Nordmann, R., 1975, "Eigenvalues and Resonance Frequency Forms of Turborotors with Sleeve Bearings Crank Excitation, External, and Internal Damping," Machine Dynamics Group, Technical University Darmstadt, F.R.G.

Rouch, K. E., and Kao, J. S., 1980, "Dynamic Reduction in Rotor Dynamics by the Finite Element Method," ASME JOURNAL OF MECHANICAL DESIGN, Vol. 102, pp. 360–368.

Spanos, P. D., Cao, T. T., Jacobson, C. A., Jr., and Nelson, D. A. R., Jr., 1988, "Decoupled Dynamic Analysis of Combined Systems by Iterative Determination of Interface Accelerations," *Earthquake Engineering and Structural Dynamics*, Vol. 16, pp. 491–500.

Tongue, B. H., and Dowell, E. H., 1983, "Component Mode Analysis of Nonlinear, Nonconservative Systems," ASME JOURNAL OF APPLIED MECHANICS, Vol. 50, pp. 204–209.

Von Pragenau, G. L., 1981, "Large Step Integration for Linear Dynamic Systems," Conference Proc. IEEE Southeastern '81, reprint Apr.

NASA National Aeronautics and Space Administration

Report Documentation Page

1. Report No.	2. Government Accession No.	3. Recipient's Catalog No.

4. Title and Subtitle	5. Report Date
Nonlinear Rotordynamics Analysis	February, 1991
	6. Performing Organization Code

7. Author(s)	8. Performing Organization Report No.
Sherif T. Noah	
	10. Work Unit No.

9. Performing Organization Name and Address	11. Contract or Grant No.
Marshall Space Flight Center Alabama 35812	NAS8-37465
	13. Type of Report and Period Covered

12. Sponsoring Agency Name and Address	14. Sponsoring Agency Code
National Aeronautics & Space Administration Washington, DC 20546-0001	Final

15. Supplementary Notes

16. Abstract

Effective analysis tools have been developed for predicting the nonlinear rotordynamic behavior of the SSME turbopumps under steady and transient operating conditions. Using these methods, preliminary parametric studies have been conducted on both generic and actual HPOTP (high pressure oxygen turbopumps) models. In particular, a novel modified harmonic balance/alternating Fourier transform (HB/AFT) method was developed and used to conduct a preliminary study of the effects of fluid, bearing and seal forces on the unbalanced response of a Multi-disk rotor in presence of bearing clearances. A computer program was developed and made available to NASA, Marshall. The method makes it possible to determine periodic, sub-, super-synchronous and chaotic responses of a rotor system. The method also yields information about the stability of the obtained response, thus allowing bifurcation analyses. This provides a more effective capability for predicting the response under transient conditions by searching in proximity of resonance peaks. Preliminary results were also obtained for the nonlinear transient response of an actual HPOTP model using an efficient, newly developed numerical method based on convolution integration. A computer program was developed and made available to NASA Marshall Flight Center. Currently, the HB/AFT is being extended for determining the aperiodic response of nonlinear systems. Initial results shows the method to be promising.

17. Key Words (Suggested by Author(s))	18. Distribution Statement

19. Security Classif. (of this report)	20. Security Classif. (of this page)	21. No. of pages	22. Price